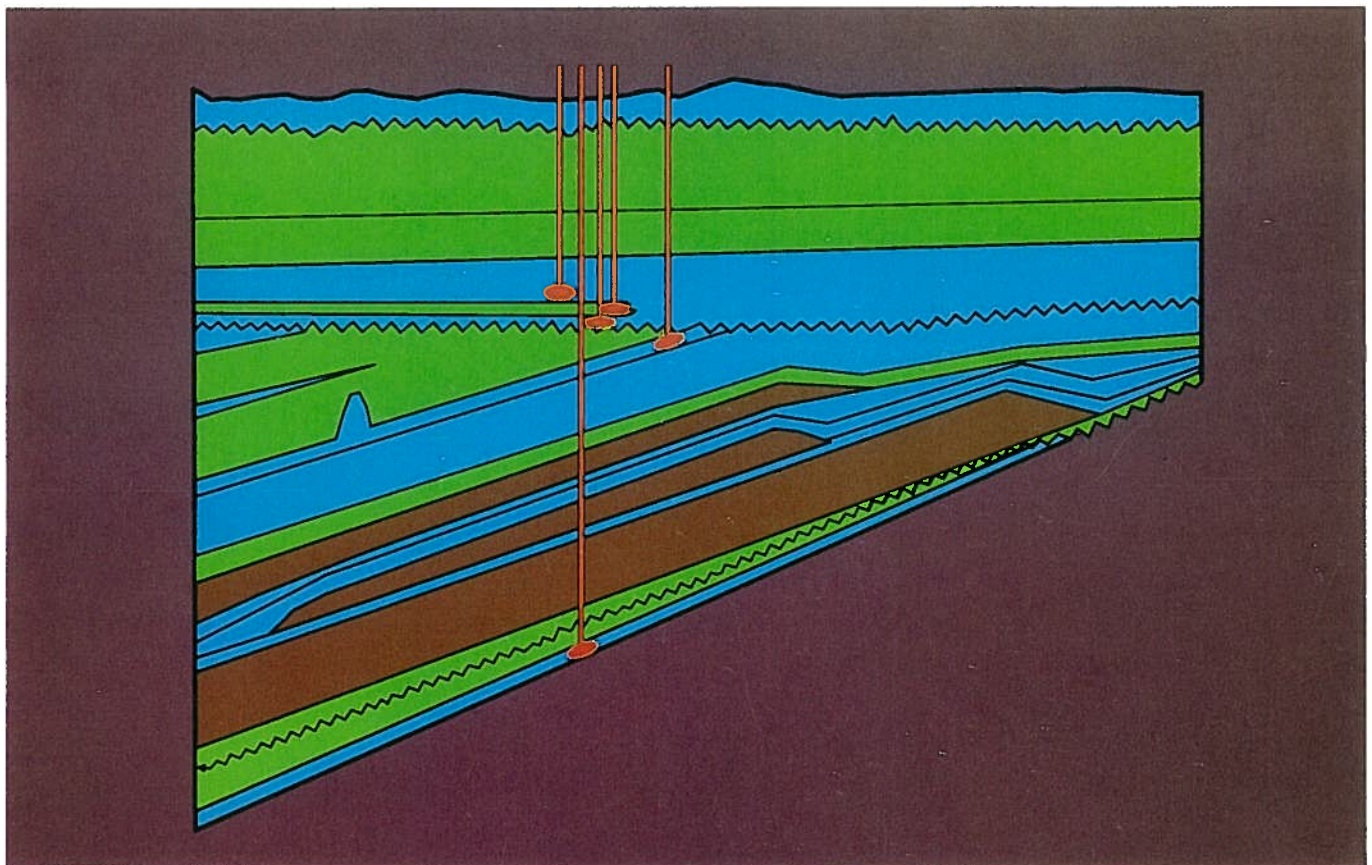


# **Evaluation of effects of deep waste injection in the Cold Lake area, Alberta**

S. Bachu, E.H. Perkins,  
Brian Hitchon, A.T. Lytviak,  
and J.R. Underschultz



**ALBERTA  
RESEARCH  
COUNCIL**

Alberta Geological Survey

# **Evaluation of effects of deep waste injection in the Cold Lake area, Alberta**

**S. Bachu, E.H. Perkins,  
Brian Hitchon, A.T. Lytviak,  
and J.R. Underschultz**

*Cover:*

Diagrammatic representation of the position of  
injection wells in the hydrostratigraphic succession.

## Acknowledgements

---

This work was jointly funded by the Alberta Research Council and Alberta Environment. The authors express their appreciation and thanks to Dr. Brian Hammond, Senior Research Manager, Research Management Division, Alberta Environment; and Mr. Ron Hicks, Athabasca River Basin Planner, Planning Division, Alberta Environment, who allowed the research team the necessary flexibility to undertake this study in an optimum manner, and provided appropriate support. The contribution of Dr. C.M. Sauveplane to the evaluation of hydrofracturing thresholds for rocks is gratefully acknowledged. Special thanks are due to Mika M. Madunicky, technical assistant to the senior author, who was responsible for project coordination and com-

pilation of both the original contract reports and this bulletin. This publication has benefited from reviews by staff at Alberta Environment, Alberta Energy Resources Conservation Board, Saskatchewan Environment, and the National Hydrology Research Institute, who provided comments on the original contract reports on which it is based. Major technical reviewing fell to Dr. Charles Kreidler, Bureau of Economic Geology, The University of Texas at Austin, and Professor Frank Schwartz, University of Alberta, to whom the authors are very grateful for their care and comments. Appreciation is also expressed to Lorne Bradley, Dale Hite, Dan Magee, Jim Matthie and Karen Parrish of Publishing and Graphics.

**Copies of this report are available from:**

Alberta Research Council  
Publications Sales  
250 Karl Clark Road  
Edmonton, Alberta  
Canada  
Phone: (403)450-5390

*Mailing address:*

P.O. Box 8330, Postal Station F  
Edmonton, Alberta  
Canada T6H 5X2

*or from:*

Alberta Research Council  
Publications Sales  
3rd Floor, 6815 - 8 Street NE  
Calgary, Alberta  
Canada T2E 7H7  
Phone (403)297-2600

# Contents

---

Abstract .....	1
Introduction .....	1
Baseline conditions .....	2
Regional geology .....	4
Regional hydrogeology .....	4
Water-rock interactions .....	6
Selection of representative formation waters .....	7
Mineralogy of injection aquifers .....	8
Correction of formation water analyses .....	11
Composition of injection waters .....	12
Calculation of potential water-rock interactions .....	12
Basal Cambrian aquifer .....	13
Cooking Lake aquifer .....	13
McMurray aquifer .....	16
Clearwater aquifer .....	18
Mannville aquifer .....	19
Geochemical effects of deep waste injection .....	20
Evaluation of hydrofracturing thresholds for rocks .....	24
In situ stress regime and failure criteria .....	24
Evaluation of breakdown pressures .....	26
Estimation of Poisson's ratio .....	27
Estimation of overburden stress and initial pore pressure .....	28
Estimation of constant $\alpha$ and breakdown pressures .....	28
Numerical simulation of pressure buildup .....	31
Mathematical and numerical modelling .....	31
Sensitivity analysis .....	32
Calibration of regional models .....	35
Lower Paleozoic system .....	35
Post-Prairie succession .....	35
Regional simulations of injection .....	37
Injection in the Basal Cambrian aquifer .....	38
Injection in the post-Prairie succession .....	40
Local hydraulic parameters .....	43
Local simulations of injection .....	46
Evaluation of the results .....	53
Conclusions .....	54
References .....	55

## Figures

Figure 1	Location of injection sites and schematic representation of the position of injection wells in the hydrostratigraphic sequence .....	3
Figure 2	Injection sites, salinity isoconcentration contours and locations of representative formation waters for five injection aquifers .....	9
Figure 3	Saturation indices of selected minerals for mixtures of formation water and injection waters, Basal Cambrian aquifer .....	14
Figure 4	Saturation indices of selected minerals for mixtures of formation water and injection waters, Cooking Lake aquifer .....	15
Figure 5	Saturation indices of selected minerals for mixtures of formation water and injection waters, McMurray aquifer .....	17
Figure 6	Saturation indices of selected minerals for mixtures of formation water and injection waters, Clearwater aquifer .....	19
Figure 7	Saturation indices of selected minerals for mixtures of formation water and injection waters, Mannville aquifer .....	21

Figure 8	Total volume of minerals precipitated/dissolved per litre of injected fluid as a function of time	23
Figure 9	Variation of fracturing gradient with depth	24
Figure 10	Example of acoustic and density logs	28
Figure 11	Finite element grid used for sensitivity analysis	33
Figure 12	Computed freshwater potentiometric surface for the Basal Cambrian aquifer	34
Figure 13	Model areas for simulation of effects of injection in the Lower Paleozoic aquifer system and the post-Prairie succession	36
Figure 14	Predicted increase in hydraulic head at the four injection sites in the Basal Cambrian aquifer, assuming regional hydraulic parameters	38
Figure 15	Predicted spread of the pressure buildup at the top of the Basal Red Beds, Basal Cambrian aquifer and Precambrian	38
Figure 16	Predicted increase in hydraulic head at the four injection sites in the Basal Cambrian aquifer, assuming high values for hydraulic parameters	39
Figure 17	Predicted spread of pressure buildup at the top of the Basal Cambrian aquifer	40
Figure 18	Predicted increase in hydraulic head at injection sites in the Mannville aquifer (Grand Rapids and Lower Grand Rapids)	41
Figure 19	Predicted increase in hydraulic head at injection sites in the Mannville aquifer (Rex Member and Lloydminster Formation)	42
Figure 20	Predicted increase in hydraulic head at injection sites in the Clearwater aquifer	43
Figure 21	Predicted increase in hydraulic head at injection sites in the Clearwater and Mannville aquifers	44
Figure 22	Predicted increase in hydraulic head at injection sites close to the pre-Cretaceous unconformity	45
Figure 23	Predicted increase in hydraulic head at injection sites in the Beaverhill Lake aquifer system	46
Figure 24	Predicted spread of hydraulic head buildup as a result of injection in Mannville, Clearwater, and McMurray aquifers	47
Figure 25	Finite element grids used for local simulation of the effects of injection	48
Figure 26	Predicted effects of injection in Lower Paleozoic aquifers at Dome and BP sites	51
Figure 27	Predicted effects of injection in post-Prairie aquifers at Dome and BP sites	51
Figure 28	Predicted increase in hydraulic head at Suncor sites	52
Figure 29	Predicted spread of hydraulic head buildup at Suncor sites	52
Figure 30	Predicted increases in hydraulic head at Murphy site	52
Figure 31	Predicted spread of hydraulic head buildup at Murphy site	52
Figure 32	Predicted effects of injection at Westmin site	53

## Tables

Table 1	Projected injection rates for the period 1985-2015	2
Table 2	Characteristics of the main aquifers	5
Table 3	Chemical composition, physical properties, and production data for formation waters from injection aquifers	7
Table 4	Comparison of major components in formation waters from the Basal Cambrian aquifer	8
Table 5	Comparison of major components in formation waters from the Beaverhill Lake aquifer system	8
Table 6	Comparison of major components in formation waters from the McMurray aquifer	8
Table 7	Comparison of major components in formation waters from the Clearwater aquifer	10
Table 8	Bulk mineral composition of the Beaverhill Lake Group	10
Table 9	Adjustments made to the formation water analyses to account for missing values for Al and SiO <sub>2</sub> , and loss of CO <sub>2</sub>	12
Table 10	Variation of tensile strength with lithology	25
Table 11	Geomechanical parameters suggested by Dusseault and Simons (1982)	27
Table 12	Estimation of Poisson's ratio for rocks at selected injection sites	29
Table 13	Estimation of overburden stress at selected injection sites	29
Table 14	Estimation of breakdown pressures for rocks at selected injection sites	30
Table 15	Characteristics and results of numerical simulations of the natural steady state flow in three regional model areas in the post-Prairie injection succession	37

Table 16	Regional estimates of hydraulic parameters .....	39
Table 17	Computed increases in hydraulic heads at the four injection sites in the Basal Cambrian aquifer .....	40
Table 18	Local versus regional values of hydraulic parameters used in simulations of the effects of injection .....	46
Table 19	Characteristics of the finite element grids and CPU time used for local simulations of deep waste disposal at selected sites .....	50



## Abstract

*The regional and local effects of underground injection of wastewater from in situ oil sands pilot plants have been evaluated at sites in the Cold Lake area, Alberta, using projected injection rates up to the year 2015. Geochemical effects were investigated in a suite of cases representative of the injection aquifers and conditions of injection in the Cold Lake Oil Sand Deposit. Although water-rock reactions will take place between the injected fluid, formation waters and minerals in the injection aquifer, only those reactions involving quartz and calcite are significant. Based on calculations of the amounts of these minerals precipitated or dissolved, the most important change that should be made to wastewater before injection is softening or the removal of carbon dioxide.*

*Fracturing thresholds were evaluated at several sites, based on the geomechanical properties of the rocks. The regional effects of deep waste disposal were simulated on a*

*large scale in terms of pressure buildups at 27 sites. Under the assumption that average values of the hydraulic parameters characterize the hydrostratigraphic succession, the numerical simulations revealed no interferences between the different injection sites for the projected duration of operations. The results of regional scale simulations allowed for the individual treatment of each injection site. Local scale simulations were performed for the same sites as were the evaluations of geochemical effects and fracturing thresholds. The results show that vertical fracturing will occur close to the respective injection well at some sites, but overlying strata are expected to prevent fracture propagation to the top of the bedrock. As a general conclusion, the effects of deep injection of wastewaters in the Cold Lake area are felt only in the area adjacent to the injection wells.*

## Introduction

The Western Canada Sedimentary Basin is very rich in hydrocarbons, with huge deposits of oil sands and heavy oil in Alberta. In the Cold Lake area, the oil sand deposits are found in the Lower Cretaceous Mannville Group at depths of a few hundred metres. Because the semi-solid bitumen does not flow freely at reservoir temperature (viscosities in excess of 10.4 Pa·s) the crude bitumen is extracted using in situ enhanced oil recovery (EOR) methods, generally based on steam injection. Following recovery of the bitumen and surface treatment of the entrained water, the resulting residual wastewaters are disposed of by injecting them into deep aquifers. In order to assess the impact of deep waste disposal on the subsurface environment, the Alberta Research Council and Alberta Environment undertook a study of the effects of deep waste disposal in the Cold Lake area. Because the primary concerns and approach to the problem were the same for both organizations, it was agreed to fund the initial and subsequent studies equally. The Cold Lake area includes pilot and commercial operations in all major oil sand and heavy oil occurrences. Most of the pilot and commercial operations either practice deep waste disposal or predict the need for deep waste disposal in the future. Accordingly, the study area was made large enough to ensure both adequate representation of the natural steady state hydrogeological regime and to eliminate artificial boundary effects in the areas selected for numerical simulation of deep waste injection.

A comprehensive study of the hydrogeology of a region defined as Tp 50-70, R 15 W3M - R 17 W4M

(60 000 km<sup>2</sup>) was carried out and the results compiled in three contract reports (Basin Analysis Group 1985, 1987, 1988) and an Alberta Research Council bulletin (Hitchon et al. 1989). The present bulletin is concerned with the regional and local effects of deep injection of residual wastewaters from the oil sands and heavy oil pilot plants in the Cold Lake-Lindberg area. Specifically, these effects relate (1) to potential water-rock interactions as they may affect permeability due to mineral precipitation or dissolution, (2) to the onset of induced fractures during sustained injection of liquid wastes, and (3) to the pressure buildup adjacent to the injection well.

The geochemical effects of deep waste disposal in the Cold Lake area are presented first, in order to evaluate possible changes in the porosity of the host aquifer as a result of mineral precipitation/dissolution. Significant changes in porosity affect the hydraulic characteristics (permeability, specific storage) of the aquifer, thereby influencing the pressure buildups resulting from injection. Given that deep waste disposal is generally a safe operation, except for possible vertical migration of wastewater through conduits such as fractures in the confining formations, it is important to know the stage at which fracturing will be initiated during the injection process. Thus, an evaluation of fracturing thresholds for rocks at sites in the Cold Lake area is presented before the numerical simulations of hydraulic head (pressure) buildups.

The regional effects of deep waste disposal were evaluated at 27 injection sites in the area in terms of hydraulic head buildups only. Local effects were



evaluated in terms of water-rock interactions and hydraulic head buildups at a limited number of sites. These sites were chosen based on the representativeness of the injection aquifer with respect to stratigraphy (Basal Cambrian, Cooking Lake, McMurray, Clearwater, and Grand Rapids aquifers), areal distribution of wells injecting into these aquifers, data availability, and when appropriate, proximity to injection sites.

Based on all these studies, it is concluded that the injection of wastewaters in the Cold Lake area has only limited local effects near the injection wells. This bulletin is presented in three sections: geochemical effects, evaluation of fracturing thresholds, and simulation of hydraulic head buildups for the projected period of 30 a.

## Baseline conditions

The Cold Lake study area is defined in terms of the Dominion Land Survey coordinates as Tp 50-70, R 15 W3M - R 17 W4M (figure 1a). The area includes 27 pilot and commercial operations in all major oil sand and heavy oil occurrences, which either practice deep waste disposal or predict the need for it in the future. Table 1 presents the location and projected rates of injection at the sites considered in this study, based on information compiled by the Planning Division of Alberta Environment. The main sources of information for defining the baseline conditions in the Phanerozoic succession in the Cold Lake area were the well data files of the Energy Resources Conservation Board (ERCB) and Saskatchewan Energy and Mines. Ap-

proximately 14 800 wells have been drilled in the area, but they are very unevenly distributed. Variations in the amount and distribution of data throughout the stratigraphic column reflect the distribution of oil and gas reservoirs. In general, the amount of data increases dramatically for formations within the Cretaceous, where most of the major oil and gas discoveries have been made.

Given that a great wealth of data exists concerning the subsurface environment, the examination and processing of the information was carried out using an automatic system for data management and data processing. This system was integrated in such a way as to provide the synthesized information required by

**Table 1.** Projected injection rates for the period 1985-2015 at deep well disposal sites in the Cold Lake study area, Alberta.

Operator	Field/Area	Location	Stratigraphic unit	Depth below KB (m)	Injection rate (m <sup>3</sup> /d)		
					Realistic 1985-1995	High 1995-2005	High 2005-2015
1 Amoco	Lindberg	09-28-55-06-W4M	Lloydminster	560	5081	12477	0
2 Bow Valley	Marie Lake	01-14-65-02-W4M	McMurray	550	1199	1499	1499
3 BP 80%	Wolf Lake	08-07-66-05-W4M	Grand Rapids	430	12887	20530	31530
4 BP 20%	Wolf Lake	10-08-66-05-W4M	Cambrian	1325	3335	5132	7883
5 Can. Occidental	Manatokan	10-12-63-08-W4M	Cooking Lake	495	1714	9487	8696
6 Can. Occidental	Lindberg	05-18-58-04-W4M	Cooking Lake	610	2637	2293	0
7 Can. Worldwide	Muriel Lake	10-16-59-04-W4M	Cummings	505	263	2847	0
8 Dome 25%	Lindberg	00-18-55-05-W4M	Rex Sand	530	1287	1287	0
9 Dome 25%	Lindberg	00-30-55-05-W4M	Rex	550	1287	1287	0
10 Dome 25%	Lindberg	00-10-56-06-W4M	Rex Member	565	1287	1287	0
11 Dome 25%	Lindberg	00-10-56-06-W4M	Cooking Lake	680	1287	1287	0
12 Dome 55%	Primrose	10-05-67-04-W4M	Cambrian	1310	3587	7173	7173
13 Dome 45%	Primrose	10-05-67-04-W4M	McMurray	540	2934	5868	5868
14 Drummond	Ardmore	13-20-62-03-W4M	Mannville C	405	723	1449	1449
15 Esso 55%	May-Ethel	08-33-64-03-W4M	Cambrian	1290	14910	12834	13328
16 Esso 45%	May-Ethel	04-17-65-03-W4M	McMurray	520	12197	10501	10905
17 Husky	Tucker Lake	13-20-64-04-W4M	McMurray	540	1311	1312	1482
18 Koch	Fort Kent	06-19-61-04-W4M	Clearwater	570	1125	1670	1287
19 Mobil	Wolf Lake (2)	06-11-64-06-W4M	Clearwater	440	252	6995	6995
20 Murphy 75%	Lindberg	05-13-58-05-W4M	L. Grand Rapids	510	1431	2324	1772
21 Murphy 25%	Lindberg	05-13-58-05-W4M	Cooking Lake	600	477	775	591
22 PanCanadian	Lindberg	10-09-56-06-W4M	Lloydminster	560	602	602	0
23 Suncor 55%	Fort Kent	05-28-61-04-W4M	Clearwater	450	923	2211	786
24 Suncor 45%	Fort Kent	00-28-61-04-W4M	Cummings	450	755	1809	643
25 Suncor	Primrose	07-14-67-03-W4M	Cambrian	?	3521	16354	16354
26 Westmin 75%	Lindberg	11-01-55-05-W4M	Lloydminster	530	1809	7602	7617
27 Westmin 25%	Lindberg	03-13-55-06-W4M	Cooking Lake	680	609	2534	2539

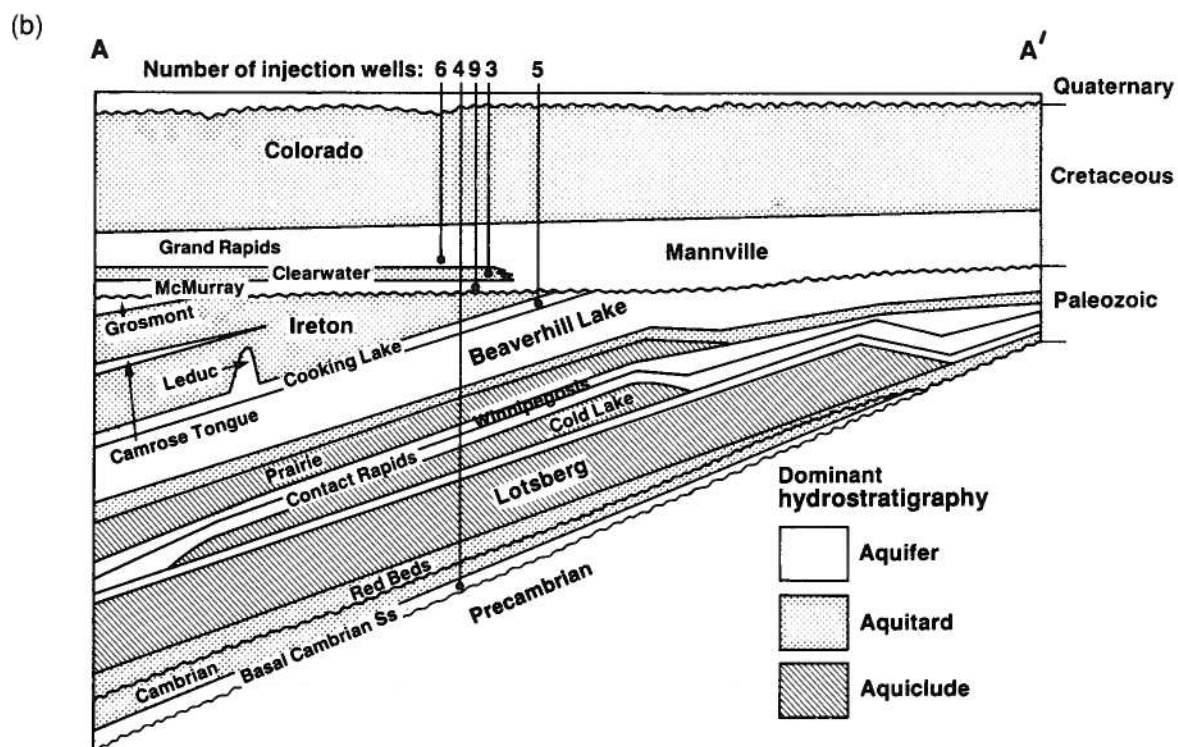
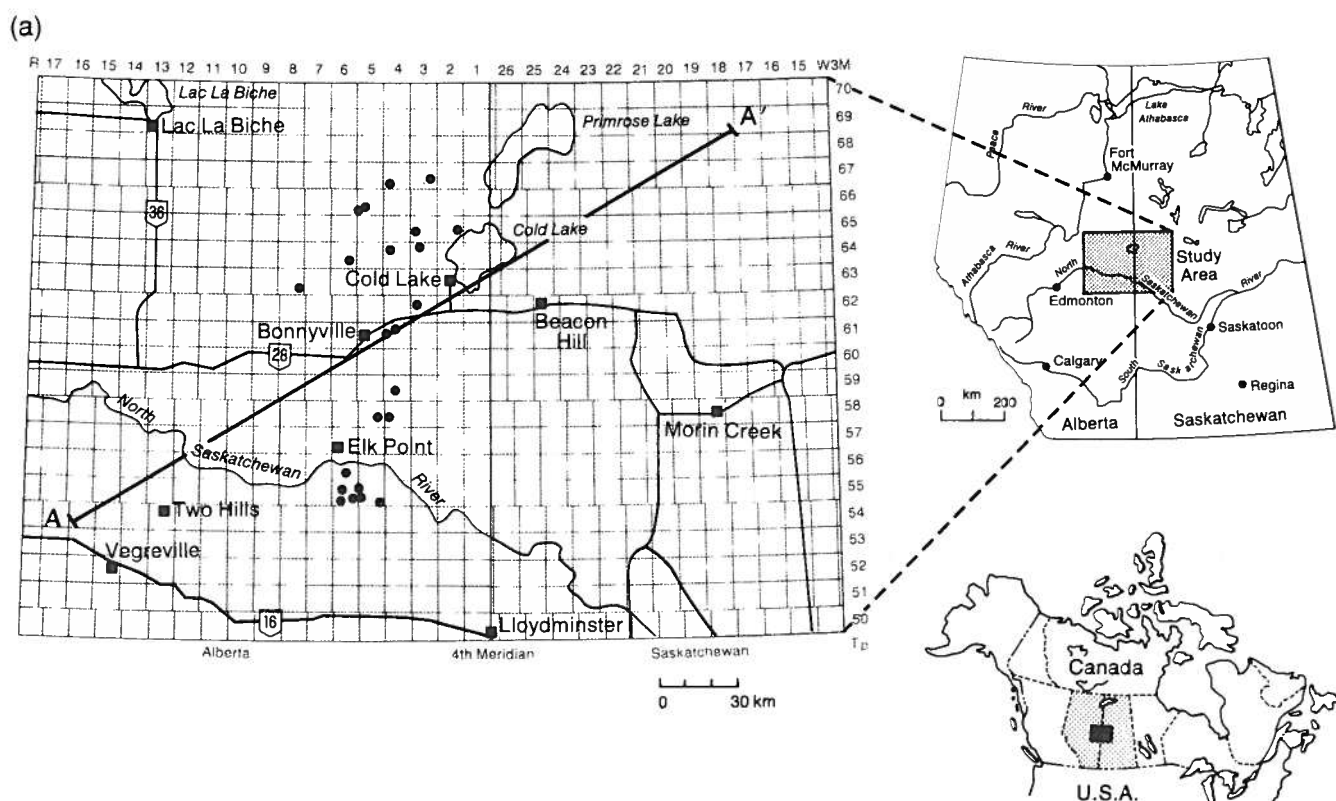


**Figure 1.** (a) Location of injection sites (•) in the Cold Lake area; (b) schematic representation of the position of injection wells in the hydrostratigraphic sequence.

the geochemical and numerical models used to study the effects of injection. The data used in the study include stratigraphic picks, chemical analyses of formation waters (1858), core analyses (46 700) and drillstem tests (2155). The criteria for data selection and error detection, and the methods and techniques used for data processing are described in Bachu et al. (1987).

All important hydrostratigraphic units were characterized by their position, geometry (isopachs) and hydraulic parameters, and the chemistry and hydrodynamics of the formation waters. In the following section of this bulletin, the regional geology and the baseline hydrogeological regime are briefly presented in order to provide the necessary framework for evaluating the effects of injection. A more detailed analysis of the natural hydrogeological and geothermal regimes in the area is given elsewhere (Hitchon et al. 1989).

## Regional geology

The Western Canada Sedimentary Basin is a westward thickening wedge of sedimentary strata which extends southwest from a zero edge at the Canadian Shield outcrop to a maximum thickness of about 6 km at the front of the Cordilleran Thrust and Fold Belt. Regional dips are between 5 and 10 m/km. The initial platform phase of the basin involved transgressive onlap of the Precambrian crystalline basement and coincides with deposition of Paleozoic sediments dominated by shallow water carbonates and evaporites. During the Late Jurassic to Paleocene interval, the continental terrace wedge was compressed, detached from its basement, and thrust over the flank of the craton to form the present eastern part of the Cordillera. This initiated the development of a foreland basin filled with Cretaceous and Tertiary clastic detritus (Porter et al. 1982). Figure 1b presents a diagrammatic dip cross section through the strata in the Cold Lake area.

As a result of Early Devonian erosion, the only Lower Paleozoic rocks found in the Cold Lake region are a succession of Middle and Upper Cambrian clastics. Epeirogenic uplift of the Peace River Arch in northern Alberta during Early Devonian time created a basin between the arch and the Meadow Lake Escarpment just south of the study area. This basin was completely filled with a series of massive halite beds (Lotsberg and Cold Lake Formations) and associated red mudstones during the Lower Devonian. The overlying Middle Devonian Winnipegosis and Contact Rapids Formations include fringing carbonate banks, patch reefs, and thin carbonate beds laid down under open marine conditions, which are commonly highly dolomitized. Overlying them are the thick salt beds of the Middle Devonian Prairie Formation which are ab-

sent in the northeast part of the study area as a result of salt dissolution.

The Middle/Upper Devonian Beaverhill Lake Group is mainly composed of interbedded carbonates and shale, with some dolomitization. The overlying platform deposits of the Upper Devonian Cooking Lake Formation are limestones, which are partially overlaid in the west by shales of the Ireton Formation. In the northwestern part of the study area, correlative with the Ireton Formation, is the Grosmont Formation, a complex series of carbonates and locally developed evaporites. The dominantly dolomitic Upper Devonian Winterburn Group is present only along the western boundary. Although Lower Carboniferous strata were once present, they were removed by late Paleozoic to early Mesozoic erosion. During Late Carboniferous, Permian, Triassic, and Jurassic times the region was an area of non-deposition. Consequently, all the Devonian rock units are truncated as a result of pre-Cretaceous erosion.

Throughout the Cretaceous there was continuous deposition of clastic sediments. The arenaceous Lower Cretaceous McMurray Formation includes onlap-offlap features and contains the oil sand deposits. It is separated from the overlying arenaceous Grand Rapids Formation by the Clearwater Formation which consists of shales and sandstones thinning toward the southeast. The McMurray, Clearwater, and Grand Rapids Formations comprise the Mannville Group, where most of the oil sand and oil and gas reserves are found. The Mannville Group is overlaid by the Colorado Group (Lower/Upper Cretaceous) which is mainly composed of shales with thin sandstones, such as the Viking Formation which wedges out toward the northeast. Shaley Upper Colorado and Lea Park strata form the bedrock beneath glacial deposits.

The top of the bedrock has an average elevation of about 540 m, with a few deep, easterly oriented channels. Quaternary sediments are very heterogeneous in nature (till, silt, and gravel).

## Regional hydrogeology

The hydrostratigraphy of the sedimentary block was first defined on the basis of the geometry and lithology of the formations. Subsequent analysis of the hydrogeological data led to grouping of individual units into ten aquifer systems, five aquitards, and two aquicludes situated between the crystalline Precambrian basement and the top of the bedrock. The main regional characteristics of the aquifer systems are presented in table 2.

The subcrop edge of the Basal Cambrian sandstone is close to the northern boundary of the study area throughout most of the region. The aquifer has a thickness of more than 150 m in the southeast corner and 75-100 m along the southern boundary. The formation

**Table 2.** Characteristics of the main aquifers in the Cold Lake area, Alberta.

Aquifer	Average thickness (m)	Average density of formation waters (kg/m <sup>3</sup> )	Average temperature (°C)	Average porosity	Regional hydraulic conductivity (m/d)	Specific storage (m <sup>-1</sup> )
Mannville	188	1007	23	0.24	0.035	0.0050
Clearwater	18	1005	23	0.27	0.037	0.0008
McMurray	60	1006	24	0.24	0.027	0.0080
Upper Devonian	38	1010	28	0.13	0.020	0.0006
Beaverhill Lake	303	1033	28	0.10	0.003	0.0004
Winnipegosis	112	1093	32	0.04	0.011	0.0007
Basal Cambrian	71	1160	40	0.23	0.043	0.0003

waters in the Basal Cambrian aquifer are very saline (240 000-310 000 mg/L total dissolved solids [TDS]), with relatively low contents of Ca and Mg, and high contents of SO<sub>4</sub>. These features suggest that the solutes are derived from evaporites, a suggestion consistent with the presence of overlying Devonian halite beds and a decrease of the salinity corresponding with the SW-NE flow of the formation waters. The Basal Cambrian aquifer is isolated from any other aquifers because of the presence above it of the Cambrian aquitard and the Lower Devonian aquiclude system.

Middle and Upper Cambrian strata (100-250 m) are generally composed of thin intercalations of sandstone and shale, basically forming a weak aquitard above the Basal Cambrian aquifer. Salinities are similar to those in the aquifer below. The Red Beds aquitard which overlies Cambrian strata is formed of Lower Devonian rocks of evaporitic-clastic origin. The massive Lotsberg and Cold Lake halite beds form the thick (up to 375 m) Lower Devonian aquiclude system which covers most of the area.

The Contact Rapids and Winnipegosis Formations are in hydraulic continuity, forming the Winnipegosis aquifer system. Salinity decreases northeastward from about 295 000 mg/L to 55 000 mg/L, with corresponding decreases in Cl, Ca, and Mg, while HCO<sub>3</sub> shows an opposite trend. These findings are consistent with an origin of the dissolved components from the dissolution of halite and anhydrite in the overlying Prairie Formation.

The Prairie Formation halite and anhydrite overlie the Winnipegosis aquifer system in the western two-thirds of the study area. Along its eastern margin, extensive salt dissolution has taken place. In areas not subjected to dissolution by meteoric water, this aquiclude is 120-160 m thick.

The stratigraphic position and hydraulic continuity of the carbonates of the Beaverhill Lake Group, and the Cooking Lake and Leduc Formations, justifies their grouping into the Beaverhill Lake aquifer system. In the western third of the study area, where this aquifer system has been preserved from erosion beneath the Ireton aquitard, thicknesses range from about 300 m to more than 500 m. East of the limit of the Ireton aquitard, as little as 100 m remains in the Cold Lake area because of erosion at the pre-Cretaceous uncon-

formity. Here, this aquifer system is in hydraulic continuity with the overlying McMurray and Mannville aquifers. The salinity decreases, structurally updip and hydraulically downflow, from more than 150 000 mg/L in the southwest to 20 000 mg/L in the northeast. The distributions of Cl, Ca, and Mg are consistent with the generally eastward flow direction. The trends for HCO<sub>3</sub> and SO<sub>4</sub> (as well as Na and Cl) are probably related to solution of evaporites from the underlying Prairie aquiclude. Accompanying this is dilution of the formation waters as they move updip from below the protective cover of the Ireton aquitard into regions with direct hydraulic connection with the fresher waters of the McMurray and Mannville aquifers.

The argillaceous lime mudstones of the Ireton Formation occur only in the western third of the area and along part of the southern boundary because of erosion at the top of the Paleozoic. Maximum thickness of this aquitard is about 250 m. The Camrose Tongue aquifer in the southwest corner of the Cold Lake area is a thin (less than 10 m) dolomite layer within the thick Ireton aquitard. The Grosmont aquifer in the northwest corner of the area is a dolomitized platform carbonate which is of approximately the same age as the Ireton Formation. The Upper Devonian carbonates of the Winterburn Group form an eroded remnant along the western boundary of the Cold Lake area.

The McMurray aquifer of the Lower Cretaceous succession is present in the northwestern half of the Cold Lake area, being defined by the presence of Clearwater shales above it. From west to east it rests on the Upper Devonian-Grosmont aquifer system, the Ireton aquitard, and the Beaverhill Lake aquifer system. The fluid flow in this aquifer is dominated by the underlying Grosmont aquifer, all the lateral flow being focused toward the area of overlap between the two aquifers. The salinities of formation waters in this aquifer decrease northward (from 100 000 mg/L to 60 000 mg/L), with corresponding decreases in Cl, Ca, and Mg.

The thin (35 m, on average) arenaceous unit within the Clearwater Formation is defined as the Clearwater aquifer. It is under- and overlaid by thin (up to 10 m) shales of the Clearwater Formation which form two aquitards, separating this aquifer from the McMurray

and Mannville aquifers. The lateral flow and the composition of formation waters in this aquifer are similar to those of the McMurray aquifer indicating that the intervening lower Clearwater shale is a weak aquitard.

The Mannville aquifer includes seven oil sand layers which generally act as weak, local aquitards. The lateral flow is weak. Salinity decreases from more than 60 000 mg/L in the southwest to less than 10 000 mg/L in the northeast, with corresponding decreases

in Cl, Ca, and Mg, and increases in  $\text{HCO}_3$ . The Mannville aquifer is overlaid by the thick (up to 700 m) Colorado aquitard system which is composed of shaley strata interbedded with thin sandstones, such as the Viking and the St. Walburg sandstones. Above it, there are shallow Quaternary channel aquifers which are characterized by hydraulic conductivities four orders of magnitude higher than in the aquifers in the Phanerozoic.

## Water-rock interactions

The geochemical effects of deep waste disposal are important on a local scale because of the potential for mineral precipitation or dissolution as a result of water-rock interactions between the injected waters and the formation fluids and rocks. The hydraulic characteristics of the rocks around the injection zone may be modified because of these geochemical effects, thus influencing the movement of injected water and the pressure buildup during the lifetime of the operation. The potential for mineral precipitation and dissolution can be determined by a variety of techniques. These range from laboratory experiments on representative cores using actual injection waters to computer codes designed to determine individual mineral saturations for given mixtures of injection and formation waters. The latter route was chosen in this study because the length of time (months to tens of years) necessary to determine low temperature water-rock interactions experimentally precluded a laboratory approach.

Water-rock interaction computer codes generally require complete analyses of both the injection water and the formation water. Knowledge of the mineralogy of the injection aquifer is also needed. Most are designed to calculate reactions under equilibrium conditions; kinetic effects are usually not evaluated. However, based on knowledge of the rates of reaction for some mineral transformations, the possibility of mineral precipitation or dissolution taking place can be inferred.

With respect to the evaluation of water-rock interactions during deep waste injection in the Cold Lake region, there were three major limiting factors: (1) the lack of complete analyses of formation waters at any of the injection sites; (2) restricted information on the composition of the injected waters, which varies as in situ recovery processes change; and (3) limited data on the mineralogy of the injection aquifers at the injection sites. Each of these limiting factors was addressed and evaluated prior to the determination of potential reactions resulting from injection.

The computer code SOLMINEQ.88 (Kharaka et al. 1988) requires detailed analyses of the waters under investigation, specifically formation and injected

waters, if interactions between the injected waters and the disposal aquifer (rock matrix plus formation water) are to be modelled. Information on the composition of the injected waters is given by Gunter et al. (1986); in general, the composition of these waters can be approximated by calculating the water composition which is in equilibrium with the mineralogy of the appropriate oil sand formation at in situ conditions. The mineralogy of the rock matrix of selected aquifers is provided elsewhere in this bulletin. All formation water analyses used in the regional evaluation of the hydrogeology of the Cold Lake area originated from the files of the ERCB. The limitations of these analyses are described by Hitchon et al. (1987) and the methods of data processing by Bachu et al. (1987). None of these analyses is suitable for water-rock interaction studies, for a variety of reasons.

In the early 1970s, samples of about one thousand formation waters were collected across Alberta through a cooperative program with the ERCB. All were from drillstem tests of then currently drilled wells, and the produced formation waters were subsampled for the Alberta Research Council. In addition to selected major element determinations made by the ERCB, selected minor and trace elements were determined at the Alberta Research Council by a variety of techniques after filtering and preservation of the samples. Bearing in mind the vicissitudes of drillstem tests and the need for appropriate field procedures if reliable information on formation water composition is to be collected, it is believed that the data resulting from the cooperative program with the ERCB are reasonably representative of in situ formation water composition. They are certainly more representative than if conventional methods had been used, though not as representative as if some determinations had been made in the field and selected aliquots preserved for laboratory analysis. With this caveat in mind, the analysis file from the cooperative program was searched for data from the Cold Lake region. A selection was made of data from appropriate injection aquifers and areally as close as possible to the 27 injection sites in the model area.

provincial Upgrader site near Lloydminster, immediately south of the study area. With the permission of Husky Oil Operations Ltd., an analysis of formation water from the Basal Cambrian sandstone at Husky Lloyd SWD B12-30-49-27-W3M is given in table 3. The analysis from the Husky well is close to the regional averages for all components mapped (figure 2a, table 4). Comparison with the local averages for mapped components near the four injection sites (table 4) shows that the formation waters near the injection sites have lower salinities, and correspondingly lower contents of Cl, Ca, and Mg, but increased amounts of HCO<sub>3</sub>, and especially, SO<sub>4</sub>.

Detailed analyses of formation waters in the Beaverhill Lake aquifer system are not available for the Cold Lake study area. The geographically nearest detailed analysis is from the Skaro field, which produces oil from the Cooking Lake Formation at 9-29-57-19-W4M. This analysis is given in table 3 (from Hitchon et al. 1971). Injection sites for disposal into the Cooking Lake Formation of the Beaverhill Lake aquifer system lie in a general N-S line, with salinities of the formation waters ranging from less than 40 000 mg/L to nearly 125 000 mg/L (figure 2b, table 5). The corresponding values for other major components are given in table 5. From the point of view of modelling water-rock interactions, the two injection sites at Tp 56 R 6 and Tp 55 R 6 were selected for study because the extrapolated regional compositional trends in this area most closely compare to the analysis of formation water from the Skaro field.

Regional salinity gradients in the McMurray aquifer have an E-W orientation, with salinities decreasing from 60 000 mg/L in the south to 10 000 mg/L in the north. In the area of the four sites which have been designated for injection into the McMurray aquifer, the regional salinity is 20 000 mg/L (figure 2c). Because of the strong compositional gradients of the regional salinity pattern for formation waters in the McMurray aquifer in the Cold Lake area and the relative distribution of injection sites and locations of detailed formation water analyses (figure 2c), only one detailed analysis is comparable (table 6) to the regional salinity around the injection sites. The analysis of this sample (table 3) is used in the water-rock modelling study.

**Table 5.** Comparison of major components (mg/L) in formation waters from the Beaverhill Lake aquifer system.

	W13-RCA-765 9-29-57-19-W4M	Regional averages around injection sites		
		63-8	58-4/5	56-6,55-6
Salinity	161 205	40 000	75 000	125 000
Cl	99 900	20 000	50 000	75 000
Ca	8 440	1 000	2 500	6 000
Mg	2 980	500	1 250	2 000
HCO <sub>3</sub>	139	300	200	200
SO <sub>4</sub>	790	1 600	300	400
Density (kg/m <sup>3</sup> )	1 110	1 030	1 060	1 090

Three sites are designated for injection into the Clearwater aquifer (figure 2d). Four detailed analyses of formation waters are available for the Cold Lake area, but none are for areas close to the injection sites (figure 2d). However, comparison of the regional average composition of formation waters around the two groups of injection sites (table 7) with the detailed analysis of RCAH 51-275A (table 3) indicates that the latter is suitable for use in water-rock modelling studies.

More than 40 detailed analyses of formation waters from the Mannville aquifer are available for the Cold Lake study area (figure 2e). For the purpose of water-rock interaction modelling, one analysis (RCAH 1-875B, table 3) has been selected from the Lindberg area.

## Mineralogy of injection aquifers

The selected representative formation water analyses, while better than 'standard' formation water analyses, are nevertheless incomplete, lacking determinations for Al and SiO<sub>2</sub> in some cases. The analyses can be corrected and modified provided that the mineralogy of the injection aquifer is known and assuming that the formation waters are in equilibrium with the minerals in the aquifers. Formations currently undergoing diagenetic reactions are not in total equilibrium; however, the diagenetic reactions will buffer the water compositions. Often, the buffered values are near equilibrium values. The formation mineralogy has been determined for most of the aquifers in this study,

**Table 4.** Comparison of major components (mg/L) in formation waters from the Basal Cambrian aquifer.

	Husky Lloyd SWD B12-30-49-27-W3M	Regional average 50-27-W3M	Average around injection sites 66-4-W4M
Salinity	308 400	300 000	260 000
Cl	188 000	175 000	150 000
Ca	1 920	3 000	1 500
Mg	1 220	1 250	500
HCO <sub>3</sub>	80	150	260
SO <sub>4</sub>	3 180	2 000	6 000
Density (kg/m <sup>3</sup> )	1 286	1 190	1 165

**Table 6.** Comparison of major components (mg/L) in formation waters from the McMurray aquifer.

	RCAH 72-475A 11-12-67-16-W4M	Regional average 65-4
Salinity	29 306	20 000
Cl	16 900	12 000
Ca	450	200
Mg	222	100
HCO <sub>3</sub>	942	800
SO <sub>4</sub>	17	50
Density (kg/m <sup>3</sup> )	1 021	1 013

In the following sections of the bulletin each injection aquifer is considered in sequence, and if appropriate formation water analyses are available the analytical data are presented in table 3. The effects of incomplete analyses and the methods to correct them will be discussed later.

## Selection of representative formation waters

Detailed analyses of formation waters from the Basal Cambrian aquifer are not available for the Cold Lake study area. The Basin Analysis Group has carried out contract work for Husky Oil Operations Ltd. at their Bi-

**Table 3.** Chemical composition (mg/L), physical properties and production data for formation waters from injection aquifers, Cold Lake area, Alberta and Saskatchewan.

Sample number	—	W13-RCA-765	RCAH 72-475A	RCAH 51-275A	RCAH 1-875B
Stratigraphic unit	Basal Cambrian	Cooking Lake Fm.	McMurray Fm.	Clearwater Fm.	Glauconitic Ss.
Location	12-30-49-27-W3M	9-29-57-19-W4M	11-12-67-16-W4M	11-26-63-12-W4M	11-20-55-6-W4M
Depth (m)	1634-1685	1120.1-1122.0	534.6-538.3	527.9-530.4	615.7-629.7
Source	Injectivity test	Wellhead, perf.	DST 1	DST 5	DST 1
Recovery	—	Pumping	27.4 m sw, gas	163 m sw, 18.3 m	61 m sw, gas
	34.83 m <sup>3</sup> /d	muddy sw	29 534.5 m <sup>3</sup> /d		
Li	—	20	4.4	7.6	6.2
Na	112 645	47 100	10 600	10 900	19 000
K	1 289	840	90	117	84
Mg	1220	2980	222	322	975
Ca	1920	8440	450	484	1430
Sr	—	300	31	41	112
Ba	0.8	—	11	10	35
Cu	2.3	0.49	*	*	*
Ag	—	—	0.3	*	0.3
Zn	0.84	2.12	*	*	5.8
Pb	0.94	—	0.6	0.4	0.3
Fe	29	0.19	0.2	*	0.2
Mn	1.2	0.7	*	*	0.2
Al	—	—	*	0.01	*
H <sub>2</sub> AsO <sub>3</sub>	0.008	—	*	2	1.3
H <sub>3</sub> BO <sub>3</sub>	—	189	64	58	58
PO <sub>4</sub>	—	—	3.7	5.5	2.3
NH <sub>3</sub>	—	—	—	—	41
SiO <sub>2</sub>	29.7	—	8.9	14	2.9
F	—	—	1.1	1.7	0.13
Cl	188 000	99 900	16 900	20 600	35 500
Br	—	296	52	55	120
I	—	15	8	9	11
SO <sub>4</sub>	3 180	790	17	47	37
HCO <sub>3</sub>	80	139	942	760	220
Cations (anal., meq/L)					
(25°C)	5130.0	2766.3	505.6	529.9	982.8
Anions (anal., meq/L)					
(25°C)	5370.3	2836.5	492.7	594.8	1005.8
Cations (calc., meq/L)	4529.9 (30°C)	2568.1 (40°C)	491.3 (30°C)	513.7 (22.8°C)	948.9 (28.2°C)
Anions (calc., meq/L)	4741.5 (30°C)	2634.1 (40°C)	477.5 (30°C)	578.6 (22.8°C)	969.4 (28.2°C)
TDS (calc.)	308 399	161 205 (40°C)	29 306 (30°C)	33 385 (22.8°C)	57 500 (28.2°C)
TDS (110°C)	—	178 700	—	33 300	60 300
TDS (ignition)	—	153 600	—	31 580	55 370
pH (laboratory)	6.2 (25°C)	6.78 (25°C)	7.3 (25°C)	7.9 (20°C)	7.61 (25°C)
pH (calc.)	6.18 (30°C)	6.66 (40°C)	7.26 (30°C)	7.86 (22.8°C)	7.45 (28.2°C)
Density (kg/m <sup>3</sup> )	1286 (15°C)	1110 (25°C)	1021 (15.56°C)	1026 (15.56°C)	1035 (15.56°C)
Refractive index	1.373 (25°C)	1.3595 (25°C)	1.3372 (21°C)	1.3388 (25°C)	1.3430 (25°C)
Resistivity (ohm m) (25°C)	0.031	0.0551	0.241	0.195	—

- = not determined  
\* = below detection

sw = salt water

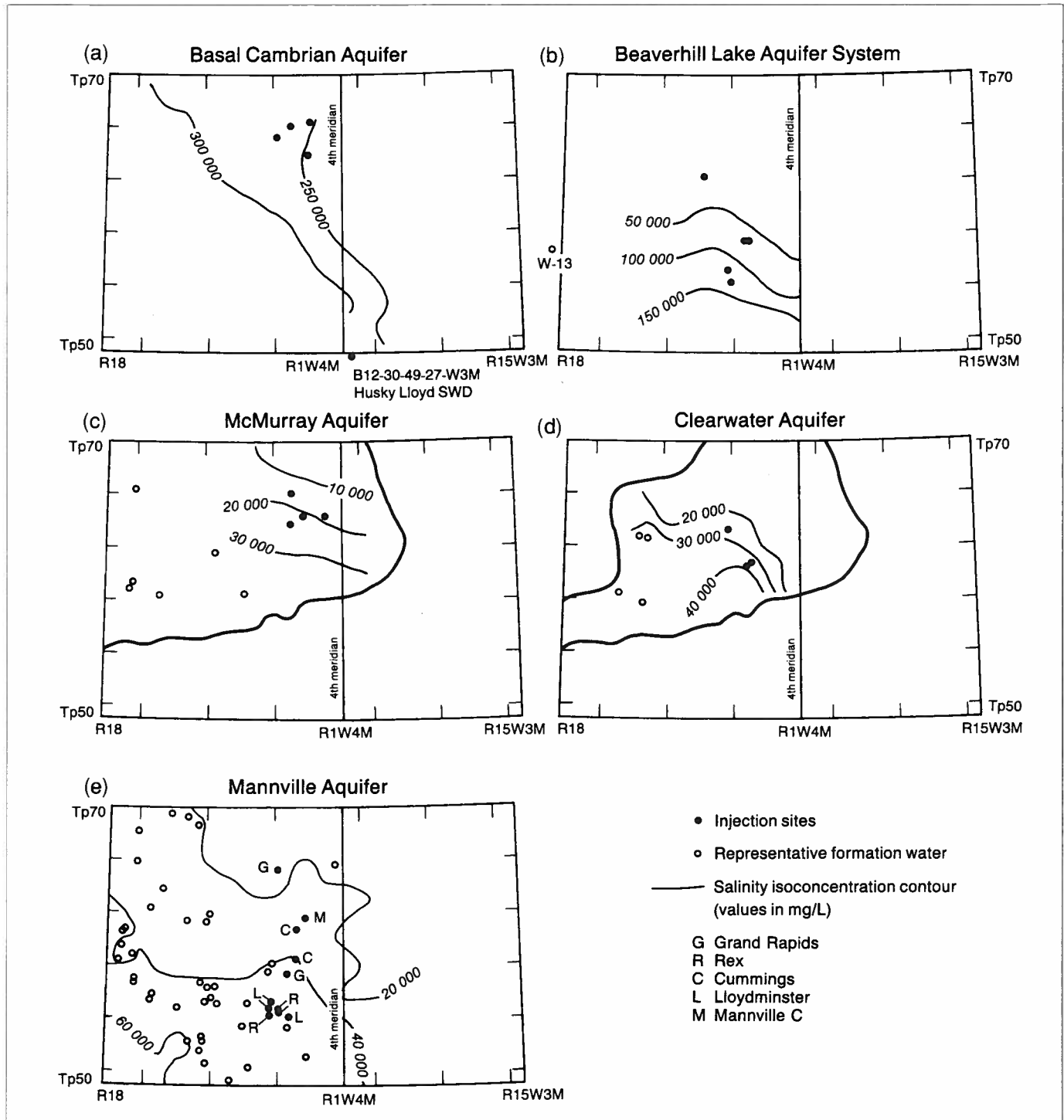


**Figure 2.** Injection sites, salinity isoconcentration contours (mg/L), and locations of representative formation waters for five injection aquifers in the Cold Lake area. (a) Basal Cambrian aquifer; (b) Beaverhill Lake aquifer system; (c) McMurray aquifer; (d) Clearwater aquifer; (e) Mannville aquifer.

but not for the Cooking Lake/Beaverhill Lake aquifer. Accordingly, a combination of X-ray diffraction (Co K-alpha radiation at 50 kV and 20 mA; scan rate 1 degree 2  $\theta$ /min; chart speed 500 mm/h), and visual and thin section examinations were made of selected cores from the Cooking Lake/Beaverhill Lake aquifer.

In general, the Basal Cambrian sandstones are fine- to coarse-grained, sub- to well-rounded, and poorly sorted (Pugh 1973; MacDonald 1987). Pebble beds and shaly laminae are common locally. Sedimentary features are often well developed, but many have been destroyed by bioturbation.



**Table 7.** Comparison of major components (mg/L) in formation waters from the Clearwater aquifer.

	RCAH 51-275A 11-26-63-12-W4M	Regional averages around injection sites	
		64-6	61-4
Salinity	33 385	27 000	35 000
Cl	20 600	16 000	21 000
Ca	484	400	700
Mg	322	200	100
HCO <sub>3</sub>	760	450	300
SO <sub>4</sub>	47	25	20
Density (kg/m <sup>3</sup> )	1 026	1 019	1 026

As of 1986, there were only seven wells with preserved core from the Basal Cambrian sandstones in the study area. As part of an M.Sc. project, MacDonald (1987) examined core from six wells and thin sections from five wells in the Basal Cambrian sandstone. The visual examination of core from Esso 83 SWD at Ethel Lake (11-22-64-3-W4M) for the interval between 1214.38 m and 1227.58 m indicated a poorly sorted dark red sandstone, intercalated with red and green shale. Bioturbation was rare. The interval between 1227.58 m and 1251.63 m consists of poorly sorted sandstones (green, yellow, and red) interbedded with 0.5-5 cm bands of red and green shales. Unfortunately, no thin section or X-ray work was performed on samples from this well.

The nearest well to Cold Lake that was examined by MacDonald (1987) was the Imperial Willingdon No. 1 well (14-14-55-15-W4M); thin sections from a depth of 1955.75 m indicated that the sample was composed of 94% quartz, 3% chlorite, 1% feldspar, and 1% kaolinite, with trace amounts of zircon and magnetite. Illite occurred as a minor pore-filling cement. Comparison of the results of these thin section examinations, X-ray diffractions, and core examinations indicates that there are only small differences in the

minerals present in small/trace amounts when compared to the Basal Cambrian sandstone elsewhere in the province (MacDonald 1987). The differences include the presence/absence of calcite, the presence/absence of anhydrite, the presence of dolomite (but not calcite) in one sample, and the replacement of magnetite by hematite.

Literature data on the mineralogical composition of the Cooking Lake and Beaverhill Lake Formations is sparse. The formations are generally described as 'carbonate rocks'. This information is insufficient for modelling purposes, and thus an X-ray diffraction (XRD) study of nine whole-rock samples was carried out. Three samples (at different depths) were taken from the BA Corbett site; four from the Arco Heart Lake site; and two from the Rothwell Frog Lake site. The samples were not chemically treated prior to XRD. Representative portions of the samples were ground to less than 20 µ and packed into aluminum sample holders. This procedure produces a randomly oriented distribution of particles in the sample. The mineralogical data are presented in table 8. These rocks are predominantly composed of calcite and dolomite, and contain between 1 and 30% quartz. No other phases are consistently present. Illite, kaolinite, and chlorite were the only clay minerals observed; smectite was not present. Pyrite, plagioclase, and potassium feldspar were also present in trace amounts.

The McMurray Formation is predominantly composed of quartz (93%), feldspar (5%), and minor chert/rock fragments (2%). Trace amounts of calcite, dolomite, siderite, pyrite, and clay minerals may be present, but only in small and variable amounts. When present, the dominant clay mineral is usually kaolinite (Mossop et al. 1981; James and Oliver 1977).

The Clearwater Formation is extremely complex and variable in its mineralogy. It is considered to be chemi-

**Table 8.** Bulk mineral composition (%) of the Beaverhill Lake Group, Cold Lake area.

Well name Depth (m)	Calcite	Dolomite	Quartz	Illite	Kaolinite	Chlorite	Plagioclase	K-feldspar	Pyrite
Rothwell Frog Lake (9-6-56-2-W4M)									
603.2	63	13	19	2	1	tr	tr	tr	1
605.0	98	-	2	-	-	-	-	-	-
BA Corbett (5-12-63-10-W4M)									
714.3	86	6	8	-	-	-	-	-	-
718.6	24	35	30	4	2	2	2	1	-
799.4	77	2	1	-	tr	-	-	-	-
Arco Heart Lake (11-26-69-10-W4M)									
647.6	86	3	11	tr	-	-	-	-	-
658.3	82	16	2	-	-	-	-	-	-
660.7	70	4	20	3	2	tr	tr	-	-
665.2	81	13	4	-	-	-	-	-	2

tr = trace

cally immature and still undergoing diagenesis. The grain-forming mineralogy of the Clearwater Formation in the Cold Lake area is composed of quartz (21%), feldspar (28%), volcanic rock fragments (23%), chert (20%), and other sedimentary and metamorphic rock fragments (8%). The fine fraction (approximately 1-5% locally, but it can be much higher) is composed of illite (43%), smectite (14%), mixed layer smectite/illite (12%), kaolinite (16%), and chlorite (15%) (Vissen et al. 1985; Harrison et al. 1981).

Mineralogically, the Grand Rapids Formation of the Mannville aquifer system is very similar to the Clearwater Formation, differing primarily in the modal amounts of the minerals. Rock fragments and chert account for much less of the total rock volume, with a corresponding increase in the modal amount of quartz. The dominant clay is kaolinite, although illite and smectite are present in significant amounts (Harrison et al. 1981). This formation is also currently undergoing diagenesis.

## Correction of formation water analyses

The selected formation water analyses are not complete; values for Al are missing for all but the sample from the Clearwater aquifer, and a value for dissolved silica is missing for the sample from the Cooking Lake aquifer. Various other cations and anions are missing in some of the analyses, but none is critical. None of the analyses measured the Eh or redox potential directly; thus, no computations involving any element with more than one redox state (Fe, Cu, etc.) can be made without a number of assumptions. In addition, all of the formation waters except that from the Basal Cambrian aquifer were supersaturated with respect to calcite. As discussed below, this indicates that the samples were not taken correctly and the molality of carbon dioxide in solution changed before they were analysed; this results in modified total inorganic carbon (TIC) and pH measurements.

When formation water analyses were not available for a specific injection site, analyses from the closest wells were used after correction of the major cation and anion values based on their regional trends. Many of the formation water analyses were missing values for total dissolved aluminum and silica; thus, these values had to be assumed. Because quartz was present in all of the formations, quartz saturation was used to calculate total dissolved silica. This assumes that quartz is in equilibrium with the aqueous phase and the pH is known; thus, the activity of the silica species in solution can be calculated by:

$$\begin{aligned}\log \bar{A}_1 &= \log a(\text{Qtz}) + \log a(w) - \log a(\text{H}_4\text{SiO}_4) \\ \log \bar{A}_2 &= \log a(\text{H}_4\text{SiO}_4) - \log a(\text{H}_3\text{SiO}_4^-) - \log a(\text{H}^+)\end{aligned}\quad (1)$$

where  $\log \bar{A}$  is the logarithm of the equilibrium constant for the subscripted equilibrium, and  $\log a$  is the logarithm of the activity subscripted phase (Qtz for quartz;  $\text{H}_4\text{SiO}_4$ ,  $\text{H}_3\text{SiO}_4^-$  aqueous silica species; w for water). By convention, the log activity of any pure, stoichiometric solid phase is zero, and the log activity of water (which is near zero) is obtained by iterative calculations. The activity of the aqueous silica species can then be directly obtained, and having calculated the activity coefficients (iteratively), the molality of these species in the aqueous phase can be calculated and summed to obtain total silica in solution. Although other minerals could be used to calculate silica in solution, those minerals present in the rocks all contain aluminum which is missing from the water analyses, hence they cannot be used.

In a similar fashion, by assuming that a clay mineral (kaolinite, smectite, or illite), when present, is in equilibrium with the formation water, in combination with quartz saturation, pH, and the analyses for some of the other cations, this allows total dissolved aluminum to be calculated. The following equations show some of the calculations which would be made if the clay mineral was a typical potassium-magnesium illite:

$$\begin{aligned}\log \bar{A}_3 &= \log a(\text{Ill}) + 8 \log a(\text{H}^+) + 2 \log a(w) \\ &\quad - 3.5 \log a(\text{H}_4\text{SiO}_4) - 0.6 \log a(\text{K}^+) \\ &\quad - 0.25 \log a(\text{Mg}^{++}) - 2.3 \log a(\text{Al}^{+++}) \\ \log \bar{A}_4 &= \log a(\text{Al}(\text{OH})_4^-) + 4 \log a(\text{H}^+) \\ &\quad - \log a(\text{Al}^{+++}) - 4 \log a(w) \\ \log \bar{A}_5 &= \log a(\text{Al}(\text{OH})_3) + 3 \log a(\text{H}^+) \\ &\quad - \log a(\text{Al}^{+++}) - 3 \log a(w) \\ \log \bar{A}_6 &= \log a(\text{Al}(\text{OH})_2^+) + 2 \log a(\text{H}^+) \\ &\quad - \log a(\text{Al}^{+++}) - 2 \log a(w) \\ \log \bar{A}_7 &= \log a(\text{Al}(\text{OH})_1^{++}) + \log a(\text{H}^+) \\ &\quad - \log a(\text{Al}^{+++}) - \log a(w)\end{aligned}\quad (2)$$

In addition to the previously calculated value for aqueous silica, values for the aqueous species of magnesium and potassium, pH, and the activity of water must be known (or obtained by iteration) for this calculation to be made.

Values calculated in this fashion must be considered approximate; they are thermodynamically consistent, they take into account all aqueous speciation, but they are the result of an equilibrium approach. Total silica may therefore be higher than the calculated equilibrium value using quartz because of the more rapid dissolution of other minerals (e.g. chalcedony) if present in quantity. In addition to the uncertainty as to whether the clay mineral is in equilibrium with the fluid, whether multiple clay minerals are present, or which specific clay mineral is in equilibrium

with the fluid, any change in the calculated values for the aqueous silica species will change total aluminum. The presence of feldspars, rock fragments, and chert fragments in several of the formations indicates that the rocks may still be actively undergoing diagenesis. When diagenetic reactions are occurring they may buffer any of the fluid components above or below their equilibrium value. In the absence of additional analytical information, these are the best assumptions that can be made and experience has shown that they are viable.

Many comprehensive studies have indicated that in any groundwater flow system in which calcite is present, the maximum that the water is supersaturated with respect to calcite is less than 0.1 SI units. If the saturation index (SI) of calcite is greater than this value, then CO<sub>2</sub> has been lost from the solution before the laboratory analysis. With the exception of the formation water from the Basal Cambrian aquifer, all of the formation waters are supersaturated with calcite. Carbon dioxide has presumably been lost from each sample of the formation waters before analysis. It is therefore necessary to 'add' CO<sub>2</sub> to the analysis until calcite saturation is reached.

The assumptions and compensatory calculations resulted in modified compositions of the formation waters. With the exception of pH which changed significantly for several waters, in general the changes were small. The largest change was for the formation water from the Cooking Lake Formation and resulted in the following: approximately 3 mg/L SiO<sub>2</sub> and 0.00002 mg/L Al were calculated to be in solution, given no analyses for either of these. The pH was changed to 6.35 from a value of 6.78, and TIC was

changed to 32.3 from 55.5 mg/L. All of the above modifications have been taken into account and the adjustments shown in table 9.

## Composition of injection waters

The composition of wastewater from an enhanced oil recovery operation is primarily dependent on the composition of the production water. However, it is also modified by treatment, length of storage time, temperature during storage, and by mixing with surface water/shallow aquifer water before disposal (to reduce the total dissolved solids). The composition of production water from enhanced oil recovery pilots is the result of the interaction of the injection water and steam with: the reservoir minerals, the formation water, the formation gases (if present), and the heavy oil/bitumen. For the purpose of modelling water-rock interactions, the initial composition is important, as are the formation temperature and pressure, the steam quality, and the length of time that the injection fluid has to react. It is clear that the composition of the produced water will vary significantly over a production cycle and that, in principle, all of the chemical reactions occurring during production could be inferred from this process.

Because of the variation in wastewater composition with respect to time, it is impossible to establish a typical composition for any given pilot. For this reason, approximately 20 different wastewaters from pilots in the Cold Lake area were used in the modelling. A number of the wastewater samples came from the same pilot but were measured at different times during the production cycle. For reasons of confidentiality, the wastewaters cannot be identified with specific pilots. Compositions are given by Gunter et al. (1986); pH values range from 1.7 to 9.0, and total dissolved solids from 1100 to 35 000 mg/L.

**Table 9.** Adjustments made to the formation water analyses in table 3 to account for missing values for Al and SiO<sub>2</sub>, and loss of CO<sub>2</sub>.

Stratigraphic unit	Component	Analysed value	Calculated value
Basal Cambrian sandstone	Al <sup>+3</sup>	—	0.00001
Cooking Lake Formation	Al <sup>+3</sup>	—	0.00001
	HCO <sub>3</sub> <sup>-1</sup>	139	80.9
	SiO <sub>2</sub> (aq)	—	3.0
	pH	6.78	6.35
McMurray Formation	Al <sup>+3</sup>	—	0.00001
	HCO <sub>3</sub> <sup>-1</sup>	942	722.3
	pH	7.3	6.51
Clearwater Formation	HCO <sub>3</sub> <sup>-1</sup>	760	785.7
	pH	7.9	6.54
Glaucconitic sandstone	Al <sup>+3</sup>	—	0.00001
	HCO <sub>3</sub> <sup>-1</sup>	220	228.2
	pH	7.61	6.72

## Calculation of potential water-rock interactions

Using the computer code SOLMINEQ.88 (Kharaka et al. 1988), each of the 20 wastewaters was mixed with the formation water from each of the aquifers, and the saturation index calculated for every mineral in the thermodynamic data base of SOLMINEQ.88 which can possibly be saturated. Plots were made of the SI values for minerals which are present in the aquifers or which were considered significant and of interest. The saturation index is a measure of the ability of a mineral to precipitate or dissolve. The SI is defined as the logarithm to the base ten of the ratio of the activity quotient for the hydrolysis reaction of a mineral to the equilibrium constant for the same reaction. If the SI is less than 0.0, the mineral (phase) should dissolve into

the fluid; if the SI is greater than 0.0, the phase should precipitate from the fluid; if the SI is 0.0, the phase is in equilibrium with the fluid. This calculation is strictly an equilibrium calculation. If the fluid is supersaturated with respect to a mineral, the mineral may not precipitate because of kinetic considerations. However, the greater the supersaturation, the more likely it is to precipitate.

The computer code SOLMINEQ.88 (Kharaka et al. 1988) was used to reduce all of the water analyses and to perform all of the geochemical modelling in this bulletin. SOLMINEQ.88 takes a water analysis and calculates the distribution of mass among all of the aqueous species in the water. The saturation indices and a number of other parameters are then calculated. SOLMINEQ.88 was then used to raise the temperature and pressure to that of the formation or injection condition, redistribute the mass among the aqueous species, and recalculate the saturation indices. Other options which can then be used (with or without a change in temperature and pressure) are to add or remove mass from the solution (in the form of arbitrary components, specified minerals, or gases); calculate volatile fractionation and partitioning into oil, water, and gas; boiling; adsorption; ion exchange; and the option most commonly used in this bulletin, the mixing of two waters (injection and formation) over the fraction of formation water from 0 to 1.

Because of the large number of wastewaters considered, individual mixing curves for each wastewater/formation water pair could not be plotted (figures 3-7). Instead, the area where all of the curves fall is shaded. If any of the curves are significantly different from the others, they have been plotted as a separate line or region. Individual curves which fall below the rest of the SI curves correspond to wastewaters which were formed from production waters in an early cyclic process.

All of the figures have the same abscissa, with values ranging from 0 to 1. A value of 0 indicates that the fluid composition used in calculating the SI values is that of the formation water, while a value of 1 indicates that the fluid composition is that of the wastewater. Data between 0 and 1 represent various mixtures of formation and wastewater. In all of the figures, the ordinate axis is the saturation index of the mineral; the range of ordinate values varies from figure to figure, but always includes a value of 0.0 because this value corresponds to saturation.

As will be discussed in more detail later, the waste injection fluids are production fluids from enhanced oil recovery pilots. They may have undergone some treatment, but their composition reflects the mineral reactions which occur in the formation at EOR temperatures and pressures (typically 100 to 300°C and pressures on or above the steam critical curve).

### Basal Cambrian aquifer

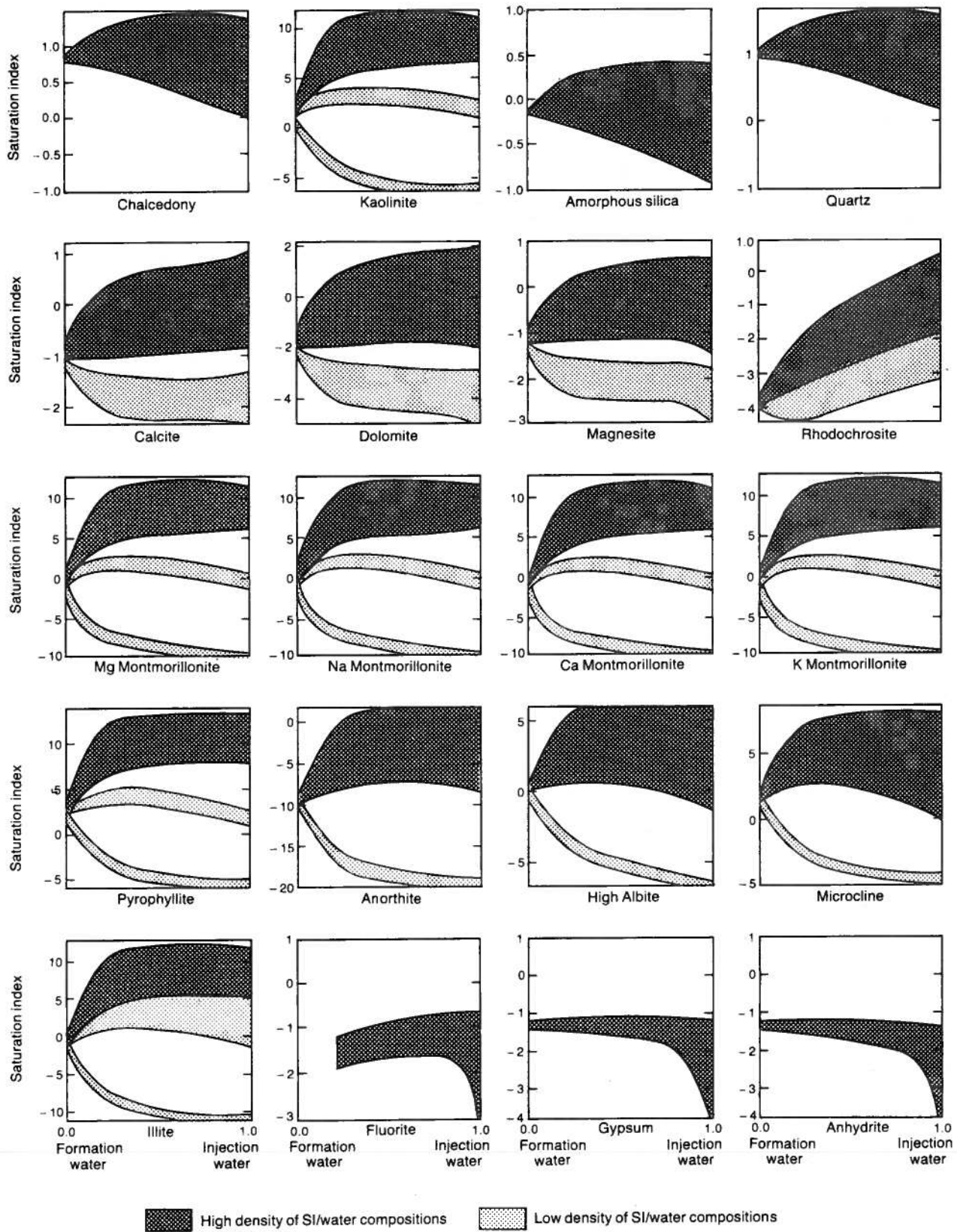
Figure 3 illustrates the effects of mixing the formation water from the Basal Cambrian aquifer with the various wastewaters.

The results can be summarized as follows. The formation water is supersaturated with quartz, with an SI of approximately 1. The injection waters and their mixtures with formation water have a range of SI values which vary from 0.8 SI units below that in the formation water to approximately 0.6 SI units above that in the formation water. The average value is therefore the same as or slightly above that for the formation water, but not significantly so. The SI values for the other silica phases (amorphous silica and chalcedony) are lower than that for quartz and the shapes of their SI curves are similar to that of quartz. Because the change in the SI for quartz is not extreme, in view of the assumptions made, quartz is not expected to precipitate in significant amounts. Formation waters are undersaturated with all of the carbonate minerals, but some of the wastewaters and their mixtures have SI values greater than zero for the carbonate minerals. The average SI value for all of the carbonates is less than zero; thus, in these waters precipitation of calcite should not be a problem. The sheet silicates and clays (kaolinite, illite, pyrophyllite, K-montmorillonite, Ca-montmorillonite, Na-montmorillonite, and Mg-montmorillonite) are all saturated (SI approximately equal to zero) in the formation water. In the wastewaters and their mixtures, the SI values of the sheet silicates and clays increase rapidly to a maximum of approximately 12. These are highly supersaturated and indicate that one or more of these phases will precipitate from solution. The SI values for the feldspars (plagioclase, microcline, and albite) increase as the proportion of wastewater increases; however, only albite and microcline are supersaturated. Because the feldspars share the same elements as the clay minerals, it is anticipated that the clay minerals will precipitate instead of them. Gypsum, anhydrite, and fluorite are undersaturated in the formation waters, wastewaters and their mixtures, and should not cause any problems.

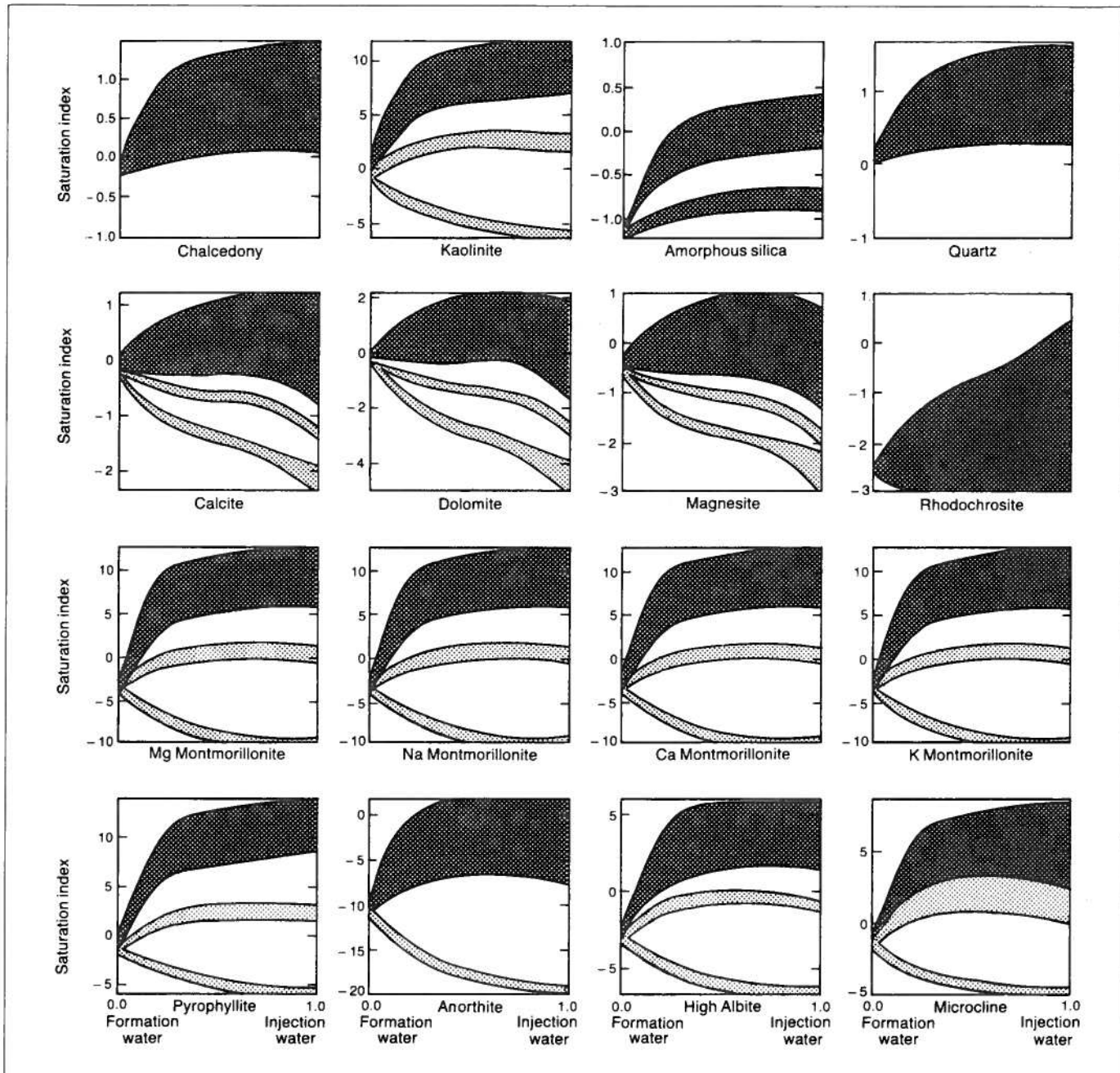
### Cooking Lake aquifer

Figure 4 illustrates the effects of mixing the formation water from the Cooking Lake aquifer with the various wastewaters.

The dominant mineral in the formation is calcite; thus, the SI values for all of the carbonate minerals are extremely important. The formation water is saturated with respect to calcite and dolomite. Some of the wastewaters and their mixtures are undersaturated with calcite and dolomite, but most are slightly saturated. An exception is the manganese carbonate, rhodochrosite, which is almost completely undersaturated. Trace amounts of Mn would be ex-



**Figure 3.** Saturation indices of selected minerals for mixtures of formation water and injection waters, Basal Cambrian aquifer.



**Figure 4.** Saturation indices of selected minerals for mixtures of formation water and injection waters, Cooking Lake aquifer.

pected in calcite, however. Dolomite has extremely slow kinetics when compared to calcite, and thus, if the solution is supersaturated with respect to the carbonate minerals, calcite (with minor amounts of Mg, Mn and probably Fe present in the structure) would precipitate from solution.

Quartz is the second most important mineral in the formation and it is assumed to be in equilibrium with the formation water. The wastewaters and their mixtures with the formation water are increasingly supersaturated with quartz, and in some wastewaters an SI value of approximately 1.3 is reached. The average trend is for SI values to increase; thus, in the Cooking

Lake aquifer, silica would be expected to precipitate from solution. The SI values for the other silica phases (amorphous silica and chalcedony) are lower than that for quartz, but the shapes of their SI curves are similar to the quartz SI curve.

The sheet silicates and clays (kaolinite, illite, pyrophyllite, K-montmorillonite, Ca-montmorillonite, Na-montmorillonite, and Mg-montmorillonite) are all undersaturated (SI less than zero) in the aquifer. In the wastewaters and their mixtures, their SI values increase by up to 12 units. These phases are highly supersaturated and certainly one or more will precipitate. The SI values of the feldspars (plagioclase,



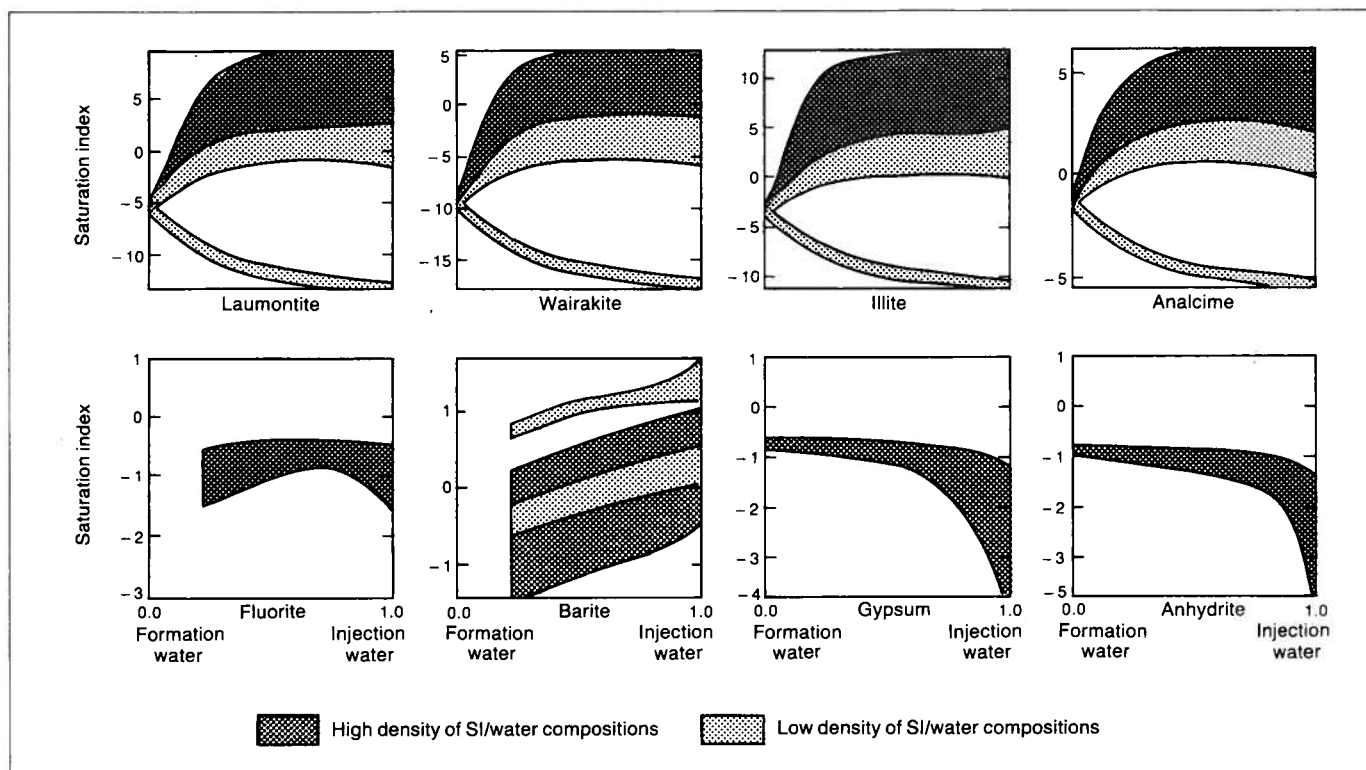


Figure 4. (continued)

microcline, and albite) are initially less than zero, but increase rapidly above zero as the proportion of wastewater increases (with the exception of plagioclase for which only a few of the solutions have SI values greater than zero). Only albite and microcline are supersaturated to any degree. Because the feldspars share common elements with the clays, and because clays precipitate much more rapidly from solution, it is anticipated that the clays will precipitate instead of the feldspars. The formation water, wastewaters, and their mixtures are undersaturated with respect to fluorite, anhydrite, and gypsum, and therefore these minerals should not cause any problems. Barite is supersaturated in the formation water, the wastewaters and their mixtures, and precipitation of this mineral may cause some formation damage. The zeolite, laumontite, is undersaturated in the formation water but most of the mixtures with the wastewaters, as well as the wastewaters themselves, are supersaturated. The zeolite, wairakite, is also undersaturated in the formation water, and in approximately half of the wastewaters and their mixtures. Almost all of the waters considered are supersaturated with respect to analcime, with only the formation water and one wastewater/formation water mixing curve having SI values less than zero. Zeolites form in low temperature environments; thus, it is possible that analcime or laumontite may form. Because these zeolites will be competing for the same ions as the clays, only one of the two groups should form in significant amounts.

#### McMurray aquifer

Figure 5 illustrates the effects of mixing the formation water from the McMurray aquifer with the various wastewaters.

The dominant mineral in the aquifer is quartz. The formation water is slightly supersaturated with respect to quartz, but all of the wastewaters and their mixtures are supersaturated with quartz, with a maximum value of approximately 1.65 SI units. The average trend is for the SI values to increase, indicating that it is extremely likely that quartz will precipitate from the wastewaters and their mixtures. The SI values for the other silica phases (amorphous silica and chalcedony) are lower than that for quartz, but the shapes of their SI curves are similar to that for quartz. The formation waters in the McMurray aquifer are in equilibrium with both calcite and dolomite. The wastewaters and their mixtures have SI values evenly distributed around an SI of zero, and although not significant, the trend is toward slightly negative values. The maximum SI value for calcite is about 1.2 while the minimum is approximately -2.4. The range of dolomite values is approximately twice as large. Because of kinetic constraints, dolomite precipitates much more slowly than calcite, and therefore calcite precipitates preferentially. Trace amounts of Mn and Mg are included in the calcite structure. The sheet silicates and clays (kaolinite, illite, pyrophyllite, K-montmorillonite, Ca-montmorillonite, Na-montmorillonite, and Mg-montmorillonite) are all undersaturated (SI less than zero) in the formation water. In the wastewaters and their mixtures, their

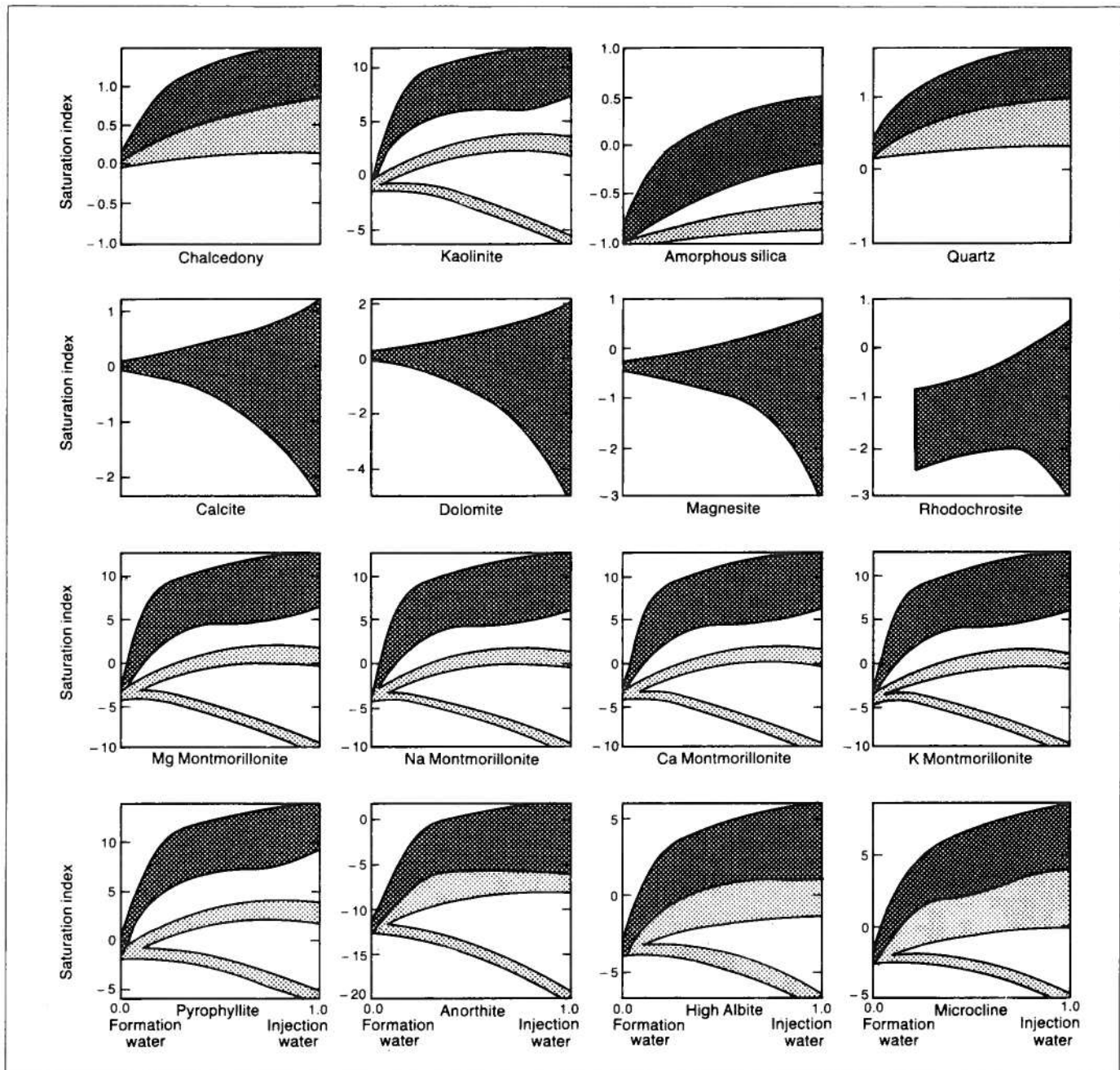


**Figure 5.** Saturation indices of selected minerals for mixtures of formation water and injection waters, McMurray aquifer.

SI values increase to 13 SI units. These phases are highly supersaturated, and certainly one or more will precipitate from solution. The SI values of the feldspars (plagioclase, microcline, and albite) are initially less than zero, but rapidly increase above zero as the proportion of wastewater increases (with the exception of plagioclase for which only a few of the wastewaters have SI values greater than zero). Only albite and microcline are supersaturated to any degree. Because the feldspars share common elements with the clays, and because clays precipitate much more rapidly from solution, it is anticipated that the clays will form instead of the feldspars. Fluorite, an-

hydrite and gypsum are undersaturated in the formation water, wastewaters and their mixtures, and will not cause any problems. Barite is supersaturated in the formation water, the wastewaters and their mixtures and, therefore, precipitation of this mineral may cause some formation damage. The zeolite, laumontite, is undersaturated in the formation water, but most of the mixtures with the wastewaters, as well as the wastewaters themselves, show supersaturation. The zeolite, wairakite, is also undersaturated in the formation water and in approximately three-quarters of the wastewaters and their mixtures. Analcime is supersaturated in many of the waters with only the forma-



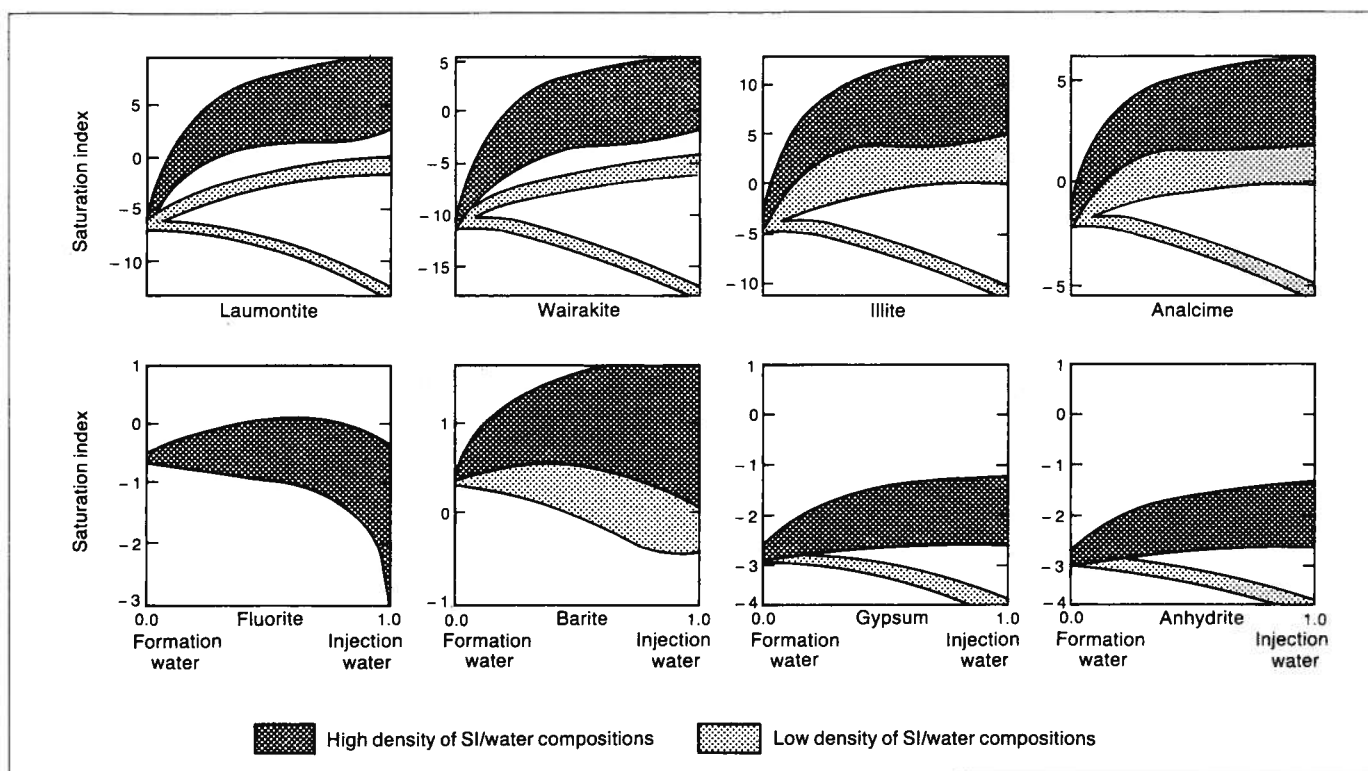


Figure 5. (continued)

tion water and several wastewater/formation water mixtures having SI values less than zero. The zeolites form in low temperature environments, thus it is possible that analcime or laumontite may form. Because these zeolites will be competing for the same ions as the clays, only one of the two groups should form in significant amounts.

#### Clearwater aquifer

Figure 6 illustrates the effects of mixing the formation water from the Clearwater aquifer with the various wastewaters. The results can be summarized as follows. Quartz is supersaturated in the formation water, with an SI of approximately 0.40. The wastewaters and their mixtures with the formation water have a range of SI values which vary from the same SI as the formation water to approximately 1.7 SI units above that of the formation water. The average value increases significantly. The SI values for the other silica phases (amorphous silica and chalcedony) are lower than that of quartz and the shape of their SI curves are similar to that of quartz. Because of the change in the SI for quartz with increasing proportions of wastewater, quartz has a significant potential for precipitation. All of the carbonate minerals are saturated in the formation water (a result of the initial assumptions) with the exception of Mn carbonate; this is probably because there is no analytical value for Mn in the formation water. The wastewaters and their mixtures have SI values which fall above and below the value for the formation water, in an approximately equal distribution.

The potential for precipitation of carbonates in some of the injection fluids is relatively high, whereas others have significant potential for dissolution if they are present in the Clearwater Formation. The problem of carbonate precipitation is thus totally dependent on the specific wastewater and cannot be generalized.

The sheet silicates and clay minerals (kaolinite, illite, pyrophyllite, K-montmorillonite, Ca-montmorillonite, Na-montmorillonite, and Mg-montmorillonite) all are supersaturated (SI significantly greater than zero) in the formation water. In the wastewaters and their mixtures, the SI values increase, on average, approximately four units. These phases are highly supersaturated and certainly one or more will precipitate from solution. The SI values of the feldspars (plagioclase, microcline, and albite) increase as the proportion of wastewater increases. Only albite and microcline are supersaturated to any degree, and because the feldspars share similar elements with the clay minerals and clay precipitates much more rapidly from solution, it is anticipated that the clay minerals will precipitate instead of the feldspars. Essentially, the diagenetic process is enhanced. Gypsum, anhydrite, and fluorite are undersaturated in the formation water, wastewaters and their mixtures, and will not cause any problems. Barite is supersaturated in the formation water, the wastewaters and their mixtures, and therefore the precipitation of this mineral may cause some formation damage. The zeolite, laumontite, is only slightly supersaturated in the formation water, but most of the mixtures with the wastewaters, as well as

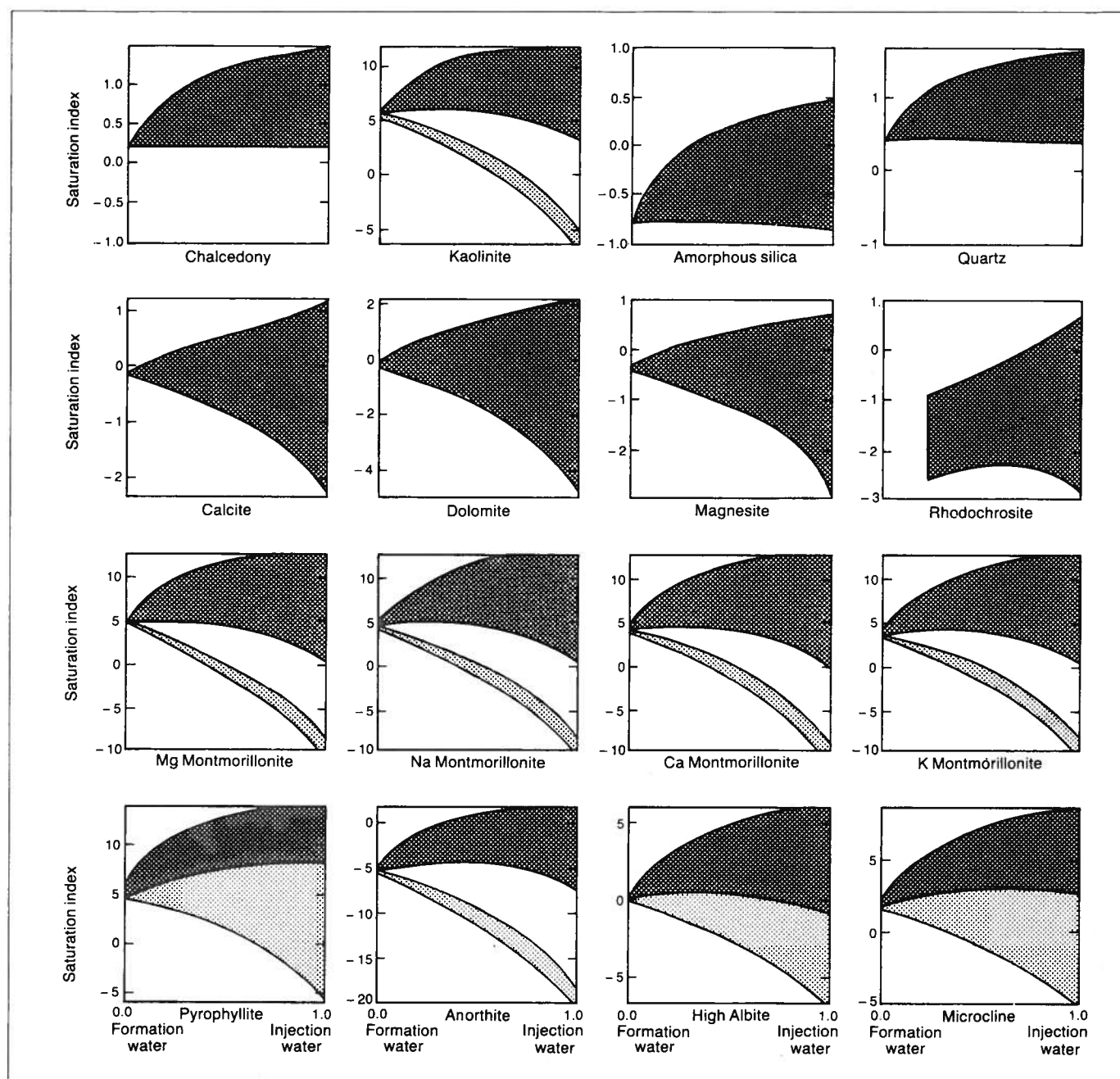


**Figure 6.** Saturation indices of selected minerals for mixtures of formation water and injection waters, Clearwater aquifer.

the wastewaters themselves, are supersaturated. The zeolite, wairakite, is undersaturated in the formation water, many of the wastewaters, and their mixtures. Analcime is supersaturated in almost all of the waters considered, with only one wastewater/formation water mixing curve having SI values less than zero. The zeolites form in low temperature environments, thus it is possible that analcime or laumontite may form. Because these zeolites will be competing for the same ions as the clays, only one of the two groups should form in significant amounts.

#### **Mannville aquifer**

Figure 7 illustrates the effects of mixing the formation water from the Mannville aquifer with the various wastewaters.

The dominant formation mineral is quartz, which is slightly undersaturated in the formation waters; this is a function of the initial assumptions. Quartz is supersaturated in all of the wastewaters and their mixtures, with a maximum value of approximately 1.7 SI units. The average trend of the SI values is increasing, thus indicating that it is extremely likely that quartz will

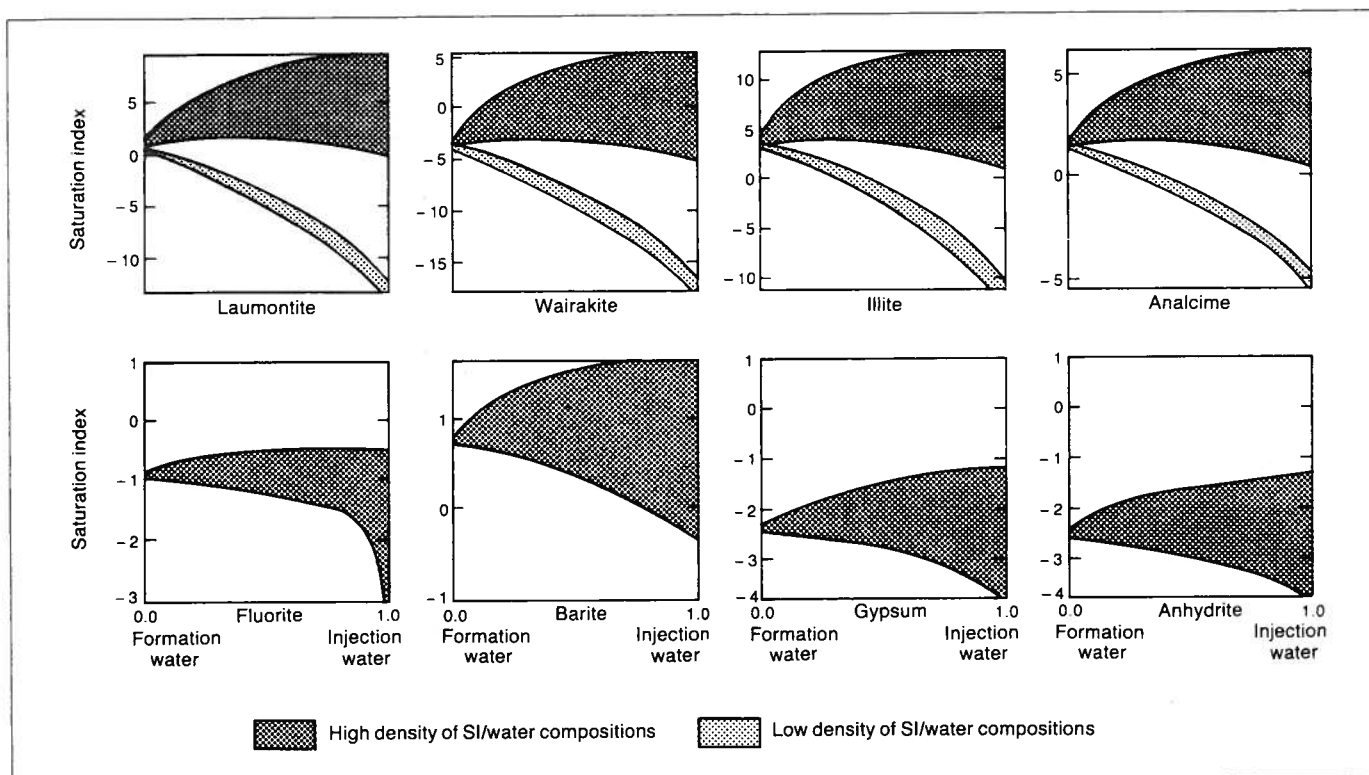


Figure 6. (continued)

precipitate from the wastewaters and their mixtures. The SI values for the other silica phases (amorphous silica and chalcedony) are lower than that for quartz but the shape of their SI curves is similar to that of quartz. The formation water of the Mannville aquifer is in equilibrium with both calcite and dolomite, in part a result of the initial assumptions. The wastewaters and their mixtures have SI values evenly distributed about an SI of zero, although not significantly so, with a trend to slightly positive values. The maximum SI value for calcite is about 1.2 while the minimum is approximately  $-2.4$ . The range of dolomite values is approximately twice as great. Because of kinetic constraints, dolomite precipitates more slowly than calcite and hence calcite will precipitate first. Trace amounts of Mn and Mg are included in the calcite structure. The sheet silicates and clay minerals (kaolinite, illite, pyrophyllite, K-montmorillonite, Ca-montmorillonite, Na-montmorillonite, and Mg-montmorillonite) are all undersaturated (SI less than zero) in the formation water and in the wastewaters and their mixtures, with the SI values increasing up to 13 SI units. These phases are highly supersaturated and certainly one or more will precipitate from solution. The SI values of the feldspars (plagioclase, microcline, and albite) are initially less than zero but increase rapidly to above zero as the proportion of wastewater increases, with the exception of plagioclase where only a few of the wastewaters have SI values greater than zero. Only albite and microcline are supersaturated to any degree, and because the feldspars share common ele-

ments with the clay minerals, and because clay minerals precipitate more rapidly from solution, it is anticipated that the clay minerals will form instead of the feldspars. Fluorite, anhydrite, and gypsum are undersaturated in the formation water, wastewaters and their mixtures, and will not cause any problems. The zeolite, laumontite, is undersaturated in the formation water, but most of the mixtures with the wastewaters, as well as the wastewaters themselves, are supersaturated. The zeolite, wairakite, is also undersaturated in the formation water and in approximately three-quarters of the wastewaters and their mixtures. Analcime is supersaturated in almost all of the waters considered, with only the formation water and one wastewater/formation water mixing curve having SI values less than zero. Prehnite is generally undersaturated, but some values are supersaturated. The zeolites form in low temperature environments, thus it is possible that analcime or laumontite may form. Because these zeolites will be competing for the same ions as the clays, only one of the two groups should form in significant amounts.

### Geochemical effects of deep waste injection

In general, all of the formation waters are either at (or near) equilibrium with the minerals observed in the formation, or they are significantly undersaturated with respect to them. This is partially a result of the assumptions made as to the amounts of  $\text{SiO}_2$  and Al in

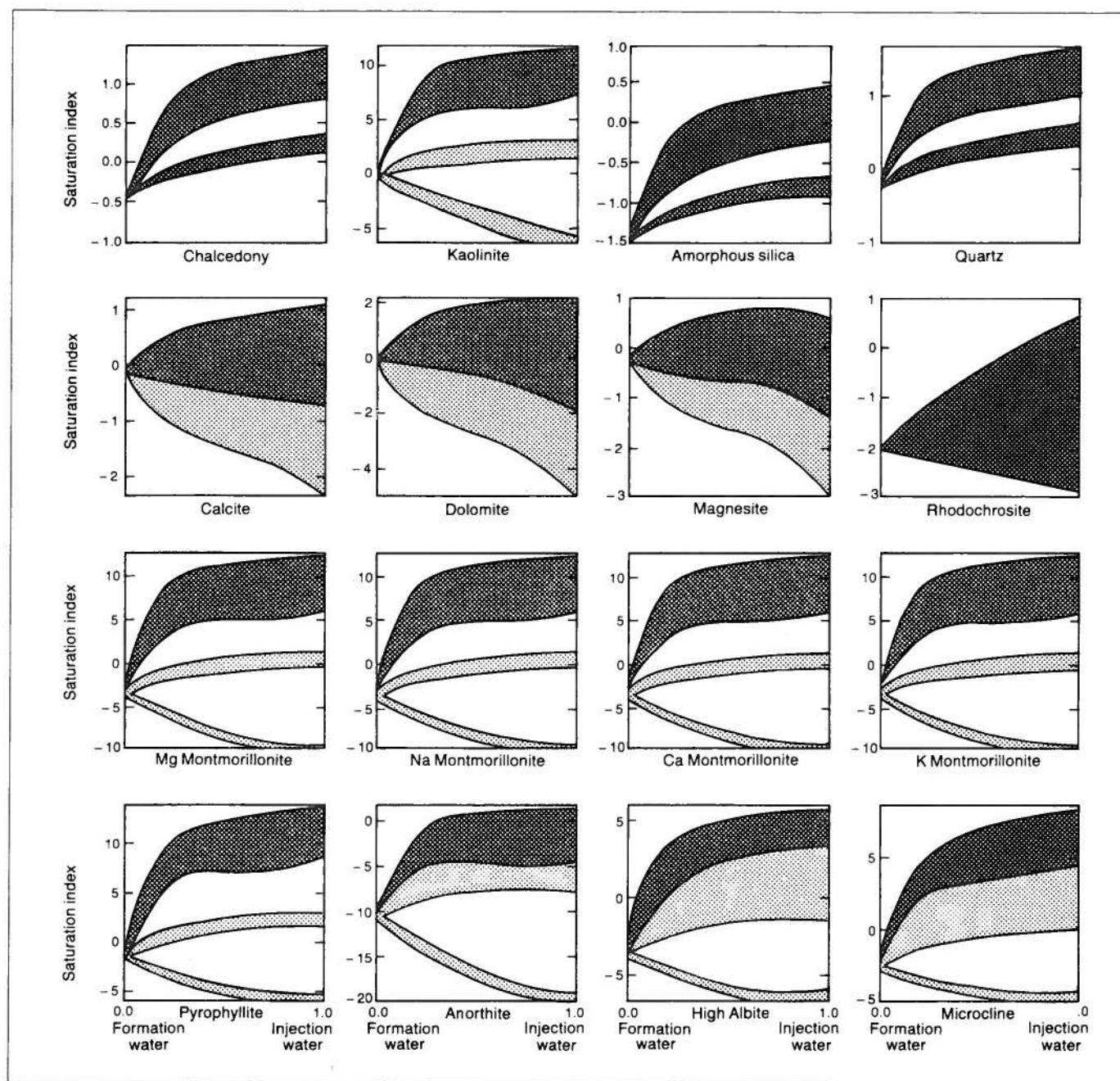


**Figure 7.** Saturation indices of selected minerals for mixtures of formation water and injection waters, Mannville aquifer.

solution, and the loss of  $\text{CO}_2$  from the water samples. The apparent undersaturation of the clay minerals in the formation waters is a result of two things: the assumed Al values, and the fact that natural clay mineral stability fields are considerably larger than those calculated because of solid solution effects. This harmony between the fluid chemistry and the mineralogy illustrates a very important point. Given sufficient time, the absence of diagenetic reactions, and no kinetic inhibitions, the formation mineralogy will control the fluid chemistry.

The wastewaters and their mixtures with the formation waters are almost always supersaturated with

respect to quartz, the clay and sheet silicate minerals, feldspars, and zeolites. This cannot be avoided and is a result of the enhanced oil recovery process. The produced fluids have come to equilibrium with the reservoir mineralogy at temperatures typically higher than  $100^\circ\text{C}$ ; at such temperatures, the solubility of  $\text{SiO}_2$  and Al is much higher. They will probably remain supersaturated until injected into an aquifer because of: (1) their short residence time in the production equipment, (2) the lack of a suitable substrate for the minerals to precipitate onto, and (3) the lack of appropriate treatment.

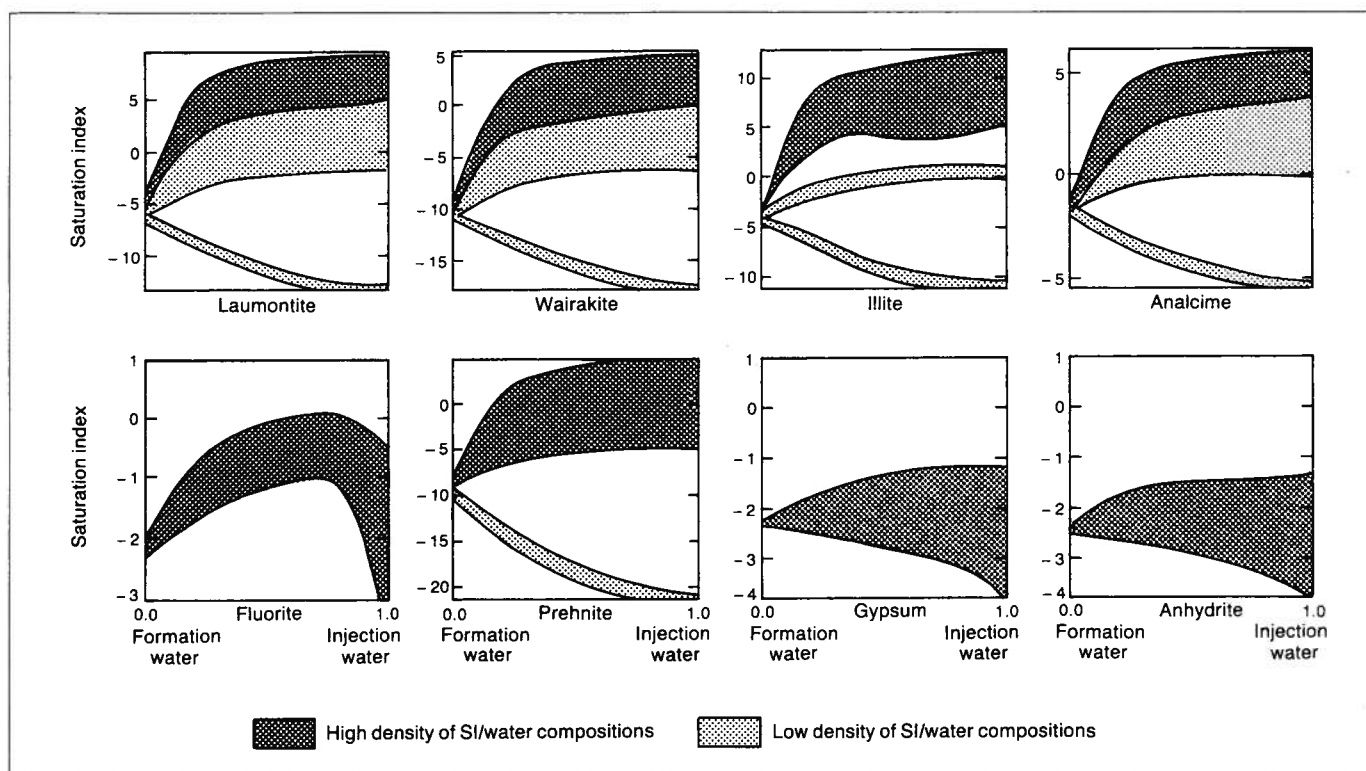


Figure 7. (continued)

Although not shown in the figures, when phosphate is present in the wastewater the fluid is typically supersaturated with the phosphate minerals chlor-apatite, fluor-apatite, and hydroxal apatite. As mentioned previously, there may be Fe minerals present with SI values significantly greater than zero, but in the absence of information about the redox state of Fe, this cannot be calculated.

The amount and identity of the minerals which will precipitate in any system with more than one supersaturated phase is currently impossible to predict. However, various constraints can be applied to determine the maximum amount of a mineral that will precipitate. Consider first the clay minerals which are typically supersaturated by ten orders of magnitude above equilibrium (SI greater than 10). Because of these high SI values and the presence of clay minerals in all aquifers, we would expect their precipitation to be rapid. However, the total amount of Al in wastewater is very small, typically of the order of 0.05 mg/L or less. Even if all the Al is used in clay formation, the number of moles of clay that can be formed per litre of solution is in the range of  $10^{-6}$  to  $10^{-7}$ . This amount is trivial and can be ignored. The local solid-solid reactions between Al-bearing phases will be far more important than this. The maximum amount of any Al-bearing mineral which can be precipitated is of a similar order of magnitude; thus, the feldspars and zeolites can be ignored.

The most significant minerals which can precipitate from or dissolve into the fluid are quartz and calcite

(dolomite is excluded because its rate of precipitation is orders of magnitude slower than calcite). If the solution has a SI value for quartz of approximately 1, then approximately  $10^{-3}$  moles can precipitate per litre of solution. If the solution has a SI value for calcite of approximately 1, then approximately  $10^{-4}$  moles per litre of calcite can precipitate.

These values are not precise because the reactions are totally dependent on the pH, the amount of each of the aqueous species in the fluid, and how the amounts of the aqueous species change during the reaction. If more than one mineral is dissolving into or precipitating from solution at one time, then they will all be affected by the rates of each reaction. These values should only serve as a guide, but they do indicate an approximate maximum amount of mineral which can be precipitated per litre of wastewater.

Values of  $10^{-3}$  moles of precipitate per litre of fluid can be important when considering large volumes of fluid and significant flow rates. If precipitation occurs quickly enough, fluid flow may be affected. Using the rates of precipitation measured for quartz at high temperatures, and extrapolating them to 25°C, the silica precipitated from solution over the lifetime of the injection period can be calculated. Over a period of 30 a, if a solution is supersaturated with quartz, approximately 20% of the available amount of silica will precipitate from solution. Approximately 50% will have precipitated after 95 a. Many formation waters are currently supersaturated with quartz and probably have

been for millennia, indicating that these calculations should be considered to be conservative.

If a solution is undersaturated with calcite, approximately 50% of the amount of calcite which can dissolve, will do so in 3 to 4 d. Over a period of 30 a, all of the calcite which can dissolve into solution must be considered to have done so. The rapid rate of dissolution and precipitation of calcite is confirmed by the lack of natural groundwaters which are supersaturated or undersaturated with calcite when this mineral is present in the formation. The rates of precipitation of calcite from a supersaturated solution are very similar to the dissolution rates.

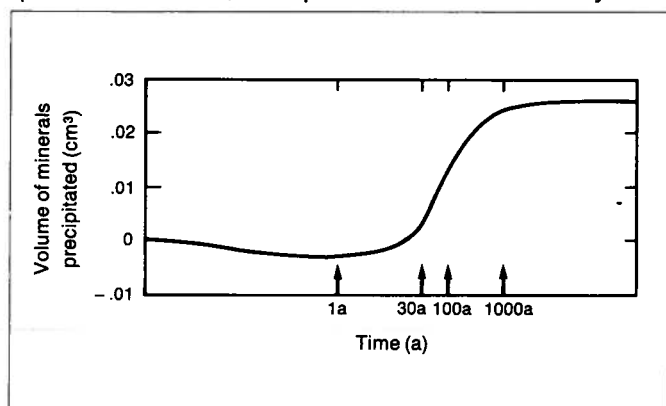
Multiple wastewater samples were taken from several of the pilots at different times; the calcite saturation index generally indicated undersaturation, though not for all of the samples. This is consistent with the SI plots for calcite in all of the wastewaters, which indicate that more than 60% of the wastewaters are undersaturated with calcite. Because the average saturation index of calcite is negative, dissolution of calcite from the aquifer would be expected, resulting in an increase in the local porosity and permeability. With the exception of the Cooking Lake/Beaverhill Lake Formation which may consist of up to 98% calcite, the total change in porosity and permeability is expected to be small because calcite is present only in trace amounts. Due to the rapid kinetic properties of calcite, all of the calcite in the area close to the well is expected to be dissolved.

Figure 8 presents the variation with time of the total volume of minerals precipitated/dissolved per litre of injection fluid in the Cooking Lake Formation. These results are indicative of the maximum possible volume change of the minerals in the formation under formation temperatures and injection pressures. They were calculated using the mineral dissolution/precipitation option of SOLMINEQ.88, and the temporal scale for the change in volume was based on available literature data for precipitation and dissolution kinetics of quartz and calcite, extrapolated where necessary. The

composition of the formation water used in this model has been discussed previously while the chosen composition of the injection water was an intermediate, near-average value. Variation of the wastewater compositions over the production cycle could modify the results, but the most significant modifier would be a change in the rate equation for quartz. Quartz is not expected to precipitate as fast as was modelled, and the injection fluid would be expected to remain partially supersaturated for a long period of time. For this reason, it is unlikely that the decrease in porosity and permeability will be as fast as is shown.

The rate at which both calcite and quartz precipitate from solution is dependent on a large number of factors, including the effective surface area for growth and the presence/absence of nucleation sites. These parameters are largely unknown in natural systems and therefore add to the uncertainty of the previous calculations. However, the relative rates at which calcite and quartz precipitate will be similar. For this reason, if treatment of wastewaters is to be considered, the most important change that can be made is to reduce the SI of calcite. This can be accomplished by softening the water, removing  $\text{CO}_2$ , modifying the pH, or increasing the residence time in a holding tank. Although considerable work has been done on water-rock interactions during EOR operations, some of which has been directed at the effects of these interactions on reservoir permeability and porosity, no information is available in the Cold Lake region for similar effects at deep waste disposal sites.

Most of the mineral reactions which will occur during the interaction of the wastewater and the minerals in the formation are endothermic; none are strongly exothermic. They will not affect the local temperature because of (1) the relatively long time period over which these reactions occur, (2) the small amount of material involved per litre of fluid, and (3) the large thermal mass of fluid and rock. The thermal effects of reaction can thus be ignored.



**Figure 8.** Total volume of minerals ( $\text{cm}^3$ ) precipitated/dissolved per litre of injected fluid as a function of time for a site injecting in the Cooking Lake Formation. Negative values indicate dissolution.



## Evaluation of hydrofracturing thresholds for rocks

Compared to other waste disposal methods, deep disposal is considered to have the advantage of isolating liquid wastes in a confined aquifer well below the horizon of human activity and potable groundwater resources. Most injected wastes move laterally in the injection zone; however, vertical migration is possible through permeable vertical conduits such as fractures and improperly abandoned wells. Of particular concern is the fracturing associated with the injection operation itself. If vertical fractures propagate all the way up to the shallow aquifers used as sources of water, then contaminant migration becomes a very real possibility. Thus, in assessing the local effects of deep waste injection in the Cold Lake area, it is necessary to evaluate the fracturing thresholds of various rocks and subsequently to compare them with predicted pressure (hydraulic head) buildups.

In reservoir engineering, hydraulic fracturing is a current practice, the objective being to increase the value of near-wellbore hydraulic parameters. It is environmentally acceptable when carried out in a controlled manner and on a relatively localized scale. The problem addressed in this study is the possibility that hydraulic fracturing may result from long-term, constant-rate injections that induce pressure buildups above the breakdown (or fracture) pressures of the injection zones (large-scale hydrofracturing). Potential upward conduits for undesirable substances may then develop in the overlying strata, damaging their integrity and modifying the flow conditions. Hydraulic fractures are most frequently vertical fractures.

The breakdown pressure ( $P_b$ ) is the reference measurement in most low-volume hydraulic fracturing experiments ('Mini-Frac'); it is the only parameter that can be easily measured and which permits comparisons between predictions and reality. Figure 9 is a classical plot of the fracturing gradient, FG (kPa/m), versus depth based on many measurements from the U.S.A. Figure 9 also shows that the variation in FG

with depth changes at about 600-800 m; beyond this, it usually remains less than 23 kPa/m, and commonly around 16 kPa/m. This can be interpreted using a model of tension failure, though it has not been verified at depths greater than 4 km. A fracture that develops vertically may pass through rocks of different lithology; its behaviour at the interface typically depends on depth and lithology. At shallow depths, one may find a horizontal 'sliding' of the fracture at the interface and no further vertical propagation. This mechanism does not occur at intermediate and greater depths, where the fracture propagates beyond the interface.

In addition to this brief overview, two points are worth noting:

(1) The hydraulic properties of the host injection zones are usually such that subsurface disposal wells are completed in formations of greater permeability than the usual 'recipients' of hydrofracturing in oil and gas production, and

(2) in spite of the impressive amount of information concerning hydrofracturing, much remains to be understood from the conceptual and predictive aspects. It remains a fairly complex process and a highly non-linear mathematical problem. Both fracture initiation and propagation are difficult to predict accurately, mainly because of the unavailability of in situ measurements of some key geomechanical properties and of the initial stress regime.

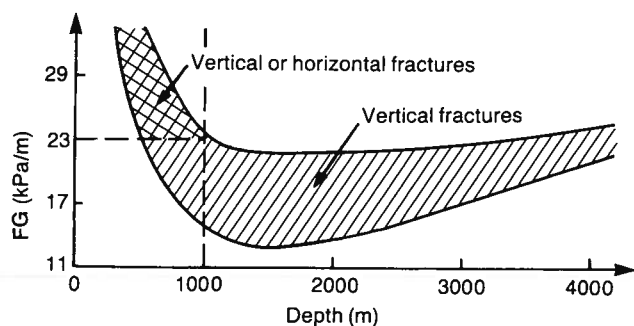
The objective of this section of the bulletin is to assess the breakdown pressures for selected injection zones in the Cold Lake area.

### In situ stress regime and failure criteria

Because of the crucial lack of in situ measurements of stress regimes, classical theories for evaluating breakdown pressures assume that: (1) one of the principal stresses is vertical; (2) the horizontal field of stress is isotropic; and (3) stress increases linearly with depth.

Following the work of Haimson (1968), it is possible to interpret fracturing pressure charts of 'Mini-Frac' tests. These analyses reveal that while assumption (1) is still satisfactory, in practice, assumptions (2) and (3) are rarely verified: horizontal stresses are rarely isotropic, and stress may vary by a few hundred kilopascals from one stratum to another at any given site.

In a purely elastic model, the overburden stress (which equals the weight of the overlying rocks above a given point) generates horizontal stresses in a simplistic fashion that does not take into account the geological history and nature of the stratum from the



FG : the fracturing gradient indicates the variation of breakdown pressure with depth

**Figure 9.** Variation of fracturing gradient with depth.

tectonic, the lithologic (diagenetic) or even the anthropogenic points of view (Warpinski et al. 1985).

In terms of tension failure, hydrofracturing implies that the fracture develops perpendicular to the lesser principal stress; this lesser stress is most frequently in the horizontal plane, which explains the common generation of a vertical fracture.

The compressive stress regime in a sedimentary basin can be resolved into three orthogonal stresses applied at any point of the basin: the maximum stress,  $S_1$ ; the intermediate stress,  $S_2$ ; and the minimum stress,  $S_3$ . In the Cold Lake area, on a local scale at the injection sites, one can assume the following conditions: the strata are horizontal, the topography is flat, and horizontal strains are small and negligible. In addition, if the elastic theory is applicable, then the maximum principal stress,  $S_1$ , is vertical and is equal to the weight of the overlying rocks, or:

$$S_1 = S_v = g \int_0^D \rho_b(z) dz \quad (3)$$

where  $\rho_b$  is the bulk density of rocks,  $g$  is the gravity acceleration,  $D$  is the depth from ground surface to the point of interest, and  $z$  is a dummy variable of integration. It is presently accepted that the minimum principal stress in the horizontal plane has an influence on the height of the vertical fracture. In addition, the upward propagation of the fracture would be more confined by overstress zones than by a change of geomechanical properties at the interface with the overlying stratum.

The type of geomechanical properties relevant to the injection zone and 'confining' layer depends on the mechanical model used in the evaluation of fracture propagation. The most commonly used theory is limited to an elastic, brittle failure, and a linear process operating at isothermal conditions. Therefore, the rocks are characterized by:

(1) Young modulus,  $E$ ; (2) Poisson's ratio,  $\mu$ ; and (3) a failure criterion which is usually related to the minimum energy required to create a fracture plane.

Often, one considers the shear modulus,  $G$ , to be related to  $E$  and  $\mu$  by:

$$2G = E/(1 + \mu) \quad (4)$$

With regard to the failure criterion, one should distinguish the first phase of hydrofracturing from the second. The first consists of a rupturing of the rock around the injection well followed by the initiation of a fracture, while the second phase is concerned with fracture propagation. The first phase is determined by the tensile strength of the rock which has to be overcome in the failure criterion. Tensile strength is defined as the maximum possible stress supported by a solid in simple tension. In non-fractured, fragile rocks (e.g. a poorly consolidated sandstone), this

stress corresponds to a decohesive failure along a plane perpendicular to the applied tension. If the rock is naturally fractured (this includes the presence of joints and/or micro-fractures), tensile strength cannot be adequately defined because of the possible propagation of fractures along existing cracks, in addition to the decohesive process. This explains why laboratory measurements of tensile strength show wide variations. The 'Brazilian test' (indirect tensile testing), however, gives the closest values when measuring decohesive failure. Different ranges can be obtained when other laboratory methods are used. An analysis of data given by Lama and Vutukuri (1978) for tensile strength,  $T$  (MPa), is presented in table 10. Where the 'Brazilian test' data only are considered, one may use:

Consolidated sandstone	$3 \leq \bar{T} \leq 5$
Massive limestone	$10 \leq \bar{T} \leq 15$
'Soft' limestone	$1 \leq \bar{T} \leq 1.5$

The rocks considered in the present study have a matrix porosity and contain fluids under pressure. Under these conditions, it is necessary to define: the total stress,  $S_{ij}$ , which would be transmitted by the dry rock; the pore pressure,  $P_f$ ; and the effective stress,  $\sigma_{ij}$ . In an elastic medium, total and effective stresses are related in the following way (Biot 1941):

$$\sigma_{ij} = S_{ij} - \alpha P_f \delta_{ij} \quad (5)$$

where  $\alpha = 1 - C_r/C_b$ , and  $C_r$  and  $C_b$  are, respectively, rock and bulk compressibility. The coefficient  $\alpha$  is often called 'Biot's poroelastic constant' because it increases with the rock porosity. This coefficient is commonly assumed to have a value of 1 for aquifers and zero for non-porous rocks. In equation 5,  $\delta_{ij}$  is the Kronecker delta, and  $S_{ij}$  represents the total stress tensor acting on an element of the fluid-filled porous medium ( $i$  face,  $j$  direction).

Let us substitute for the real medium an elastic medium which is infinite, homogeneous, and isotropic. It has a Poisson's ratio  $\mu$  and a homogeneous, two-dimensional, yet anisotropic stress regime ( $S_{H \max}$ ,  $S_{H \min}$ ). Let us assume that this elastic medium has a circular opening (the well). If the centre of the coordinates is at the well axis and the abscissa cor-

**Table 10.** Variation of tensile strength  $T$  (MPa) with lithology (after Lama and Vutukuri 1978).

Material	No. of determinations	Tensile strength		
		Minimum	Average	Maximum
Sandstone	94	0	10	28
Limestone	84	3.4	13	22.5
Dolomite	6	2.6	6	10
Siltstone	17	0	14	28
Shale	26	0	5.5	12
Salt/Gypsum	12	0	1.5	2



responds to the  $S_{H \max}$  direction, one may identify a point in space by its polar coordinates  $(r, \theta)$ .

If  $P$  is the fluid pressure at the wall of the wellbore, it can be verified that:

$$\begin{aligned} S_r &= P \\ S_\theta &= S_{H \max} + S_{H \min} \\ &\quad - 2(S_{H \max} - S_{H \min}) \cos 2\theta - P \end{aligned} \quad (6)$$

in an impermeable medium, with  $S_\theta$  minimum for  $\theta = 0$ , and that:

$$\begin{aligned} \sigma_r &= 0 \\ \sigma_\theta &= \sigma_{H \max} + \sigma_{H \min} - 2(\sigma_{H \max} - \sigma_{H \min}) \cos 2\theta \\ &\quad - (1+\mu)(P-P_f) \end{aligned} \quad (7)$$

in a permeable medium, with  $\sigma_\theta$  minimum for  $\theta = 0$ . The effective principal (horizontal) stresses at 'infinity' are  $\sigma_{H \max}$  and  $\sigma_{H \min}$ . Their values are therefore independent of time and can be expressed by:

$$\begin{aligned} \sigma_{H \max} &= S_{H \max} - P_f \\ \sigma_{H \min} &= S_{H \min} - P_f \end{aligned} \quad (8)$$

assuming  $\alpha = 1$ .

Using the elastic theory, and assuming that the criterion of tensile strength is a valid one for fracture initiation, the fracture direction is perpendicular to the maximum tension, i.e. to the minimum in situ stress in this case.

If failure occurs when the minimum tangential stress,  $S_\theta$ , is such that  $(S_\theta)_{\min} + T = 0$  for  $P = P_b$ , then:

$$P_b \geq (3 S_{H \min} - S_{H \max} + T) \quad (9)$$

for an impermeable medium, and:

$$(P_b - P_f) \geq (3\sigma_{H \min} - \sigma_{H \max} + T)/(1 + \mu) \quad (10)$$

for a permeable medium.

Equation 9 is the same as that derived by Hubbert and Willis (1957) and later used by Bredehoeft et al. (1976). It assumes "a non-penetrating fluid in a tectonically relaxed area having reasonably gentle topography, where it can be assumed that the maximum principal stress is vertical and collinear with the axis of the borehole" (Bredehoeft et al. 1976, p. 251).

According to Haimson and Fairhurst (1969) the denominator of equation 10 should be:

$$2 - \alpha \frac{1 - 2\mu}{1 - \mu}$$

which yields  $1/(1-\mu)$  rather than  $(1+\mu)$  when  $\alpha=1$ . Only when  $\mu$  is small, are the two expressions approximately equivalent.

Equation 9 represents the usual basic equation for evaluating breakdown (or fracture) pressures.

## Evaluation of breakdown pressures

Examination of equations 9 and 10 reveals that, even when assuming the values of the intrinsic properties  $\mu$  and  $T$ , the evaluation of  $P_b$  requires knowledge of the horizontal principal stress field. In the absence of 'Mini-Frac' test results, and for the purposes of this study, additional assumptions have to be made in order to arrive at a working method to evaluate  $P_b$ .

The most common assumption is that a horizontal constraint exists, i.e. strains in the  $x$  and  $y$  directions are equal and nil. In this case, Biot's stress/strain relations can be solved noting that  $\mu = \lambda/2(G+\lambda)$ , where  $\lambda$  is the Lamé constant, and assuming a horizontal isotropic stress field. This yields:

$$\sigma_{H \min} = \sigma_{H \max} = \frac{\mu}{(1 - \mu)} \sigma_v \quad (11)$$

where  $\sigma_v$  is the vertical effective stress.

Denoting the total vertical stress by  $S_v$ , defined as in equation 3, and assuming  $\alpha = 1$ , Eaton (1969) combined equations 9 and 11 to first obtain:

$$S_{H \min} = \frac{\mu}{(1 - \mu)} (S_v - P_f) + P_f \quad (12)$$

and then:

$$P_b \geq \frac{\mu}{1 - \mu} (S_v - P_f) + P_f \quad (13)$$

The derivation of equation 13 assumes that  $T = 0$  and that the failure criterion is simply  $P_b \geq S_{H \min}$ , as opposed to  $P_b \geq 2S_{H \min}$ , which is what equation 9 would yield for  $T = 0$ . Using  $\mu = 1/4$  in equation 13 yields the equation recommended by Hubbert and Willis (1957):

$$P_b \geq (S_v + 2 P_f)/3 \quad (14)$$

Anderson et al. (1973) have proposed another equation for the Gulf Coast area, noting that for weakly cemented sandstones the formation cannot withstand a positive strain in the tangential direction of the borehole. This means that the failure criterion is nil effective tangential stress in Biot's sense ( $\alpha$  not equal to 1 or 0), which corresponds to  $T + \alpha P_f = 0$ . Combining and rearranging equations 5, 9, and 11, it is easy to prove that

$$P_b \geq \frac{2\mu}{1 - \mu} S_v + \frac{1 - 3\mu}{1 - \mu} \alpha P_f \quad (15)$$

is another form of the same failure criterion. Anderson et al. (1973) recommend the use of  $\alpha \approx \phi_D$ , where  $\phi_D$  is the porosity from density logs; for  $\mu$ , they suggest the use of an area-dependent linear relation between  $\mu$  and a 'shale index' defined by  $(\phi_s - \phi_D)/\phi_s$ , where  $\phi_s$  is the sonic log porosity. The coefficients of this linear relation require data from 'Mini-Frac' tests.

Equation 15, although more accurate than equation 13, is often criticized for its suggested evaluations of  $\alpha$  and  $\mu$ , which are viewed as being unrealistic. Equation 13, Eaton's equation, is not based on a realistic failure

criterion and is more empirical than equation 15. Both equations assume an isotropic horizontal stress field. In spite of these limitations, both equations are commonly used. They make use of the relation expressed by equation 11 which clearly stipulates that the weight of the overlying rocks is the only source of stress and that the horizontal elongations are nil. According to Jaeger and Cook (1976), it is reasonable to assume that even in the absence of tectonic structures and seismicity, a region must be subject to some tectonic stress. They suggest the existence of a superposed horizontal stress,  $S_t$ , which increases uniformly with depth or  $\sigma_v$ . It has been demonstrated that reverse faulting must occur when the horizontal effective stress becomes approximately three times greater than the vertical effective stress (Hubbert 1945). If there is no superposed tectonic stress, then the relation of equation 11 may accurately represent a minimum horizontal effective stress  $\sigma_{H \min}$ . It is therefore legitimate to define  $S_t$  as:

$$0 \leq S_t < 3\sigma_v - \frac{\mu}{1-\mu} \sigma_v = \frac{3-4\mu}{1-\mu} \sigma_v \quad (16)$$

Actual estimation of in situ tensile strengths is very difficult, if not impossible, but one can make the assumption that any interval of sedimentary rock is intersected by natural discontinuities (joints and partings) across which the tensile strength,  $T$ , is effectively zero. However, except for some specific zones or lithologies, this is not a very accurate assumption. Stress release at borehole walls which occurs during the drilling process is a well documented phenomenon which generates microcracks and supports the concept of a zero tensile strength.

## Estimation of Poisson's ratio

In the laboratory, Poisson's ratio is measured under static conditions (uniaxial compression or tension) and by dynamic methods (resonance, ultrasonic testing). Static and dynamic results indicate that the ratio ( $\mu$  dynamic)/( $\mu$  static) varies, typically, between 1.1 and 1.8 (Balmer 1953). Although closer to in situ values because they account for zones of weaknesses and anisotropies, the dynamic values of Poisson's ratio obtained from laboratory methods on cores are usually less reliable than those derived from acoustic-log methods.

The classical approach (Schlumberger's Mechanical Properties Log, MPL) for evaluating Poisson's ratio from acoustic logs is to use the empirical relation between  $\Delta t_p$  and  $\Delta t_s$  proposed by Pickett (1963) for typical lithologies, where  $\Delta t_p$  is the transit time for compressional wave velocity measured with the acoustic log, and  $\Delta t_s$  is the transit time for shear wave velocity. When  $\Delta t_s$  is derived from  $\Delta t_p$  using Pickett's proposed relations, then Poisson's ratio is calculated as:

$$\mu = \frac{1-2R^2}{2(1-R)^2} \quad (17)$$

where  $R = (\Delta t_p/\Delta t_s)$ .

One should be aware that this method can be seriously inaccurate because the recognition of shear wave arrivals in most sedimentary sections is generally impossible. Pickett's relations can generate significant errors in the evaluation of  $\mu$  (McLennan et al. 1982) and therefore a weak link exists in this procedure.

In the Cold Lake area there are insufficient 'Mini-Frac' test results and MPL data to evaluate in situ values of Poisson's ratio for the injection intervals. Yet, the error introduced in the evaluation of breakdown pressures can be significant. Dusseault and Simmons (1982) discuss properties of the materials that constitute the bulk of the injection aquifers in the Cold Lake area and suggest the values shown in table 11.

Application of the above MPL technique for a sandstone would give a value of  $\mu=0.15$ , with a typical compressional transit time of  $\Delta t_p=200 \mu s/m$ . This is an important underestimation of the above values for  $\mu$ .

Alternately, if the pairs of geomechanical parameters suggested by Dusseault and Simmons (1982) are approximately correct for the studied injection aquifers, one may devise another method for evaluating Poisson's ratio.

Beginning with the well-established relation (Lama and Vutukuri 1978, Vol. II, p. 196):

$$\rho_b/(\Delta t_p)^2 = E \frac{(1-\mu)}{(1+\mu)(1-2\mu)} \quad (18)$$

where  $\rho_b$  is the bulk density, one may combine data from digitized density and acoustic logs of the injection intervals to compute the left hand side of equation 18 and then use a reasonable value (or a range of values) for  $E$  to solve equation 18 for  $\mu$ . This new method has been applied using the data given by Dusseault and Simmons (1982):  $6 \leq E \leq 11$  GPa for the poorly consolidated sandstones of the Mannville, Clearwater, and McMurray aquifers, and  $15 \leq E \leq 25$  GPa for the limestone of the Beaverhill Lake aquifer. An example of the density and acoustic curves used in this analysis is presented in figure 10. In the absence of available geophysical logs for the Lower Paleozoic

**Table 11.** Geomechanical parameters suggested by Dusseault and Simmons (1982) for the Cold Lake area.

Aquifer	Poisson's ratio	Dynamic Young's modulus E
	$\mu$	(GPa)
Mannville	0.35	6.8
Clearwater	0.35	7.1
McMurray	0.32	11.0
Beaverhill Lake	0.25	34.7

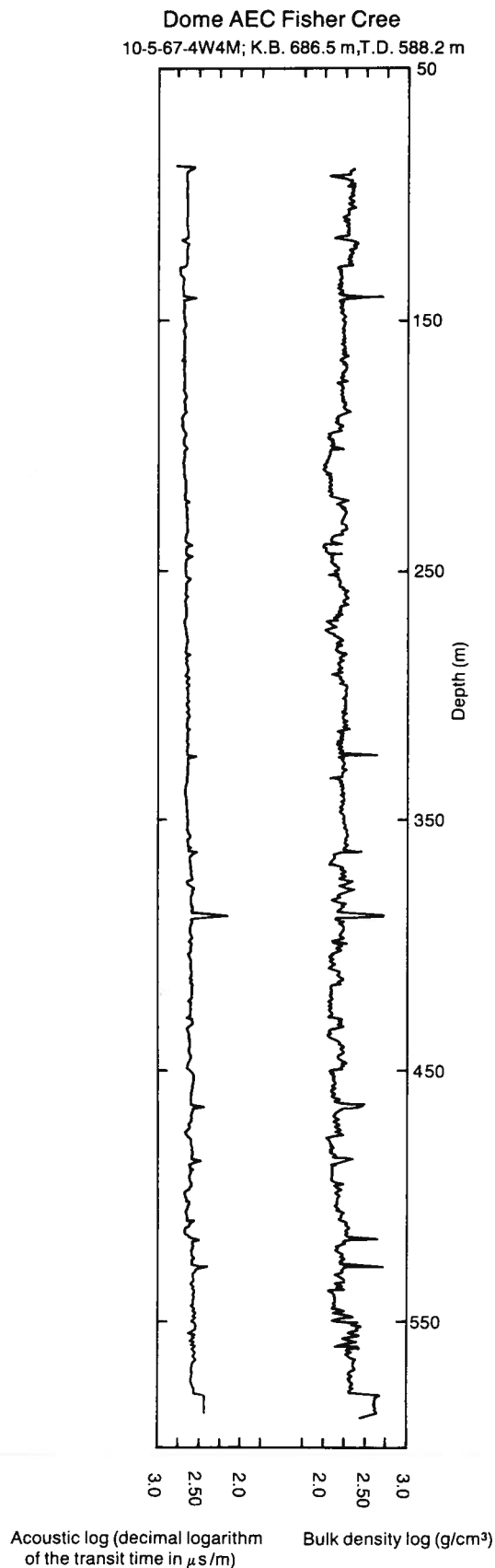


**Figure 10.** Example of acoustic and density logs used in the study.

aquifer system, literature values for the static Poisson's ratio have been used. It is felt that the error introduced should be minimal for a well-consolidated sandstone at the greater depths of injection in this aquifer.

Poisson's ratio was automatically calculated using this method; it was applied to the actual intervals, or to equivalent intervals when no log was available for a specific injection well. The numerical values and the range of Poisson's ratio are summarized in table 12 which also contains a recommended value to be used for the injection interval.

### Estimation of overburden stress and initial pore pressure

Calculation of the definite integral of equation 3 is done automatically on the basis of either actual density/depth curve or users' supplied average values for missing intervals. Average values are obtained at equivalent subsea elevations from neighbouring wells. The overburden stress,  $S_v$ , is calculated at the mid-point of the injection interval. The results of the calculations are summarized in the last column of table 13. It can be verified that these results are lower than the predictions obtained with the commonly used average lithostatic gradient of 22.62 kPa/m (1 psi/ft), or even with a more experimental regression relation based on the data of Bell and Babcock (1986) (penultimate column table 13).

### Estimation of constant $\alpha$ and breakdown pressures

As suggested by Anderson et al. (1973),  $\alpha$  is evaluated as  $\phi_D$ , the density log porosity, which is calculated using the following relation:

$$\alpha \approx \phi_D = \frac{\rho_b - \rho_{ma}}{\rho_w - \rho_{ma}} \quad (19)$$

where  $\rho_{ma}$  is the dry matrix density,  $\rho_w$  is the pore fluid density, and  $\rho_b$  is the bulk density derived as an average for the injection interval. For  $\rho_{ma}$ , the mean values of hundreds of laboratory measurements from Lama and Vutukuri (1978) were used, e.g. 2434 kg/m<sup>3</sup> for sandstone and 2500 kg/m<sup>3</sup> for limestone. For  $\rho_w$ , the regional average values of in situ formation water densities were used (table 2). The results of the calculations for the coefficient  $\alpha$ , and the corresponding breakdown pressures, are presented in table 14 for selected sites in the Cold Lake area. The lack of calibrating data from 'Mini-Frac' tests explains why the final results of table 14 are expressed in terms of a range of possible values rather than a single value.

In situations when fracturing cannot be avoided, additional modelling should be performed in order to predict the propagation of the fracture, especially at

**Table 12.** Estimation of Poisson's ratio for rocks at selected injection sites.

Operator name/ Injection aquifer	Location	Interval depths (m) and dominant lithology	Mean 'static (laboratory) Poisson's ratio'	Standard deviation for 'static (laboratory) Poisson's ratio'	'Dynamic Poisson's ratio'		Recom- mended 'dynamic Poisson's ratio'
					for E= 6GPa <sup>1</sup>	for E= 11GPa <sup>1</sup>	
Westmin/Mannville (A)	11-1-55-5-W4M	512-524	L.SS.	0.19 (117)	0.10	0.424	0.375
Westmin/Mannville (B)	11-1-55-5-W4M	558-567	L.SS.	0.19 (117)	0.10	0.425	0.376
Westmin/Beaverhill Lake	3-13-55-6-W4M	634-708	LIME.	0.24 (152)	0.07	0.391 <sup>2</sup>	0.322
Murphy/Mannville	5-13-58-5-W4M	509.4-511.7	L.SS.	0.19 (117)	0.10	0.404	0.328
Murphy/Beaverhill Lake	5-13-58-5-W4M	584.1-595.6	LIME.	0.24 (152)	0.07	0.391 <sup>2</sup>	0.322
Suncor/Clearwater	5-28-61-4-W4M	412-458	L.SS.	0.19 (117)	0.10	0.394(4)	0.299
Suncor/McMurray (A)	5A-28-61-4-W4M	443.8-452.3	L.SS.	0.19 (117)	0.10	0.397(4)	0.308
Suncor/McMurray (B)	5A-28-61-4-W4M	499.6-502.6	L.SS.	0.19 (117)	0.10	0.403(4)	0.322
BP/Mannville	8-7-66-5-W4M	422.5-440.7	L.SS.	0.19 (117)	0.10	0.400(10)	0.315
BP/Lower Paleozoic	10-8-66-5-W4M	1321-1329	SS.	0.19 (117)	0.10	[0.29]	[0.19]
Dome/McMurray	10-5-67-4-W4M	468.5-487.0	L.SS.	0.19 (117)	0.10	0.402	0.323
Dome/Lower Paleozoic	10-5-67-4-W4M	1302-1320	SS.	0.19 (117)	0.10	[0.29]	[0.19]

L.SS. – Poorly consolidated sandstone; SS. – Sandstone; LIME. – Limestone (massive)/shaley limestone

1 E = 'Dynamic' Young Modulus.  $6 \leq E \leq 11$  GPa for poorly consolidated sandstone

2 for 'soft' case, with E = 15GPa

3 for 'stiff' case, with E = 25GPa

( ) number of values averaged

[ ] values estimated (no geophysical logs available)

the level of lithological interfaces where the geomechanical properties change and where further upward propagation might be stopped. Azimuths of fracture propagation may be inferred from Bell and Babcock (1986). Preliminary modelling of fracture propagation can be done using, for example, the

analytical but approximate solutions of Nordgren (1972). More accurate modelling requires the use of three-dimensional simulators (Chouet 1986; Settari and Cleary 1984). An appreciation of fracture penetration through an interface can be had from reviewing the works of Biot et al. (1983) and Labudovic (1984).

**Table 13.** Estimation of overburden stress at selected injection sites.

Operator name/ Injection aquifer	Location	Estimated pore pressure	Depths to mid-points of injection intervals	Overburden <sup>1</sup> stress from empirical correlation with depth	Overburden <sup>2</sup> stress from integration of density logs
		(MPa)	(m)	(MPa)	(MPa)
Westmin/Mannville (A)	11-1-55-5-W4M	3.75	518.3	12.84	10.91
Westmin/Mannville (B)	11-1-55-5-W4M	4.28	562.5	13.92	11.89
Westmin/Beaverhill Lake	3-13-55-6-W4M	5.30	682.0	16.95	14.68
Murphy/Mannville	5-13-58-5-W4M	3.30	510.5	12.65	10.49
Murphy/Beaverhill Lake	5-13-58-5-W4M	4.11	596.5	14.81	12.38
Suncor/Clearwater	5-28-61-4-W4M	3.35	435.0	10.75	9.21
Suncor/McMurray (A)	5A-28-61-4-W4M	3.36	448.0	11.08	9.49
Suncor/McMurray (B)	5A-28-61-4-W4M	3.88	501.0	12.41	10.68
BP/Mannville	8-7-66-5-W4M	2.83	440.7	10.90	9.02(3)
BP/Lower Paleozoic	10-8-66-5-W4M	11.66	1325.0	33.08	29.40(4)
Dome/McMurray	10-5-67-4-W4M	2.78	540.0	13.39	11.26
Dome/Lower Paleozoic	10-5-67-4-W4M	11.06	1311.0	32.73	29.24

1  $S_v = 2.509 \times 10^{-2} D - 0.16065$ , where  $S_v$  is the overburden stress and D is the depth (inferred from Bell and Babcock 1986)

2 using best estimates for bulk density when logged intervals are missing

( ) number of values averaged from neighbouring locations

**Table 14.** Estimation of breakdown pressures,  $P_b$  (MPa), for rocks at selected injection sites.

Operator name/ Injection aquifer	Location	Results from Eaton's equation 13		Results from Anderson's et al. equation 15		
		$\bar{P}_b$	Range of $P_b$	$\alpha$	$\bar{P}_b$	Range of $P_b$
Westmin/Mannville (A)	11-1-55-5-W4M	8.05	7.21- 9.02	0.21	12.93	10.58-15.69
Westmin/Mannville (B)	11-1-55-5-W4M	8.87	7.98- 9.90	0.18	14.17	11.58-17.20
Westmin/Beaverhill Lake	3-13-55-6-W4M	9.75	8.46-11.32	0.14	13.98	10.13-18.65
Murphy/Mannville	5-13-58-5-W4M	6.81	5.71- 8.17	0.25	10.26	7.30-13.93
Murphy/Beaverhill Lake	5-13-58-5-W4M	8.04	6.90- 9.42	0.15	11.79	8.55-15.72
Suncor/Clearwater	5-28-61-4-W4M	5.85	4.86- 7.16	0.26	7.98	5.16-11.72
Suncor/McMurray (A)	5A-28-61-4-W4M	6.09	5.08- 7.40	0.26	8.54	5.70-12.22
Suncor/McMurray (B)	5A-28-61-4-W4M	7.11	6.05- 8.47	0.20	10.18	7.09-14.16
BP/Mannville	8-7-66-5-W4M	5.68	4.82- 7.00	0.15	8.33	5.95-11.98
BP/Lower Paleozoic	10-8-66-5-W4M	15.82	13.42-18.91	0.04 <sup>1</sup>	15.77	14.04-24.11
Dome/McMurray	10-5-67-4-W4M	6.83	5.50- 8.48	0.22	10.77	7.44-14.93
Dome/Lower Paleozoic	10-5-67-4-W4M	15.32	12.86-18.48	0.04 <sup>1</sup>	15.59	13.95-23.97

$\bar{P}_b$  – mean value obtained for the breakdown pressure  
<sup>1</sup> estimated

In the next section, the injection of wastewater is numerically simulated, and the resulting pressure buildups are compared with the estimated breakdown

pressures, in order to evaluate the possibility of hydrofracturing at injection sites.

# Numerical simulation of pressure buildup

## Mathematical and numerical modelling

The objective of mathematical modelling and simulation of formation water flow and fluid injection in the Cold Lake study area is to provide a predictive tool for determining the effects of deep waste injection on the natural hydrogeological regime in the region in terms of hydraulic head buildup. Due to the complexity of the stratigraphic geometry and the variability of properties of the fluid and solid matrix in the subsurface environment, numerical modelling was used for studying the effects of deep waste disposal. The first step in the modelling process was to calibrate a numerical model for simulation of steady-state natural flow of formation waters within the complex hydrogeological system in the Cold Lake study area. After calibration, the system was perturbed by injecting fluids at specified rates. For a given hydrostratigraphic configuration, the system response when using different values for the hydraulic properties was indicative of the effects of injection in the various aquifers in the succession. The modelling process was carried out in two stages. First, the effects of injection were simulated on a regional scale at the 27 sites listed in table 1, using regional values for hydraulic parameters. The purpose of regional-scale modelling is to check for interference (superposition of effects) between various injection sites, assuming average values for hydraulic parameters. However, the local values of hydraulic conductivity and specific storage could be different from the values used in regional-scale simulations. Also, the resolution of the regional-scale grid is too coarse for a proper estimation of the pressure buildups at the injection wells themselves, because the results of numerical simulations are representative only for an equivalent distance which is proportional to the grid spacing. For these reasons, the effects of injection were simulated in the second stage on a local scale at selected sites. Local values for hydraulic parameters were used in order to compare the hydraulic head buildups with the fracturing thresholds that are indicated by breakdown pressures.

The mathematical model for fluid flow in porous media consists of a set of partial differential equations together with appropriate boundary and initial conditions that express conservation of mass and momentum over the region of interest. In the analysis of the natural hydrogeological regime in the Phanerozoic succession in the Cold Lake area (Hitchon et al. 1989) it was shown that, although the density of formation waters is variable, it is still possible to neglect buoyancy effects. The driving-force ratio (DFR) defined by Davies (1987) was computed on a regional scale for each aquifer, with values below the threshold over

which buoyancy effects should be accounted for. Davies (1987) studied the effects of buoyancy in a single aquifer, whereas injection in the Cold Lake area takes place both in a single aquifer (Basal Cambrian) and in a multiaquifer system in the Mannville Group. However, the density of formation waters in the multiaquifer system is sufficiently close to freshwater density (Hitchon et al. 1989) to allow the effects of buoyancy to be neglected. It is conceivable that in some places the local values of DFR exceed the threshold value because of local variations in the elevation gradient (subsurface topography) or in the hydraulic gradient. Still, for the purposes of this study, it is believed that the equivalent freshwater head approximation is valid because, as a result of injection, the external driving force will increase at the injection sites, thereby diminishing the influence of the internal buoyancy force. Assuming the validity of using equivalent freshwater hydraulic heads, the unsteady saturated flow in porous media of a slightly nonhomogeneous fluid is described by the following partial differential equation (Bear 1972), obtained by combining the continuity and momentum (Darcy's law) equations:

$$\text{div}[\bar{K}\text{grad}(H)] - Q = S_s(\partial H/\partial t) \quad (20)$$

where  $\bar{K}$  is the hydraulic conductivity tensor,  $S_s$  is specific storage,  $Q$  is the strength of sources/sinks,  $H$  is hydraulic head, and  $t$  is time.

The model FE3DGW (Finite Element 3-Dimensional GroundWater) was selected for the numerical simulation of fluid flow. This model was developed by Pacific Northwest Laboratory (U.S.A.), and a complete description of the numerical formulation and the pertinent software is given in Gupta et al. (1984a, 1984b).

In assessing the results of numerical modelling, one has to take into account the approximations and assumptions made at each step in the data processing procedures and in the numerical simulation. A first approximation is made when values at nodes in a regular grid of freshwater hydraulic heads are obtained from an irregular distribution of real (measured) values. The regular grid distribution depends (among other factors) on its resolution, the initial data size and sample distribution, the gridding method, the parameters and constraints of the method itself, and the interpolation and extrapolation procedures. In the graphical representation of the regular grids as contour maps there are approximations and differences depending on the grid resolution and on the interpolation method. In the mathematical and numerical modelling, basic assumptions are made regarding the flow (e.g. neglect of buoyancy effects), the porous matrix (e.g. homogeneity within each

hydrostratigraphic unit), and the boundary conditions, and approximations inherent in the discretization process and the method (finite element or finite difference). In addition, there are approximations in the gridding and contouring of the computed values at the nodes in the finite element grid, for comparison with the initial maps of freshwater hydraulic heads. As a result, one cannot expect a complete match between observed and computed data.

The grid resolution is also very important for using and interpreting the results. The hydraulic head values obtained at a node representing an injection site are *not* the actual values at the injection well. They actually represent the values to be found at an equivalent distance (radius),  $r_e$ , from the well. This distance depends on the type and scale of the model, the grid resolution, and the characteristics of the hydrostratigraphic system. In two-dimensional finite difference modelling, there are expressions to compute the equivalent radius,  $r_e$ , for a well centred in an isotropic grid block of dimensions  $\Delta x$  and  $\Delta y$  (Peaceman 1983):

$$r_e = 0.140(\Delta x^2 + \Delta y^2)^{1/2} \quad (21)$$

There are also expressions which take into account the horizontal anisotropy of the aquifer. Beljin (1987) has shown that the well radius,  $r_w$ , and the blocksize,  $\Delta x$ , also have an influence on the nodal correction,  $r_e$ . Very few attempts have been made to extend these results to multi-aquifer or multi-layered well systems.

In finite element modelling, there are no such expressions to compute the equivalent radius of a node. Charbeneau and Street (1979) used finite element modelling and applied a correction to the hydraulic head around a well, but their method cannot be used here because they assign the discharge to an element instead of a node. Besides, their correction can be applied only to simpler cases (confined or leaky aquifers). The FE3D GW model used for predictive simulations of the effects of injection in the Cold Lake study area is a three-dimensional, finite element, multilayered (in a very complex structure) model, with injection occurring at the grid nodes rather than the block centres. Therefore, it is impossible to compute an equivalent radius of equivalence,  $r_e$ , using a formula similar to equation 21.

The results of mathematical modelling depend on the values of hydraulic parameters and on boundary conditions. Besides these factors, the results of numerical simulations depend on the spatial and temporal discretization, namely the size of the grid and time steps. Fine grids and small time steps bring about more accurate results at the expense of increased computer resources. A sensitivity analysis is usually necessary to define the parameters to which the modelling is sensitive, and to find the optimum solution between the conflicting needs of accuracy and computational costs.

## Sensitivity analysis

For modelling purposes it is necessary to define a bounded three-dimensional region with appropriate boundary conditions for fluid flow. Because the present investigation is directed at the feasibility and effects of deep injection of liquid wastes, the region must be centred approximately around the injection sites and include the prospective injection aquifers and the stratigraphic successions which could be affected. The actual and proposed injection aquifers are in the Mannville Group, Cooking Lake Formation, and Basal Cambrian sandstone (table 1, figure 1).

In the central region of the Cold Lake study area, around the injection sites, there are six aquifer systems (Basal Cambrian, Winnipegosis, Beaverhill Lake, McMurray, Clearwater, and Mannville) which are separated by two aquiclude systems (Lower Devonian and Prairie) and four aquitards (Basal Red Beds, Ireton, Clearwater, and Colorado). The Mannville, Clearwater, McMurray, and Beaverhill Lake aquifers are in contact, in one way or another, within the area around the injection sites. Therefore, they cannot be treated individually, but must be considered as a single, multilayered system. This system is separated from the Basal Cambrian aquifer by a succession comprised of, in descending order, the Prairie aquiclude (140-160 m thick), the Winnipegosis aquifer system, the Lower Devonian aquiclude (up to 300 m thick), and the Basal Red Beds aquitard. Based on the thickness and areal extent of the Prairie and Lower Devonian aquicludes, the two injection zones were considered separately, assuming that no effects would propagate from one zone to another. This assumption was later confirmed by the results of numerical simulations. Therefore, the following two hydrostratigraphic successions were considered for numerical simulations: (1) the Lower Paleozoic succession between the Precambrian basement (impervious bottom) and the bottom of the Lower Devonian aquiclude (impervious top); and (2) the post-Prairie succession between the Prairie aquiclude (impervious bottom) and the top of the bedrock (top of the Colorado aquitard). A previous study in the Cold Lake area (Basin Analysis Group 1985) showed that the Quaternary and Phanerozoic hydrostratigraphic successions can be separated as a result of a strong permeability contrast (about four orders of magnitude) and a negligible cross-formational flow at the top of the bedrock (about  $6 \times 10^{-3}$  mm/a). The separation of the two injection successions was necessary for simulation reasons because available computer resources were not able to handle the number of nodes and elements required to model the entire Phanerozoic succession.

In the Cold Lake study area there are no lateral hydraulic boundaries for the hydrostratigraphic systems below the top of the bedrock. Only geometric boundaries separate the different units, with changes

in the values of hydraulic parameters at interfaces. The values of the hydraulic head along the lateral boundaries of various model areas were obtained from the surfaces of freshwater hydraulic heads as defined in the analysis of the hydrogeological regime in the Cold Lake area (Hitchon et al. 1989). The hydraulic heads at the top of the bedrock were considered to be the same as those at the water table, approximated by the ground surface for the purpose of this study.

A finite element grid composed of 486 surface nodes and 465 surface elements was designed to cover the central region of the Cold Lake study area (figure 11), taking into account all the injection sites and the relevant stratigraphic and hydrostratigraphic boundaries. The grid is finer around the injection sites and coarser toward the edges. The sensitivity analysis with regard to the size of the time step and the radius of influence was performed for a single layer aquifer in order to save on computer resources. The Basal Cambrian aquifer was chosen because it is isolated, being completely sandwiched between an aquiclude (Precambrian) and an aquitard (Basal Red Beds), which itself is covered by another aquiclude (Lower Devonian). The hydraulic heads along the external contour of the finite elements grid, obtained from the surface of freshwater hydraulic heads, were imposed as boundary conditions. The computed potentiometric surface (figure 12) differs from the observed one by 4.23%, with a maximum difference of 7%. Given all

the assumptions and approximations, this match is considered to be good. The FE3DGW model performs a mass balance for the model area, which shows that the net lateral crossflow through the area is  $95 \text{ m}^3/\text{d}$ , and that the total volume of water in this unit (porosity 0.12) is  $182.8 \text{ km}^3$ . The small value for lateral discharge through the area results from the very low permeability of the aquifer.

The only hydraulic parameter in a steady-state fluid flow model is the hydraulic conductivity. The steady-state equation

$$\text{div}[\bar{K}\text{grad}(H)] = 0 \quad (22)$$

for a single aquifer with constant hydraulic conductivity depends only on the boundary conditions. Using the same boundary conditions of prescribed hydraulic heads, simulations for different cases of hydraulic conductivity produce identical distributions of hydraulic heads. Therefore, a sensitivity analysis of the influence of hydraulic conductivity on the steady-state natural flow is not relevant to the study.

Another factor which could influence the solution to equations 20 or 22 is the choice of boundary conditions. However, as previously discussed, the only boundary conditions in the study area are the values of hydraulic head from the natural potentiometric surfaces and the no-flow condition at the top or bottom of the aquifer-aquitard systems bounded by aquicludes.

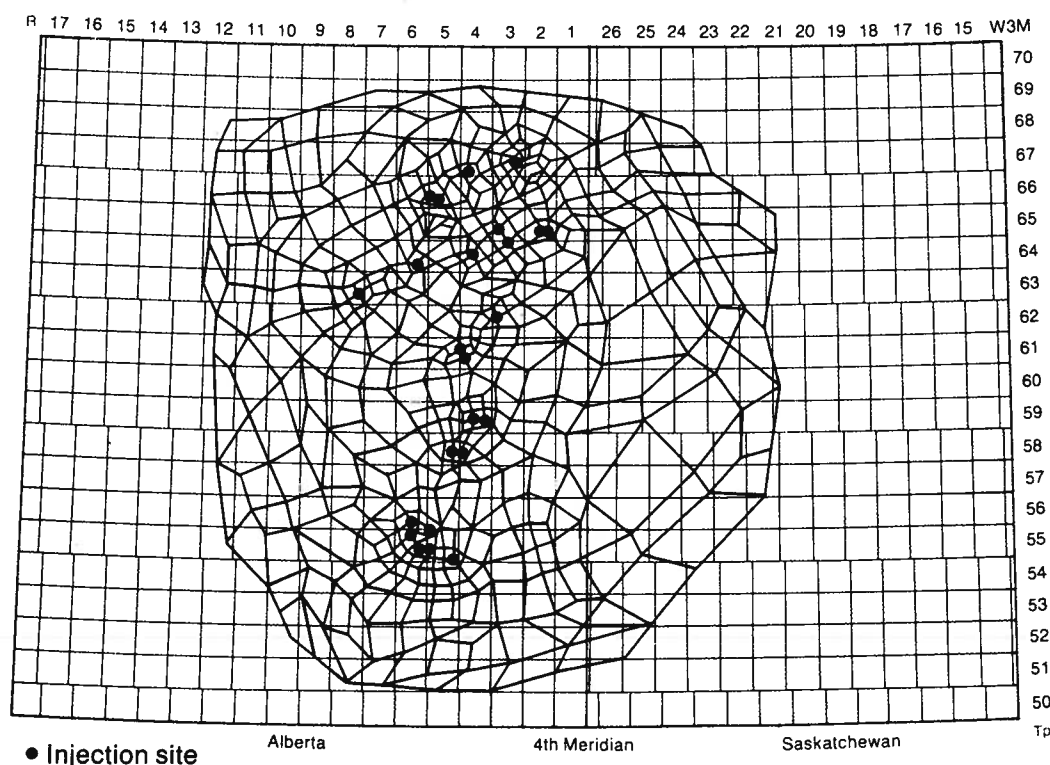


**Figure 11.** Plan view of the finite element grid used for sensitivity analysis, Cold Lake study area.



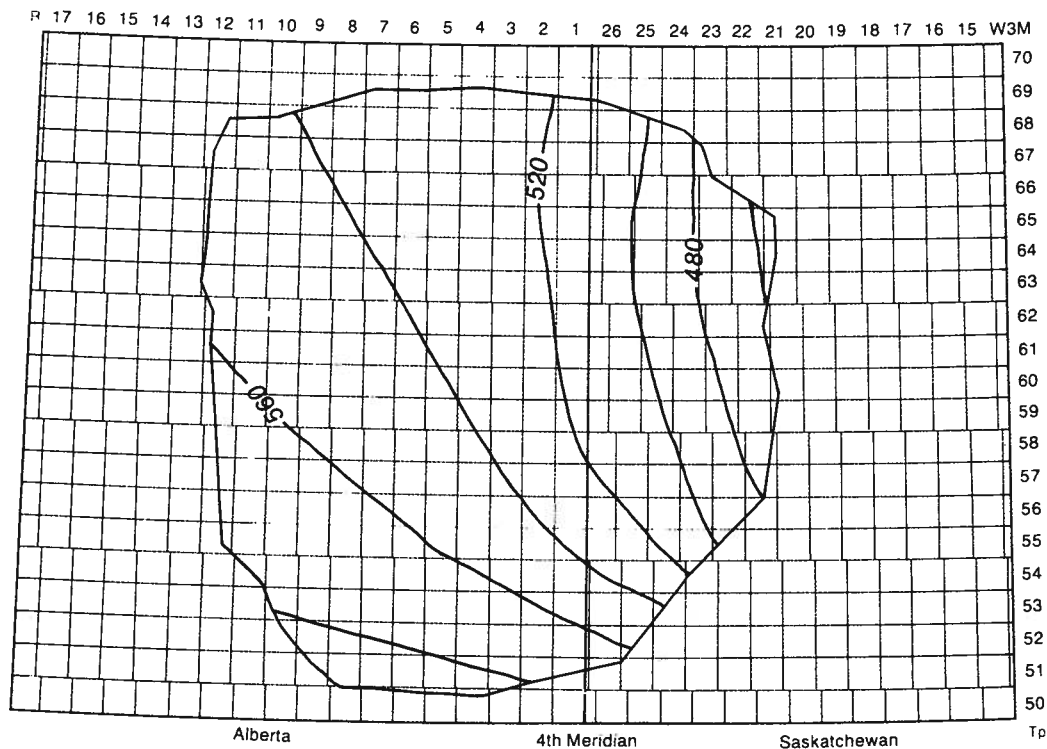


**Figure 12.** Computed freshwater potentiometric surface (m) for the single-layered Basal Cambrian aquifer, Cold Lake study area.

Therefore, the influence of the boundary conditions cannot be analysed and assessed.

A sensitivity analysis with respect to the size of the time step was performed for injection in a single well at 8-33-64-3-W4M, at a constant injection rate of  $14\,100\text{ m}^3/\text{d}$ . This well was chosen because it is the site (of the four injection wells in the Cambrian) with the highest average injection rate over the 30 a period (table 1). Runs were performed for time step sizes of 1, 10, 30, and 60 d, for 70 time steps each. The initial hydraulic head at this injection site was 511 m. For simulations with time steps of 1, 10, 30, and 60 d, the hydraulic heads at the injection site after 60 d were 515.44, 515.41, 515.34, and 515.26 m, respectively. The differences between the computed hydraulic heads with different time steps are larger in the early stages of simulation and become smaller with time. For example, after 2100 d of injection (approximately 3 a) the hydraulic head at the injection site computed with time steps of 30 and 60 d, is 605.66 m, and 605.64 m, respectively. These results are expected because the hydraulic head buildup per time interval is higher at the beginning of injection and becomes smaller as the total hydraulic head buildup tends asymptotically toward a steady-state value. For this reason, it is desirable to have smaller time steps, at least in the early stages of simulation. The difference in computed values using different time steps depends on aquifer characteristics (e.g. thickness, hydraulic conductivity). The situation analysed here is one of the

most critical when compared to the others because of a combination of the following factors: (1) it has one of the highest injection rates; (2) it has a lower hydraulic conductivity (Basal Cambrian versus Mannville or Beaverhill Lake aquifers); and (3) it is a thinner aquifer (relatively speaking) when compared to the injection aquifers higher in the succession. For other projected cases of injection, it is expected that there will be smaller differences between hydraulic heads (computed using different time steps) as a result of any combination of the following factors: a lower rate of injection, greater aquifer thickness, and higher permeability (hydraulic conductivity). Based on this reasoning and on the asymptotic decrease in the differences between computed hydraulic heads for different time steps, a time step of 60 d was used in all the predictive simulations in order to save on computer resources. The duration of 30 a (1985-2015) is equivalent to 183 time steps of 60 d each.

The radius of influence of the injection well was checked by simulating the injection of  $14\,100\text{ m}^3/\text{d}$  for the full length of the 30 a period. Assuming a porous aquifer only (no natural or induced fractures), the cone of hydraulic head buildup at the end of the projected period did not spread beyond about 5 km (half a township) around the injection well. At steady-state (equilibrium), at this injection rate, the hydraulic head buildup will probably spread over most of the Cold Lake study area, but this situation will be reached only after a period of time several orders of magnitude

(tens of thousands of years) larger than the 30 a period of injection analysed here. The radius of influence depends on the rate of injection, hydraulic characteristics, and geometry of the aquifer. Again, the simulated case is more representative of extreme conditions mainly because of a high rate of injection in a thin aquifer. The fact that the cone of hydraulic head buildup is about 10 km (the size of a township) or less in size indicates that the model area (figure 11) can be reduced (in order to save on computer resources) without imposing artificial constraints at the boundaries – constraints which would distort the solution. An attempt was made to find an equivalent radius,  $r_e$ , for the Basal Cambrian aquifer using a trial-and-error method. A simulation of injection of  $14\,100\text{ m}^3/\text{d}$  (at a single site) was performed for a single-layer isotropic aquifer having the local characteristics of the Basal Cambrian sandstone. The hydraulic head increase after 30 a was matched with the analytical solution resulting in an equivalent radius for the injection node of about 700 m. This compares relatively well with the results of using, although incorrectly, relation 21 for computing the value of the equivalent radius,  $r_e$ .

## Calibration of regional models

### Lower Paleozoic system

The Lower Paleozoic aquifer system is defined by four top surfaces (Basal Red Beds, Cambrian, Basal Cambrian sandstone, and Precambrian). The four injection sites are situated in the northern part of the Cold Lake study area (table 1). A smaller model area (figure 13a) was selected from the finite element grid defined previously (figure 11). The number of surface nodes for the smaller model area in the Lower Paleozoic aquifer system is 237, defining 217 surface quadrilateral elements. Because Cambrian strata are not present (as a result of erosion) in the northernmost part of the model area, the total number of nodes and elements in the three-layer system is 827 and 566, respectively. No potentiometric surfaces were previously defined in this succession except for the Basal Cambrian aquifer. The boundary conditions for this succession were defined as prescribed hydraulic heads along the contour of the model area at the top of the Basal Cambrian sandstone. In addition, the boundary conditions were prescribed at three other nodes at the top of the Basal Red Beds for which hydraulic head values were available from drillstem tests, for a total of 31 nodes. Therefore, the number of unknowns in the system is 796 hydraulic head values. The difference between the computed and observed potentiometric surface at the top of the Basal Cambrian aquifer averages 1.4%, with a maximum value of 6%. This match is considered to be good for the natural steady-state flow regime. One of the important results of the natural steady-state simulation is that it provided information regarding the distribution

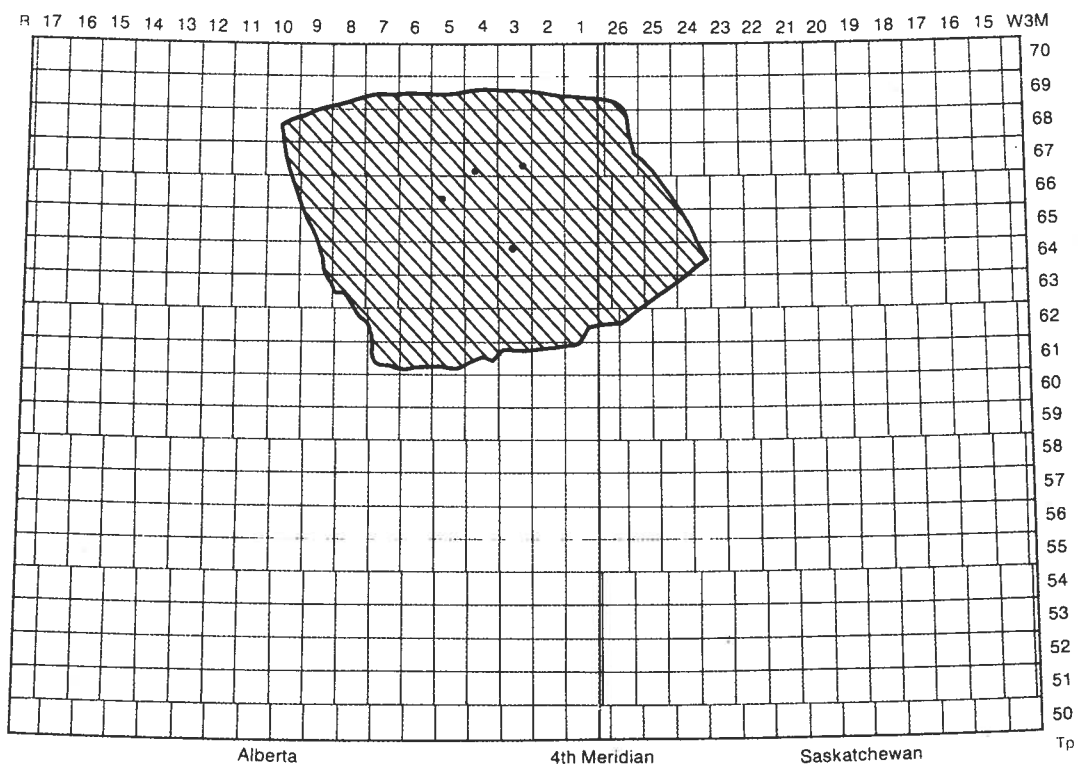
of hydraulic head values everywhere in the system, including at the top of the Cambrian and Basal Red Beds. This information was missing in the previous analysis of the natural fluid flow regime. The distribution of hydraulic heads is necessary in the predictive simulations as an initial condition of the system at the beginning of injection.

### Post-Prairie succession

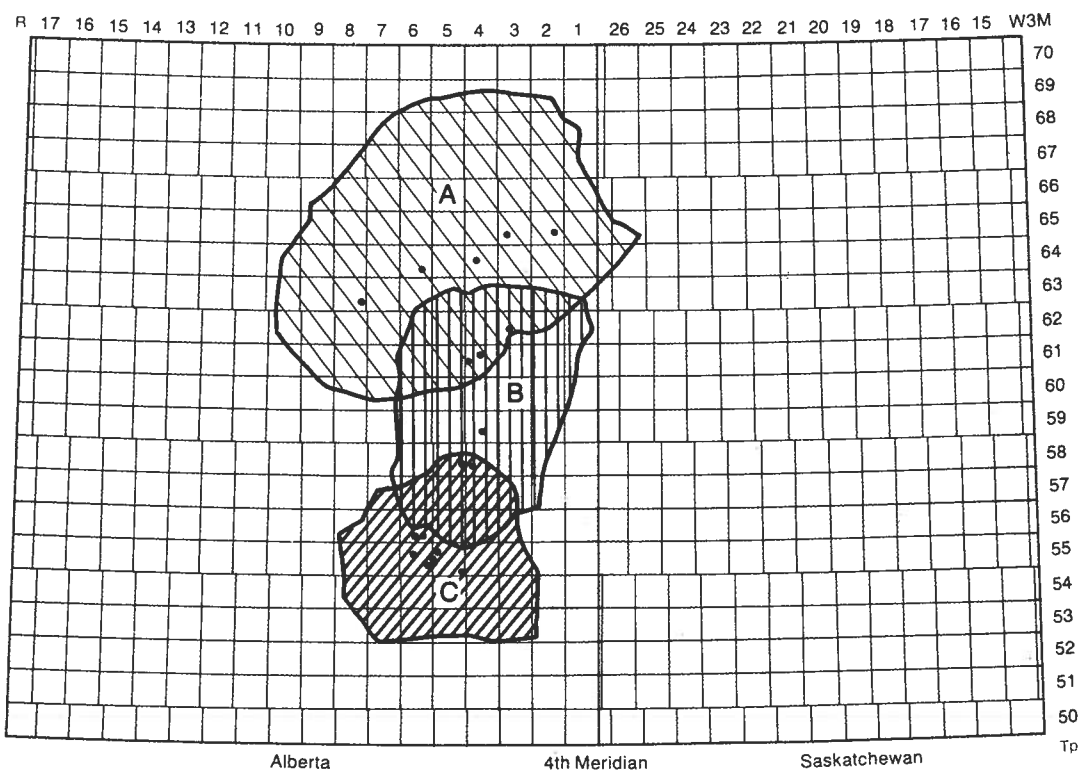
The upper injection succession between the top of the bedrock and the top of the Prairie aquiclude is much more complex. The surfaces defining the top of the Prairie aquiclude, Elk Point Group, Beaverhill Lake aquifer system, Mannville aquifer, and the top of the bedrock cover the entire model area as defined in figure 11. The surfaces defining the top and bottom of the Ireton Formation and the upper and lower Clearwater shales are only partially present; this is a result of either erosion or nondeposition. Furthermore, there are seven oil sand layers in the Mannville Group which have to be taken into account because of their distinct hydraulic properties. Using the initially devised finite element grid (figure 11) for such a complex structure means having to solve a system with approximately ten thousand unknown hydraulic head values at the nodes in the three-dimensional grid. Keeping in mind that the CPU time required to solve such a system is approximately proportional to the square of the number of unknowns, this becomes a prohibitive task. Also, the memory of the computer system used for simulations would not permit such a large number of unknowns. Based on the previous sensitivity analysis concerning the spread of hydraulic head buildup around the injection sites, and taking into account the location and rates of injection, the post-Prairie injection succession was divided into three regional model areas: (A) northern, (B) central, and (C) southern (figure 13b). The finite element grids in each model area are based on the initial finite element grid (figure 11), requiring only the renumbering of the nodes and elements in each of them. The model areas were designed to overlap in order to examine the possibility of a spread of pressure buildup from one injection site toward another (or cluster of injection sites). The validity of this separation into three model areas was later confirmed by the results of predictive simulations.

There are no surfaces of freshwater hydraulic heads to define the initial hydraulic heads and the boundary conditions at all the interfaces between different hydrostratigraphic systems in the post-Prairie succession. Only the tops of the bedrock, the Mannville, Clearwater and McMurray (bottom of the lower Clearwater shale) aquifers, and the Beaverhill Lake aquifer system have corresponding surfaces of freshwater hydraulic heads (Hitchon et al. 1989). The hydraulic head surface at the top of the Mannville Group is only partially defined in the northern area. This information

(a)



(b)



● Injection site

**Figure 13.** Outline of the model areas for simulation of the effects of injection. (a) Lower Paleozoic aquifer system; (b) post-Prairie succession: A. Northern, B. Central, and C. Southern.

**Table 15.** Characteristics and results of numerical simulations of the natural steady-state flow regime in three regional model areas in the post-Prairie injection succession.

		Northern area (A)	Central area (B)	Southern area (C)
No. of surface nodes		231	110	98
No. of surface elements		213	95	84
Total no. of nodes		2550	1384	954
Total no. of elements		2251	1172	841
No. of nodes with boundary conditions		353	204	94
No. of unknowns		2197	1180	860
Mannville*	Average	2.16	1.16	1.58
	Maximum	5.77	3.38	4.68
Clearwater*	Average	4.30	1.58	0.55
	Maximum	8.40	2.43	0.67
McMurray*	Average	3.91	3.23	0.98
	Maximum	8.21	8.01	1.49
Beaverhill Lake*	Average	3.03	1.19	2.19
	Maximum	10.50	4.67	5.70

\*Difference between computed and observed potentiometric surfaces (in percent)

was used to simulate the natural steady-state conditions in the three regional model areas above the Prairie Formation. The simulation was necessary for calibrating the model and obtaining the distribution of hydraulic heads at every point in the system so that they could be used as initial conditions in the predictive simulations. Table 15 presents the characteristics and results of the calibration of the natural steady-state flow regime in the three regional model areas in the post-Prairie injection succession.

It should be noted here that the numerical simulation of natural steady-state flow in the post-Prairie succession provided hydraulic head values for every node in the system. Hydraulic head distributions were thus obtained for the top and bottom of every oil sand layer. The hydraulic head distributions at the top and bottom of the Upper and Lower Grand Rapids oil sand layers are basically no different from the hydraulic head distribution at the top of the Mannville aquifer. The same can be said for the top of the McMurray oil sands in the area where the Clearwater shales are absent. Where the Clearwater shales are present, the hydraulic head distribution at the top of the McMurray oil sands is no different from the hydraulic head distribution at the top of the McMurray Formation. The hydraulic head distribution at the bottom of the McMurray oil sands is more similar to the hydraulic head distribution at the top of the Beaverhill Lake aquifer system than it is to the one at the top of the McMurray Formation. These results confirm the findings of the analysis of the natural flow regime: the oil sand layers in the Mannville Group act as intermediate to weak aquitards and, on a regional scale, the fluid flow in the Mannville Group bypasses them (Hitchon et al. 1989).

The match between computed and observed hydraulic heads in the three post-Prairie model areas is considered to be good, if one takes into account the approximations in data processing and the lack of information for many of the hydrostratigraphic units. Once the numerical model is calibrated for each of the regional model areas, predictive simulations can be performed in order to study the regional and local effects of deep waste injection in the Cold Lake area. The results of the simulation of natural steady-state flow are used as initial conditions for the predictive simulations, and the results of the simulation of injection are compared with these initial conditions.

## Regional simulations of injection

The FE3DGW model used for simulating the effects of injection is deterministic and therefore unable to take into account geostatistical distributions of hydraulic parameters or the uncertainty associated with their determination. The value for any parameter is constant (at least in a volume element), but for regional-scale simulations the same value was allocated to an entire hydrostratigraphic unit. The analysis of the natural fluid flow regime in the Cold Lake study area produced, among other things, estimations of regional values of the hydraulic parameters for the hydrostratigraphic systems (Hitchon et al. 1989). Table 16 presents these values, as well as low and high values for hydraulic conductivities and specific storage; these are values which define an accepted range of variability on a regional scale. It must be pointed out that the low and high values in table 16 are not the minimum and maximum values in point data distributions. The estimated regional value is used as a most probable (normal) case in simulations. Theoretically, a low value in a deterministic model signifies the worst case for fluid flow and hydraulic head buildup, representing an upper limit for the regional effects of injection. The play of hydraulic parameters (equation 20) is such that, for lower hydraulic conductivities the injected fluid moves away more slowly resulting in greater hydraulic head buildups. For the case of a lower specific storage, less injected fluid can be 'absorbed' in the fluid-solid matrix system, again resulting in a greater hydraulic head buildup. The highly improbable combination of a low hydraulic conductivity and a low specific storage in all of the hydrostratigraphic systems represents the worst possible case (a very pessimistic scenario). The opposite combination of high values for both parameters represents the best case, a particularly optimistic scenario. In the beginning, it was intended that predictive simulations for all three cases be performed: normal, worst, and best. However, after simulating the effects of injection using representative regional values for the hydraulic parameters, it became apparent that it was not always necessary to run simulations for the

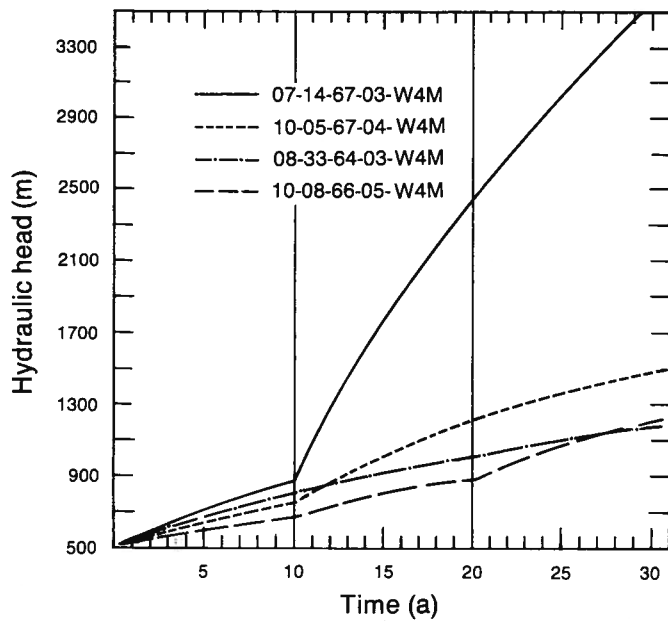


**Figure 14.** Predicted increase in hydraulic head at the four injection sites in the Basal Cambrian aquifer, assuming regional values for hydraulic parameters.

best case. Therefore, in order to save on computer resources, generally only the most probable and worst cases were simulated on a regional scale for the given sites and rates of injection.

#### Injection in the Basal Cambrian aquifer

The results of the simulation of injection at the four sites in the Basal Cambrian aquifer are presented in figure 14 as variation in hydraulic head during the entire period of injection, assuming regional values for hydraulic parameters. The change in the shape and slope of hydraulic head increase is evident for those cases in which the change in the rate of injection is significant. The different hydraulic head buildups at the four injection sites are the result of differences in rates of injection and in the geometry (thickness) of the Basal Cambrian aquifer at the sites (the hydraulic conductivity and specific storage being the same). At the Esso (08-33-64-3-W4M) and BP (10-08-66-05-W4M) sites, the thickness of the Basal Cambrian aquifer is approximately 33-36 m. At the Dome site (10-05-67-04-W4M), although the rates of injection are lower than at Esso and comparable to those at BP, the hydraulic head increase is larger because the injection aquifer is thinner. At the Suncor site (07-14-67-03-W4M), the theoretical hydraulic head buildup is very high. This is a result of the very high rates of injection projected for the final 20 a (more than  $16\,000\text{ m}^3/\text{d}$ ) in an area where the host aquifer is very thin (18 m). The Cambrian aquifer system (post-Basal sandstone) is absent at the BP, Dome, and Suncor sites.

Figure 15 shows the spread of the cone of hydraulic head buildup at the tops of the Basal Red Beds (top of

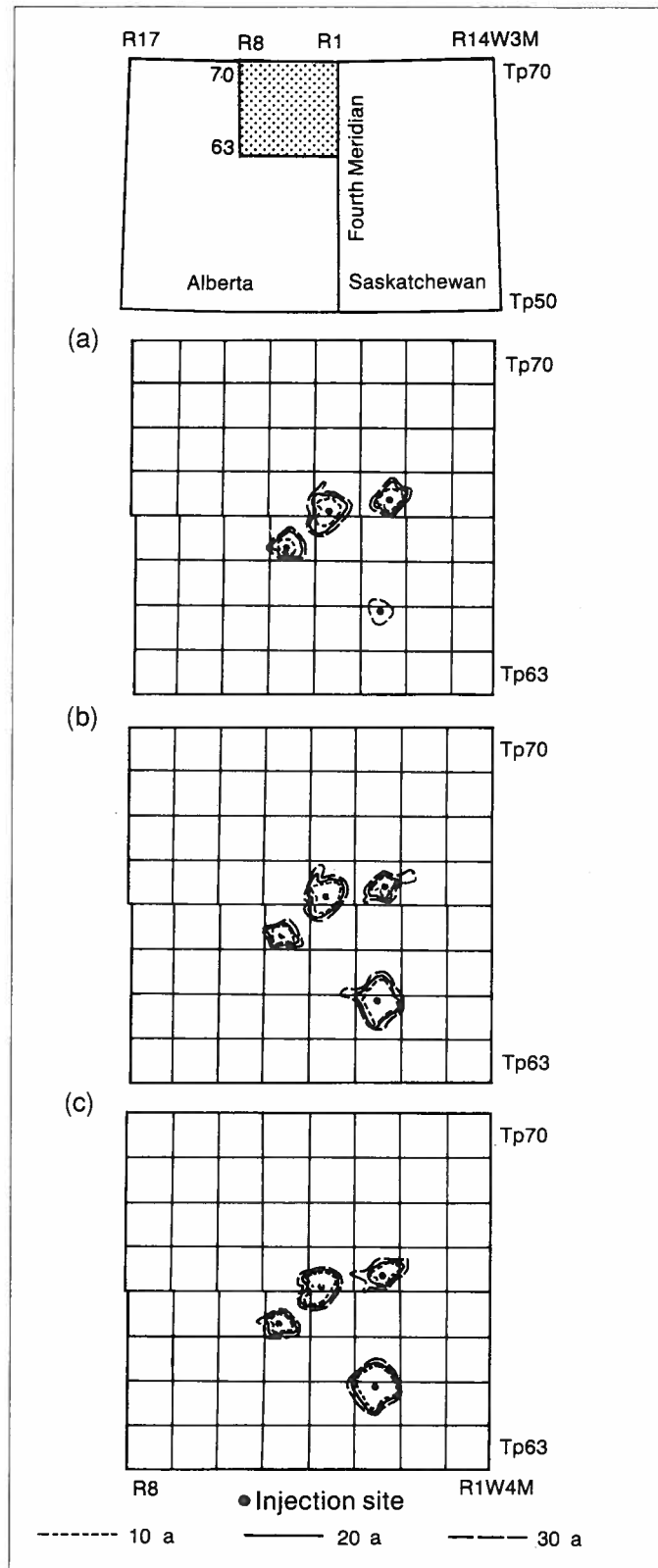


**Figure 15.** Predicted spread of the pressure buildup at the top of: (a) Basal Red Beds; (b) Basal Cambrian aquifer; and (c) Precambrian, assuming regional values for hydraulic parameters.

the Lower Paleozoic succession), the Basal Cambrian aquifer, and the Precambrian (bottom of the Lower Paleozoic succession). The spread of hydraulic head buildup is defined by the 10 m contour line which marks the difference between the hydraulic heads at the FEM nodes at any time step, and the initial hydraulic heads at the beginning of predictive simulations. The value of 10 m was chosen because it represents approximately 2% (on average) of the initial hydraulic heads in the entire hydrostratigraphic succession. This is well within the error margin of all the measurements, and processing and interpretation of the data.

In those areas where the Cambrian aquifer system (post-Basal sandstone) is present, there is no significant propagation of hydraulic head buildup at the top of the succession (Esso site). Where the Basal Red Beds directly overlies the Basal Cambrian sandstone, the effects of injection at the top of the Basal Cambrian aquifer propagate at the top of the succession. The increase at the top of the succession is about 50 to 70% of the increase at the top of the aquifer, with a corresponding area of influence (figure 15a). There is also a significant hydraulic head increase at the bottom of the injection aquifer (figure 15c). In any case, the results of simulation indicate that there is no interference between the injection sites during the projected period of 30 a, assuming regional values for hydraulic parameters.

Using high hydraulic conductivity and high specific storage values, the increase in hydraulic head at the injection sites is seen to be 60-65% lower than in the case in which average hydraulic parameters were used (figure 16). Figure 17a presents the predicted spread of hydraulic head buildup after 10, 20, and 30 a at the four injection sites at the top of the injection aquifer (assuming high regional values for hydraulic parameters).

The worst possible circumstance (low hydraulic conductivity and low specific storage) proved to be a totally unrealistic situation from the point of view of the ef-

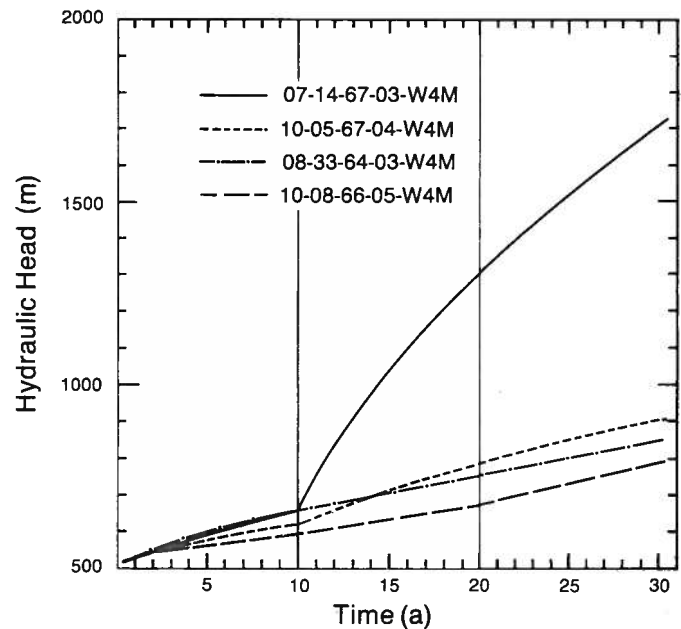


**Figure 16.** Predicted increase in hydraulic head at the four injection sites in the Basal Cambrian aquifer, assuming high values for hydraulic parameters in the Lower Paleozoic aquifer system.

fects of injection – the rock would have been fractured long before the end of the injection period. For this reason, two less extreme cases are presented: (1) low hydraulic conductivity and average specific storage; and (2) average hydraulic conductivity and low specific storage. Table 17 presents the computed hydraulic heads at the four injection sites after 10, 20, and 30 a for the two less extreme cases. Figures 17b and 17c present the spread of hydraulic head buildup at the top of the injection aquifer for these two combinations of values for hydraulic parameters. It can be seen that a lower value for specific storage has a more drastic effect on the hydraulic head buildup than does a lower hydraulic conductivity value. Under conditions of low hydraulic conductivity, after a period of 20 a there will be interference between the BP (10-08-

**Table 16.** Regional estimates of hydraulic parameters.

Aquifer (system)	Hydraulic conductivity K (m/d)			Anisotropy $K_h/K_v$	Specific storage Ss ( $m^{-1}$ )		
	Low	Representative	High		Low	Representative	High
Post-Viking	—	—	—	—	$3.0 \times 10^{-3}$	$4.7 \times 10^{-3}$	$6.9 \times 10^{-3}$
Viking	$2.0 \times 10^{-4}$	0.035	1.300	—	$3.0 \times 10^{-4}$	$4.0 \times 10^{-3}$	$6.8 \times 10^{-3}$
Mannville	$1.3 \times 10^{-4}$	0.035	2.400	90.0	$1.1 \times 10^{-3}$	$5.0 \times 10^{-3}$	$8.5 \times 10^{-3}$
Clearwater	$3.8 \times 10^{-4}$	0.037	4.200	200.0	$1.4 \times 10^{-4}$	$8.0 \times 10^{-4}$	$1.1 \times 10^{-3}$
McMurray	$9.2 \times 10^{-4}$	0.027	9.900	120.0	$3.6 \times 10^{-4}$	$8.0 \times 10^{-3}$	$1.2 \times 10^{-2}$
Grosmont	$1.2 \times 10^{-3}$	0.017	8.300	10.0	$9.5 \times 10^{-5}$	$5.5 \times 10^{-4}$	$1.4 \times 10^{-3}$
Camrose Tongue	$3.4 \times 10^{-3}$	0.022	2.100	40.0	$1.0 \times 10^{-4}$	$4.4 \times 10^{-4}$	$8.9 \times 10^{-4}$
Beaverhill Lake	$6.0 \times 10^{-5}$	0.003	0.077	0.5	$1.2 \times 10^{-5}$	$4.0 \times 10^{-4}$	$1.5 \times 10^{-3}$
Winnipegosis	$6.3 \times 10^{-5}$	0.011	0.210	0.8	$1.9 \times 10^{-5}$	$6.5 \times 10^{-4}$	$6.0 \times 10^{-3}$
Basal Red Beds	$5.0 \times 10^{-4}$	0.011	0.038	110.0	$1.2 \times 10^{-5}$	$2.0 \times 10^{-4}$	$4.4 \times 10^{-4}$
Cambrian	$2.0 \times 10^{-3}$	0.043	0.170	80.0	$1.7 \times 10^{-5}$	$2.8 \times 10^{-4}$	$5.3 \times 10^{-4}$

$K_h$  - horizontal hydraulic conductivity (essentially the representative K of this table)

$K_v$  - vertical hydraulic conductivity from core plug data

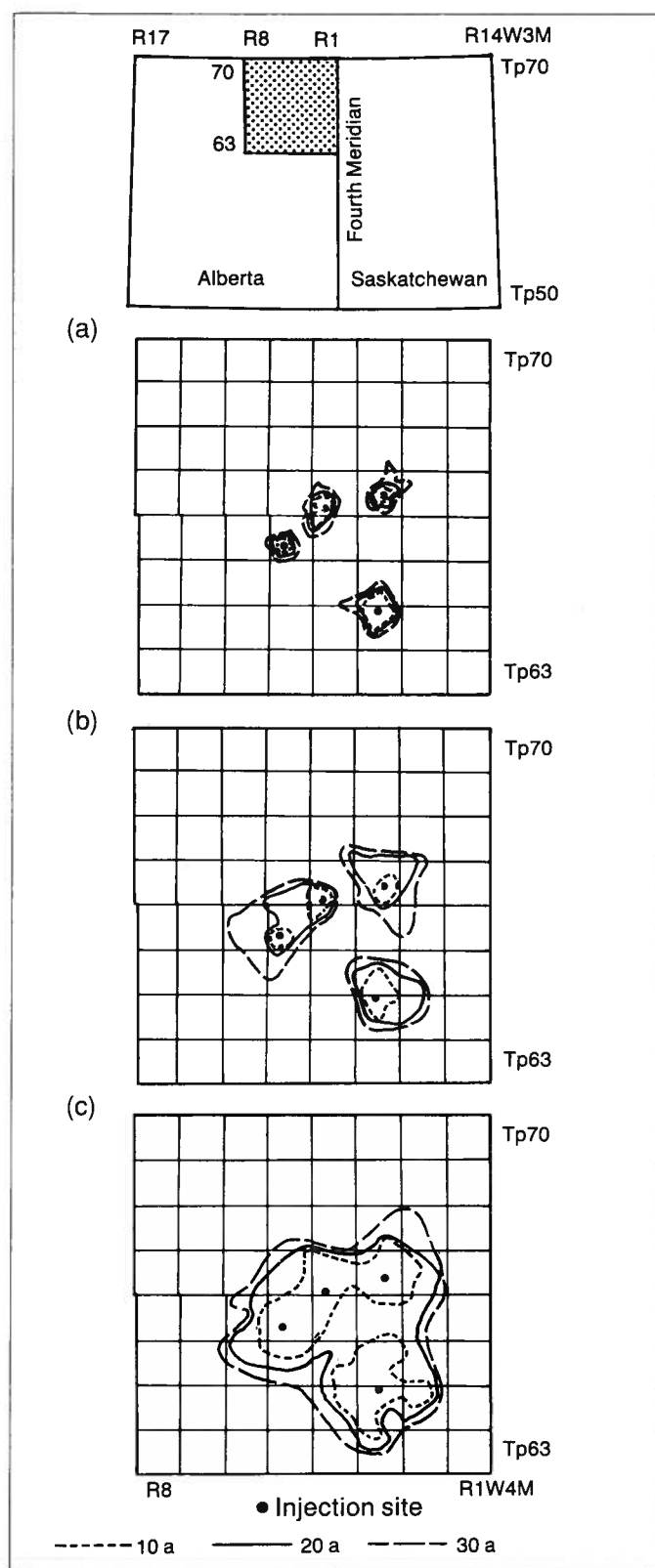


**Figure 17.** Predicted spread of the pressure buildup at the top of the Basal Cambrian aquifer in the Lower Paleozoic aquifer system assuming: (a) high values for both hydraulic conductivity and specific storage; (b) low hydraulic conductivity and regional average specific storage; and (c) regional average hydraulic conductivity and low specific storage.

**Table 17.** Computed increases in hydraulic heads at the four injection sites in the Basal Cambrian aquifer for conditions of either low hydraulic conductivity, or low specific storage, for periods of 10, 20, and 30 a.

Location	Time of injection	Hydraulic head (m)					
		Low hydraulic conductivity			Low specific storage		
		10 a	20 a	30 a	10 a	20 a	30 a
08-33-64-03-W4M		1084	1486	1872	2766	3215	3556
10-08-66-05-W4M		780	1136	1681	1470	2136	3117
07-14-67-03-W4M		1090	3505	5745	2793	9532	11033
10-05-67-04-W4M		867	1508	2122	2011	3645	4102

66-05-W4M) and Dome (10-05-67-04-W4M) sites (figure 17b). In the case of low specific storage, there will be interference between the Suncor, Dome, and BP sites after 10 a, and between all four injection sites after 20 a (figure 17c).

However, these worst conditions are not likely to occur for the following reason. The FE3DGW model used for simulations is a fluid flow model only. As such, the mathematical solution allows for any value of pressure buildup. In reality, the pressure will increase until the fracturing threshold is reached. At that point, fracturing will occur, increasing the hydraulic conductivity around the injection site. The fracturing and the increase in the real value of hydraulic parameters around the injection sites will release pressure, effectively slowing down the hydraulic head buildup. Vertical fracturing may allow cross-formational flow between the injection aquifer and other aquifers higher in the succession. However, that should not be the case in this particular situation. The Basal Cambrian aquifer is overlaid by the Basal Red Beds aquitard and by the Lower Devonian aquiclude (about 300 m thick in the area). Fractures would most likely propagate through the Basal Red Beds aquitard. It is possible that some fracturing may also occur at the bottom of the Lower Devonian aquiclude. However, these fractures are unlikely to propagate all the way through it because of the elastoplastic properties of salt, the major constituent of the aquiclude (Lotsberg and Cold Lake Formations). Even if some fractures were to propagate completely through the Lower Devonian aquiclude to the overlying Winnipegosis aquifer system, another thick (160 m) salt aquiclude (Prairie Formation) overlying this aquifer system would prevent any farther propagation.

#### Injection in the post-Prairie succession

While injection in the Lower Paleozoic aquifer system takes place in a single aquifer (Basal Cambrian sandstone), injection in the post-Prairie succession occurs in different aquifers or sections, all of them interconnected. As explained previously, the predictive simulations were performed on three overlapping model areas. However, the results are presented by



individual injection sites (in terms of hydraulic head increase) and by planes of injection (in terms of the spread of hydraulic head buildup). The average values for hydraulic conductivity in the aquifers of the post-Prairie succession are of the same magnitude as those of the Basal Cambrian aquifer, while the values for specific storage are generally one order of magnitude higher (see table 16). Also, with the exception of the Clearwater aquifer, the thicknesses of the aquifers at the injection sites are greater than that of the Basal Cambrian aquifer. The oil sands are a barrier to flow only in the case of widespread strata such as in the Upper and Lower Grand Rapids Formation. On the other hand, the rates of injection in the post-Prairie succession are lower than in the Lower Paleozoic aquifer system, with the exception of the BP-Grand Rapids site (8-7-66-5-W4M). As a result, it is expected that the effects of injection in the post-Prairie succession will be less than in the Basal Cambrian aquifer. Indeed, the results of the simulations indicate that for the normal situation (regional values for hydraulic parameters), the increase in hydraulic head at the end of a 30 a period is minimal. With the exception of the BP site (8-7-66-5-W4M), the increase in hydraulic head is less than 10% of the initial hydraulic head. In some cases, the increase is so small that it is well within the limits of the noise in the system, i.e. it is in the range of the cumulated errors from measuring to modelling. Even for the BP site, the increase in hydraulic head is only from 525 m to 590 m. Based on these results, no simulations for the best case (high values for hydraulic parameters) were performed. It could be said that the normal case is the best case. The worst possible scenario (low values for both hydraulic conductivity and specific storage) was simulated for the post-Prairie injection succession. Figures 18 to 23 present the increase in hydraulic head at each individual injection site for both the normal and worst cases. For the Dome site at 10-5-67-4-W4M, the depth of the point of injection falls midway

between the top of the Paleozoic and the top of the McMurray Formation. For this reason, the rate of injection was split into two equal parts (allocated at each node) defining the top and bottom of the interval (figures 21c, 21d). For a few injection sites in the Lindberg area, an artificial (fictive) surface was introduced in order to have FEM nodes at specific depths of injection. Otherwise, the injection depths were sufficiently close to an actual node defining a surface as to be allocated to that node. Due to the resolution of the FEM grid, the two Suncor injection sites at Fort Kent (5-28-61-4-W4M and 6-28-61-4-W4M) could not be differentiated and were therefore lumped into a single site with a cumulated injection rate (figure 21b). In the worst case scenario, it can be seen from figures 18 to 23 that the increase in hydraulic heads at the injection sites is generally within the range of natural hydraulic head values in the post-Prairie succession. At seven sites, the increase in hydraulic heads is between 800 and 1100 m.

Figure 24 presents the spread of hydraulic head buildup in four different planes of injection for the worst possible combination of hydraulic parameters. For the normal situation, the buildups are so small that, using the same 10 m contour interval as a marker, it is not significant to represent them. There is no interference between the different injection sites in the post-Prairie succession using average hydraulic parameters. In the worst case scenario, there is some interference in the cluster of injection sites in the Lindberg area (figure 24a) and at the top of the McMurray aquifer in the central area (figure 24c). In addition, the spread of hydraulic head buildup is greater for injection into the Clearwater sandstone aquifer (figure 24b), and the McMurray aquifer between the McMurray oil sands layer and the bottom of the Clearwater shale (figure 24c), as a result of the injection aquifers being thinner in these areas. The southern contour of the hydraulic head buildup spread in these two cases is almost coincident with the boundary of

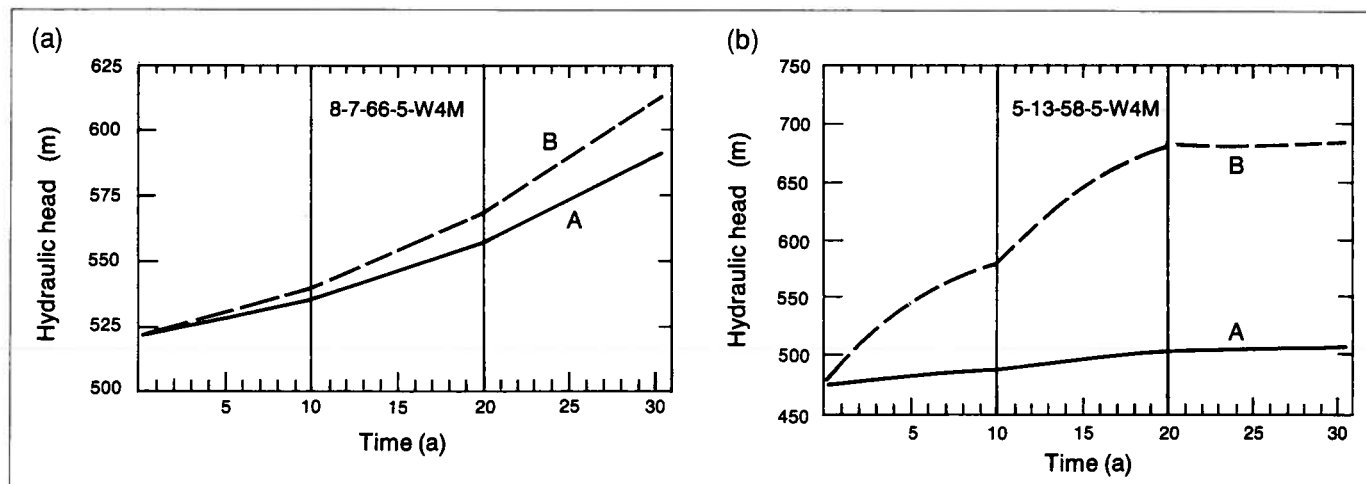


**Figure 18.** Predicted increase in hydraulic head at injection sites in the Mannville aquifer: (a) Grand Rapids; (b) Lower Grand Rapids; assuming A. regional average values for hydraulic parameters, and B. low values for hydraulic parameters.

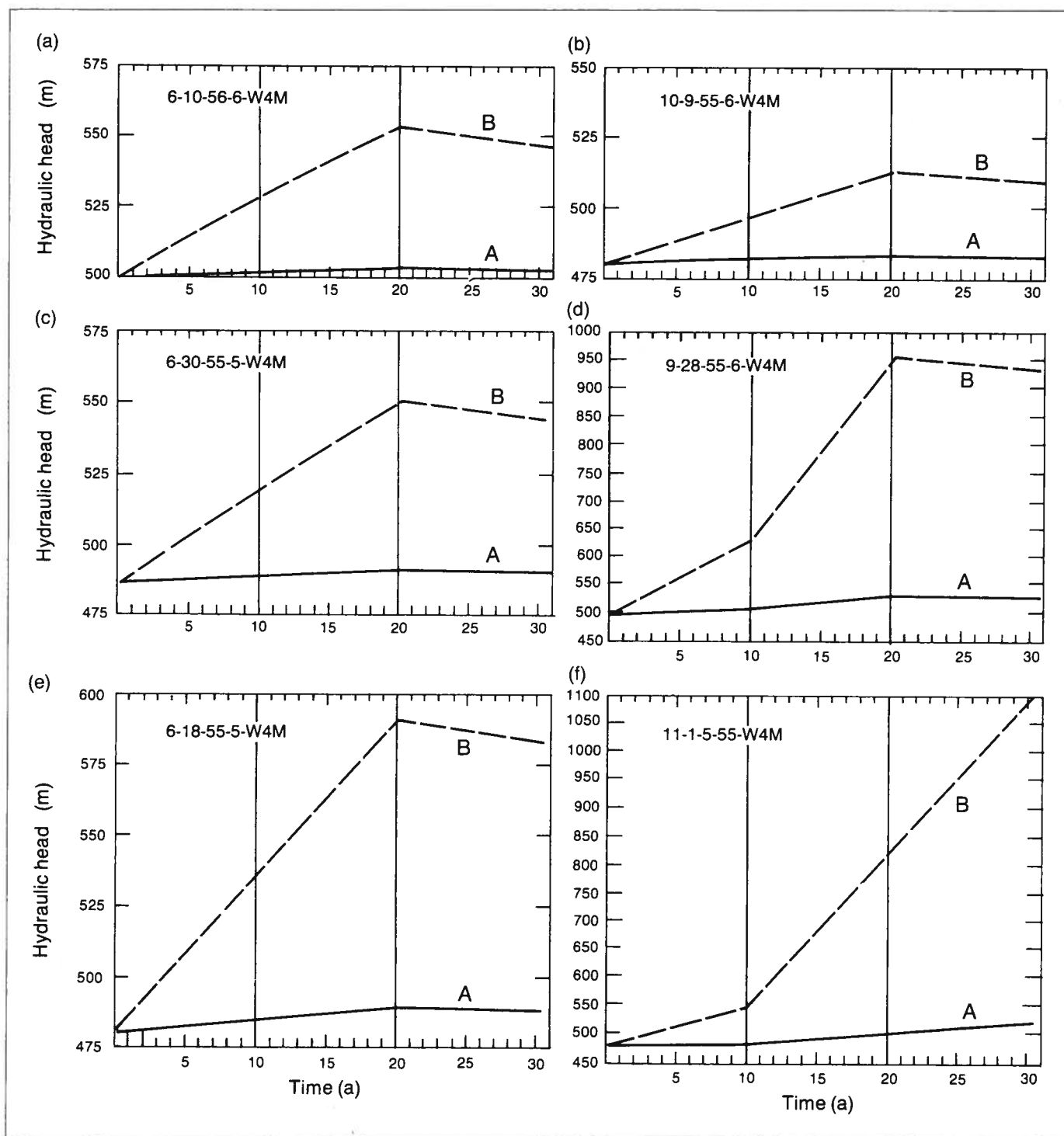


**Figure 19.** Predicted increase in hydraulic head at injection sites in the Mannville aquifer. (a), (c) and (e) in the Rex Member; (b), (d) and (f) in the Lloydminster Formation; assuming A. regional average values for hydraulic parameters, and B. low values for hydraulic parameters.

the Clearwater Formation. South of this boundary, the thickness of the injection aquifer increases rapidly with a corresponding drop in the hydraulic head buildup. There is no interference between the injection wells at the bottom of the McMurray aquifer (figure 24d). Very little pressure buildup takes place at the top of the Mannville Group, and that which does is well within

the limits of natural hydraulic heads in the system. These results show that consideration of the entire post-Mannville succession as a single aquitard is basically a correct approach in terms of the regional effects of injection.

The modelling of the effects of injection used considerable computer resources. For example, a com-

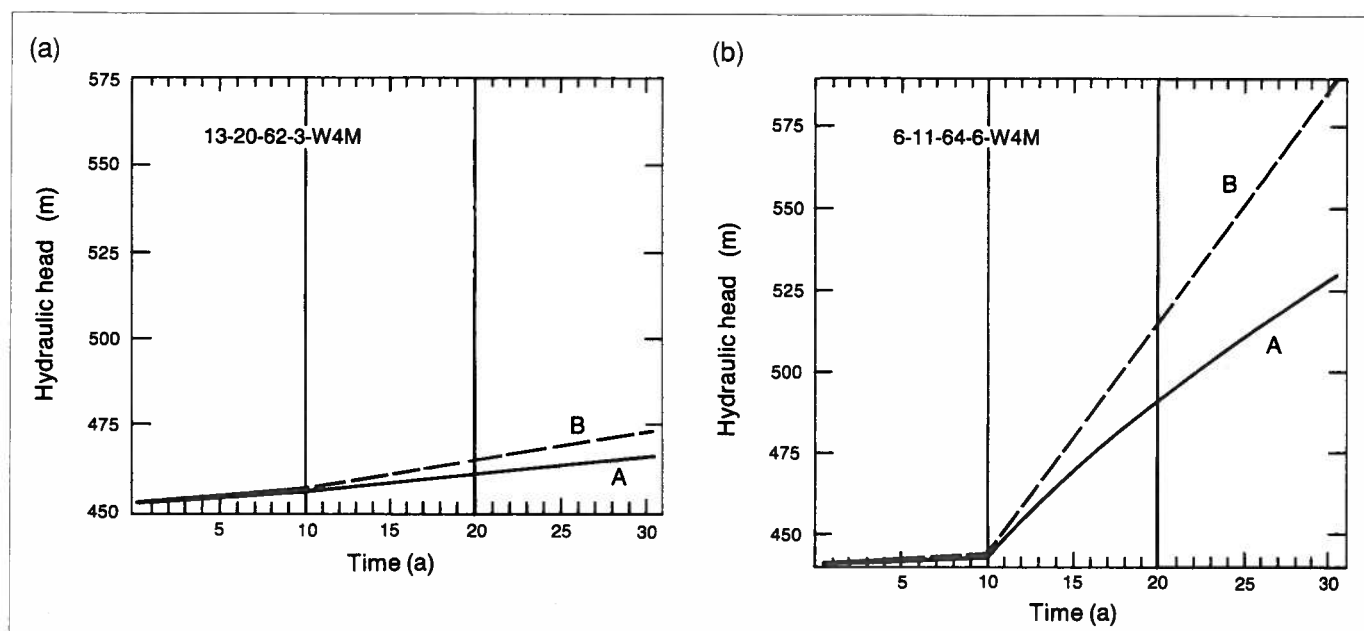


**Figure 20.** Predicted increase in hydraulic head at injection sites in the Clearwater aquifer. (a) Mannville C; and (b) Clearwater; assuming A. regional average values for hydraulic parameters, and B. low values for hydraulic parameters.

plete run for the northern area in the post-Prairie succession (2197 unknowns, 183 time steps) used about 20 h and 33 min CPU time on a VAX11/780 computer. Generally, the amount of CPU time required for simulations is directly proportional to the square of the number of unknowns. This rule was verified in the present simulations upon comparison of the computer resources used for different model areas. The need for large amounts of computer memory during the simulations was also significant.

In conclusion, using average values to characterize hydraulic parameters, numerical simulations on a regional scale revealed no interference between the different injection sites. If minimum values for hydraulic conductivity and/or specific storage are considered, the numerical simulations show (in some cases) areas of superposition of the effects of injection from different sites. In terms of hydraulic head buildups, the results of numerical simulations presented so far apply on a regional scale, starting from a distance of 500-1000 m from the individual injection wells. To determine what may happen closer to the wells, a much finer grid must be used in numerical simulations. Because of the limitations of computer resources, it is not possible to use a finer grid for simulations on a regional scale. However, the injection sites can be modelled individually, on a local scale, based on the results obtained so far which indicate that there will probably be no interference between the wells.

The above conclusions are subject to the following caveats: (1) there is a degree of uncertainty associated with the determination of aquifer characteristics; and (2) the hydraulic conductivity and specific

storage values used thus far in the simulations are regional and characteristic of the entire Cold Lake area (not of any particular site). In order to simulate the effects of injection in terms of hydraulic head buildup at selected individual sites, local values for hydraulic parameters have to be used for all hydrostratigraphic units at each injection site.

### Local hydraulic parameters

The first task was to find values for hydraulic parameters at the injection wells themselves for use in the simulations. However, the latest version (July 1987) of the ERCB data base (installed at the Alberta Research Council and used in the study) does not contain any information of this type at the specific injection sites for the formations under consideration. Therefore, the local values for hydraulic parameters had to be estimated based on data within given distances from the respective sites. These distances varied from site to site and from formation to formation, depending on data availability.

In most instances, the radius of the data search was of the order of 20-30 km, but in a few cases, a lack of data imposed the use of regional values. In addition, the number of values found within this radius was, on the average, less than 5 for aquifers in Paleozoic strata and between 10 and 20 for aquifers in the Cretaceous. This is important in the sense that the values used in the numerical simulations may be more representative for each individual model area around an injection site than are the regional values used in the simulations of the regional effects of injection. However, these values may still not be representative

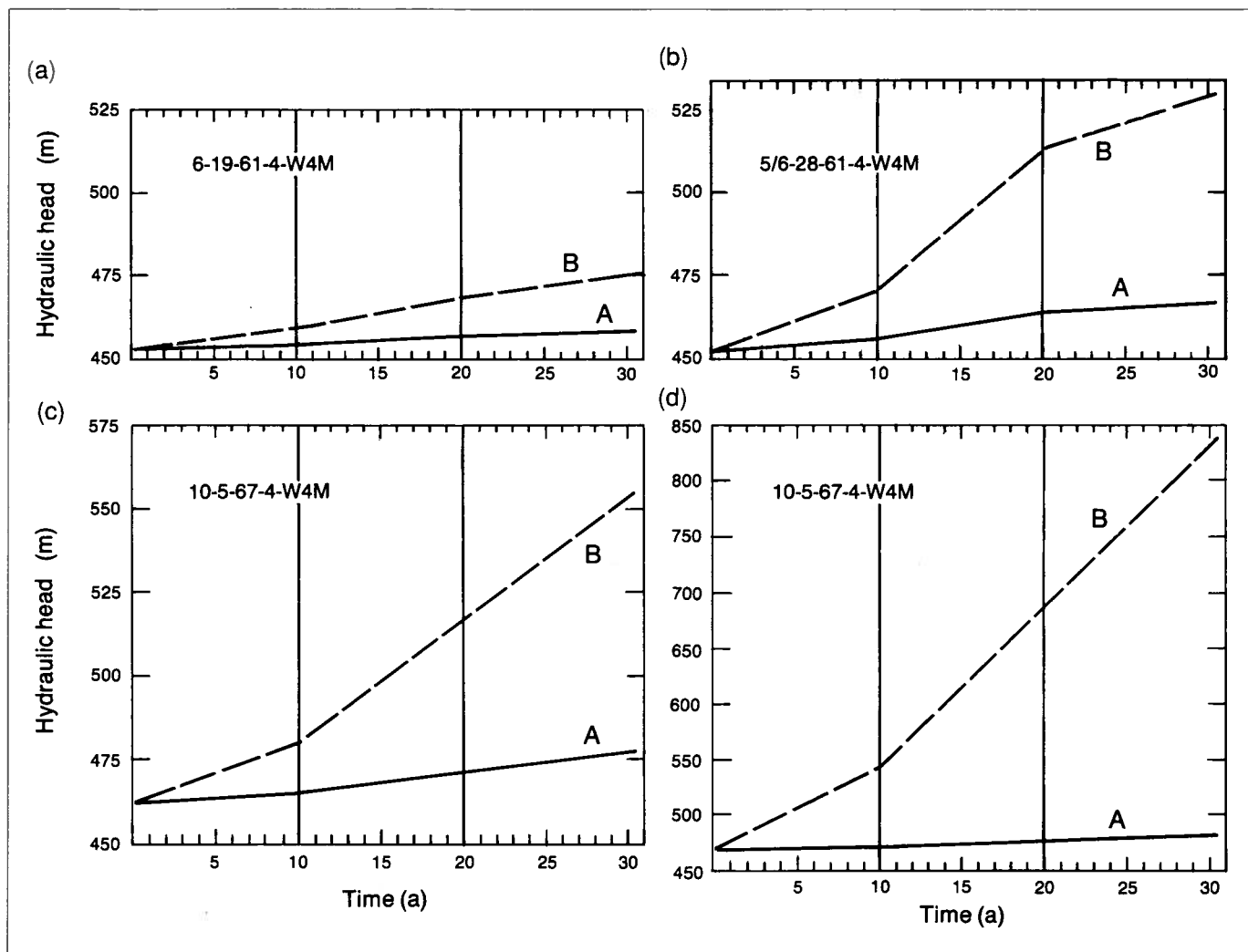


**Figure 21.** Predicted increase in hydraulic head at injection sites in the Clearwater and Mannville aquifers. (a) Clearwater Formation; (b) Lloydminster and Clearwater Formations; (c) and (d) top of the McMurray Formation; assuming A. regional average values for hydraulic parameters, and B. low values for hydraulic parameters.

for the areas around the injection sites themselves. No range of variation is given for the local values for hydraulic parameters because the data samples are too small and too scattered to define corresponding high and low values. Overall, there is a question of the representativeness of such a small data sample. Therefore, the results of numerically modelling the local effects of injection must be considered bearing in mind that there exists an uncertainty associated with the determination of aquifer characteristics, particularly the hydraulic head buildup at the nodes representing injection sites.

The values for hydraulic conductivity and specific storage (for the host aquifers at selected injection sites) used in the numerical simulations of the local effects of injection are presented in table 18. Local values were used for all the hydrostratigraphic units in the succession, but they are not shown because the effects of injection are limited mainly to the host aquifer, as will be seen later. The regional values used

previously are also given for comparison purposes. It can be seen that the local values for hydraulic conductivity are greater than the regional ones by a factor varying from 1.4 for the Grand Rapids Formation to 6.7 for the Cooking Lake Formation. The Clearwater Formation, with a local:regional values ratio of 21.6, is outside this range. This means that, using equation 20, the hydraulic head buildup at the injection sites will be proportionally smaller for local simulations than for regional simulations, if all other elements and parameters are the same (geometry, specific storage, and FEM grid). For specific storage, the ratio of local values to regional ones varies between 0.1 at an injection site in the Grand Rapids Formation and 3.6 for the Basal Cambrian sandstone. No local values were found for the sites in the McMurray Formation and Lloydminster sandstone. Therefore, the regional values for specific storage were used in the numerical simulations at these sites. The variations in specific storage values have a similar effect on the results of

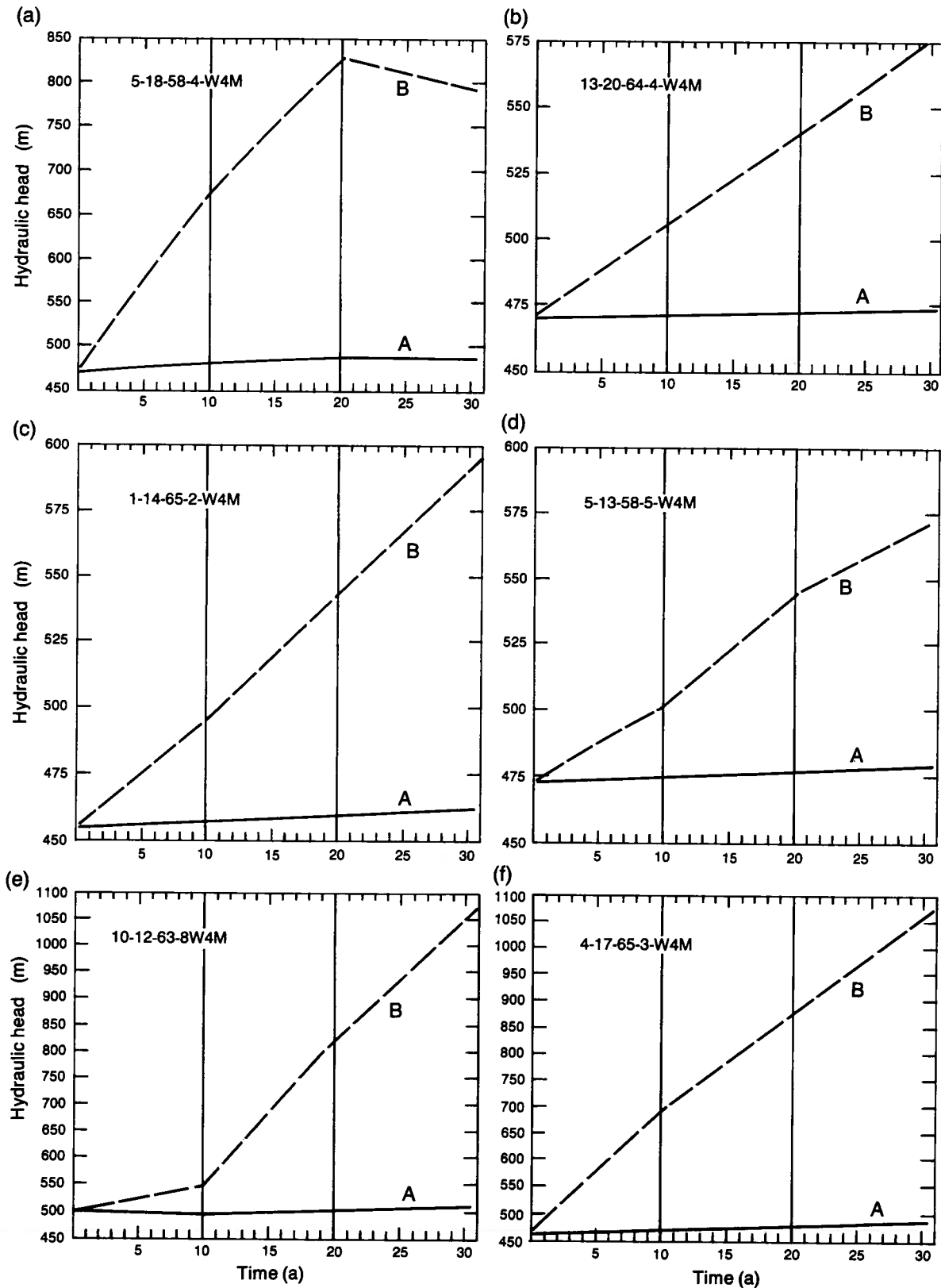


**Figure 22.** Predicted increase in hydraulic head at injection sites close to the pre-Cretaceous unconformity. (a), (c), (d) and (e) at the top of the Cooking Lake Formation; (b) and (f) at the bottom of the McMurray Formation; assuming A. regional average values for hydraulic parameters, and B. low values for hydraulic parameters.

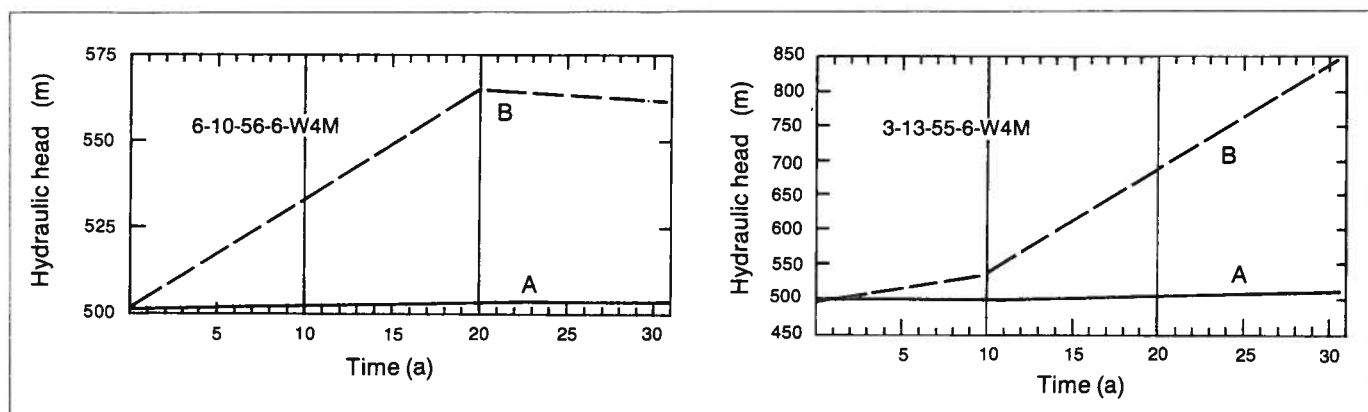


**Figure 23.** Predicted increase in hydraulic head at injection sites in the Beaverhill Lake aquifer system at the bottom of the Cooking Lake Formation; assuming A. regional average values for hydraulic parameters, and B. low values for hydraulic parameters.

numerical simulations as do the variations in hydraulic conductivity, i.e. higher specific storage means lower hydraulic head buildup and vice versa.

It should be mentioned here that the hydraulic conductivity values presented in table 18 are actually values for the horizontal component of the hydraulic conductivity tensor. There were not enough data available to determine local values for the vertical hydraulic conductivity for any of the sites considered for local simulations. Consequently, regional values for anisotropy of hydraulic conductivity (table 16) were used in the simulations. This aspect must also be considered in relation to the degree of confidence in the data used and the corresponding results of numerical simulations.

For the purposes of local-scale simulations, the initial intention was to consider the effects of

geochemical reactions between injected water and the formation water and rocks, on hydraulic parameters such as porosity and permeability (and therefore, on specific storage and hydraulic conductivity). Geochemical modelling of water-rock interactions has shown that these effects are negligible over the predicted period of 30 a of deep waste injection. Moreover, even if certain effects had been considered, the uncertainty and error associated with the determination of local values for hydraulic parameters are much larger than these possible effects, particularly over relatively 'large' areas (more than 100 km<sup>2</sup>) such as those considered in the local simulations. Geochemical reactions in the vicinity of the injection sites must be considered, but this cannot be done even at the scale of local simulations because the scale for geochemical reactions is 2 to 3 orders of magnitude less than the scale for local simulations.

**Table 18.** Local versus regional values for hydraulic parameters used in simulations of the effects of injection in the Cold Lake area.

Site location/ formation	Local values		Regional values	
	K <sub>h</sub> (m/d)	S <sub>s</sub> (m <sup>-1</sup> )	K <sub>h</sub> (m/d)	S <sub>s</sub> (m <sup>-1</sup> )
11-1-55-5-W4M/ Lloydminster	0.10	5.0x10 <sup>-3</sup>	0.035	5.0x10 <sup>-3</sup>
3-13-55-6-W4M/ Cooking Lake	0.02	5.5x10 <sup>-4</sup>	0.003	4.0x10 <sup>-4</sup>
5-13-58-5-W4M/ Lower Grand Rapids	0.10	5.0x10 <sup>-4</sup>	0.035	5.0x10 <sup>-3</sup>
5-13-58-5-W4M/ Cooking Lake	0.02	5.0x10 <sup>-4</sup>	0.003	4.0x10 <sup>-4</sup>
5-28-61-4-W4M/ Clearwater	0.80	4.0x10 <sup>-4</sup>	0.037	8.0x10 <sup>-4</sup>
6-28-61-4-W4M/ Cummings	0.10	8.0x10 <sup>-3</sup>	0.027	8.0x10 <sup>-3</sup>
10-8-66-5-W4M/ Cambrian	0.10	1.0x10 <sup>-3</sup>	0.043	2.8x10 <sup>-4</sup>
8-7-66-5-W4M/ Grand Rapids	0.05	7.5x10 <sup>-3</sup>	0.035	5.0x10 <sup>-3</sup>
10-5-67-4-W4M/ Cambrian	0.10	1.0x10 <sup>-3</sup>	0.043	2.8x10 <sup>-4</sup>
10-5-67-4-W4M/ McMurray	0.10	8.0x10 <sup>-3</sup>	0.027	8.0x10 <sup>-3</sup>

## Local simulations of injection

The ten injection sites selected for local simulations of hydraulic head buildup are distributed over the entire Cold Lake area in Alberta, and include all of the host aquifers. However, some of them are at the same location but different injection depths, and others are relatively close to each other. This distribution made it possible to delineate only five model areas for local simulations, covered by appropriate finite element grids. One area in the north (figure 25a) includes two Basal Cambrian sandstone injection sites (10-8-66-5-W4M and 10-5-67-4-W4M). For the post-Prairie succession, a northern model area (almost identical to the Cambrian one, but with fewer surface elements) includes sites with injection into the Grand Rapids (8-7-66-5-W4M) and McMurray (10-5-67-4-W4M) Formations. A north-central area (figure 25b) includes two sites which are very close to each other: in the Clearwater Formation at 5-28-61-4-W4M, and in the Cummings sandstone at 6-28-61-4-W4M. A south-central

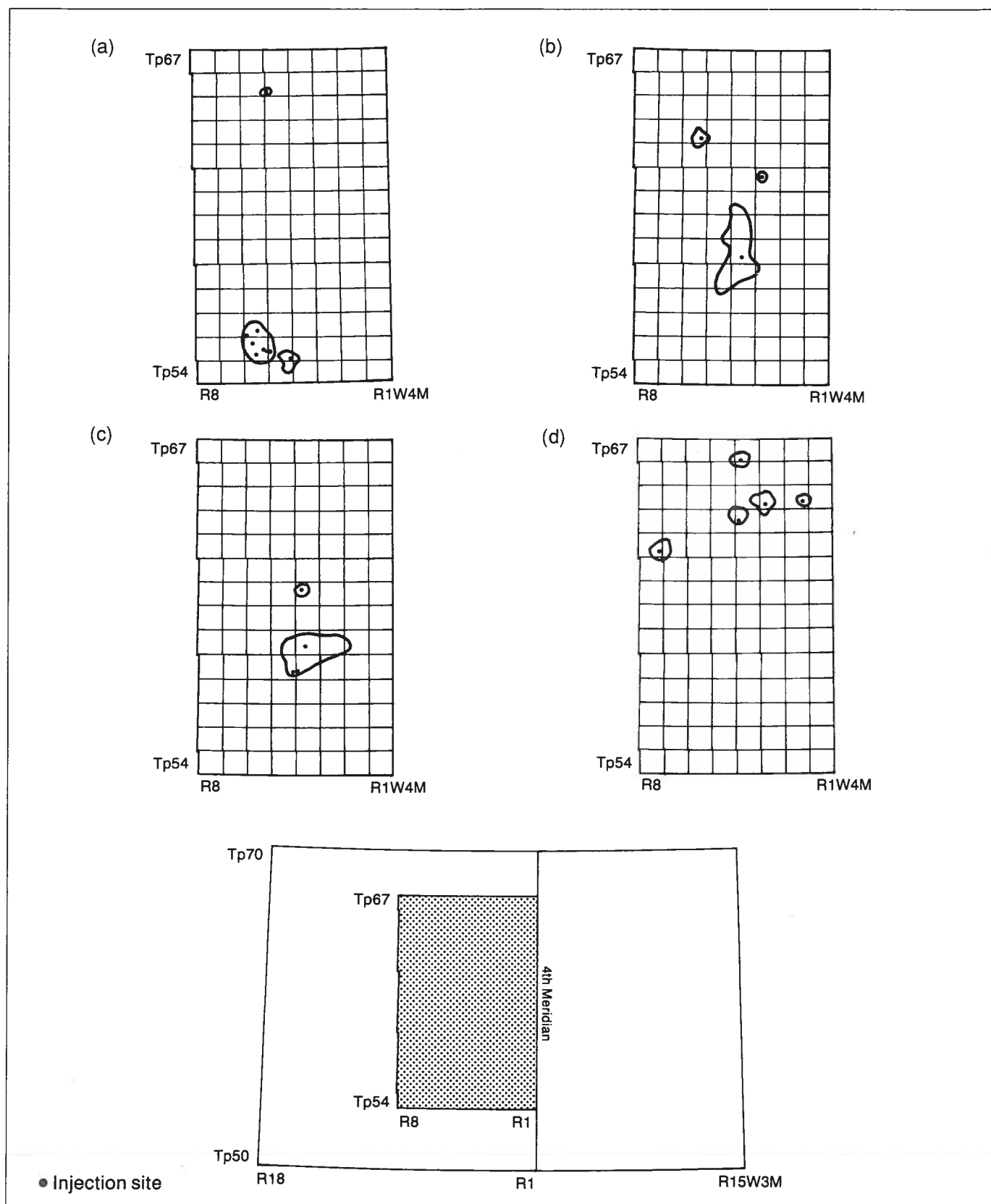


**Figure 24.** Predicted spread of hydraulic head buildup as a result of injection in the Mannville, Clearwater and McMurray aquifers. (a) Mannville Group; (b) Clearwater sandstone; (c) top of the McMurray Formation (also in some places at the top of the Cooking Lake Formation); assuming low values for hydraulic parameters for the injection aquifers (the contour represents the 10 m isoline of hydraulic head increase after 30 a).



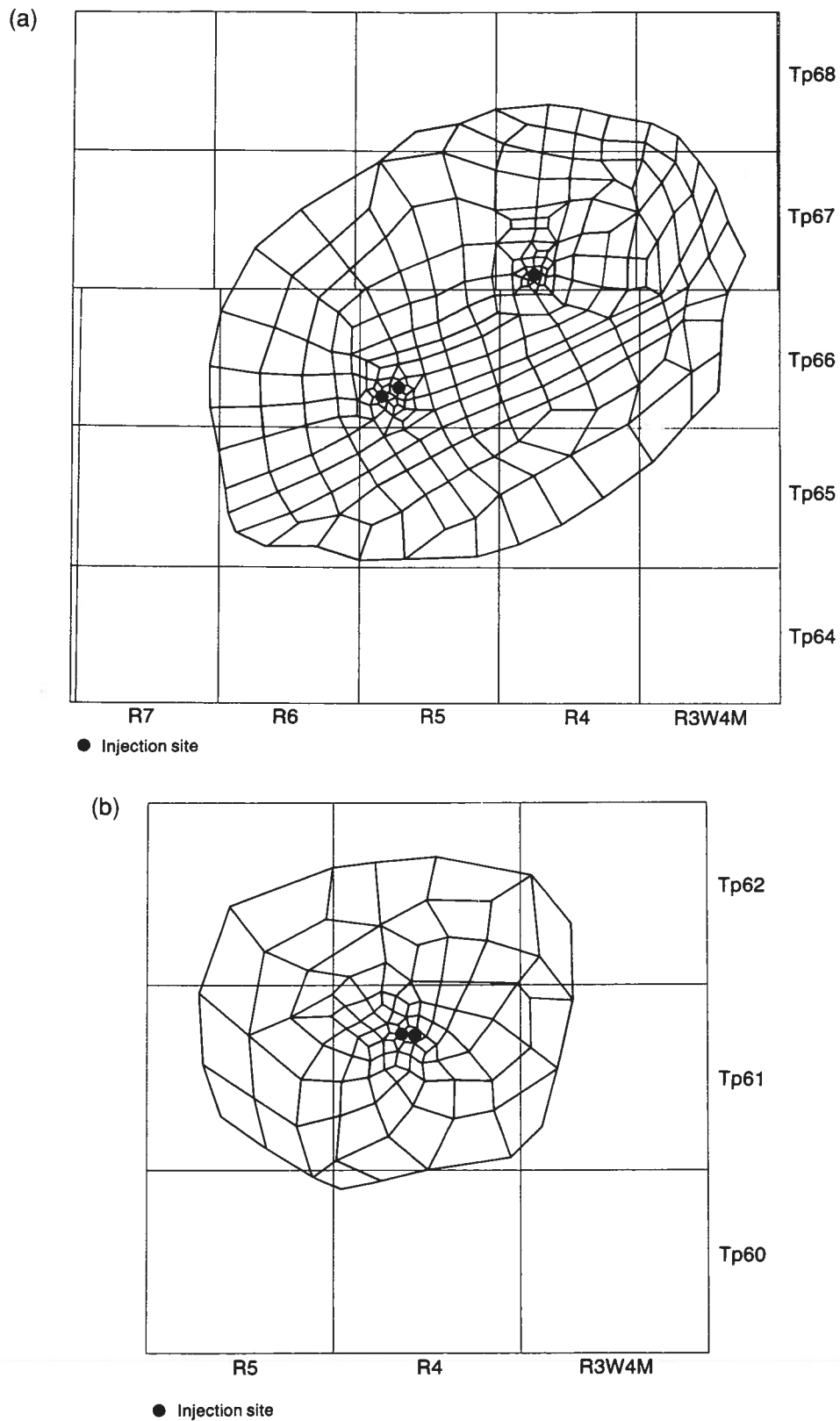


**Figure 25.** Plan view of the finite element grids used for local simulation of the effects of injection in the Cold Lake area. (a) Lower Paleozoic, northern area; (b) post-Prairie, north-central area; (c) post-Prairie, south-central area; and (d) post-Prairie, southern area.

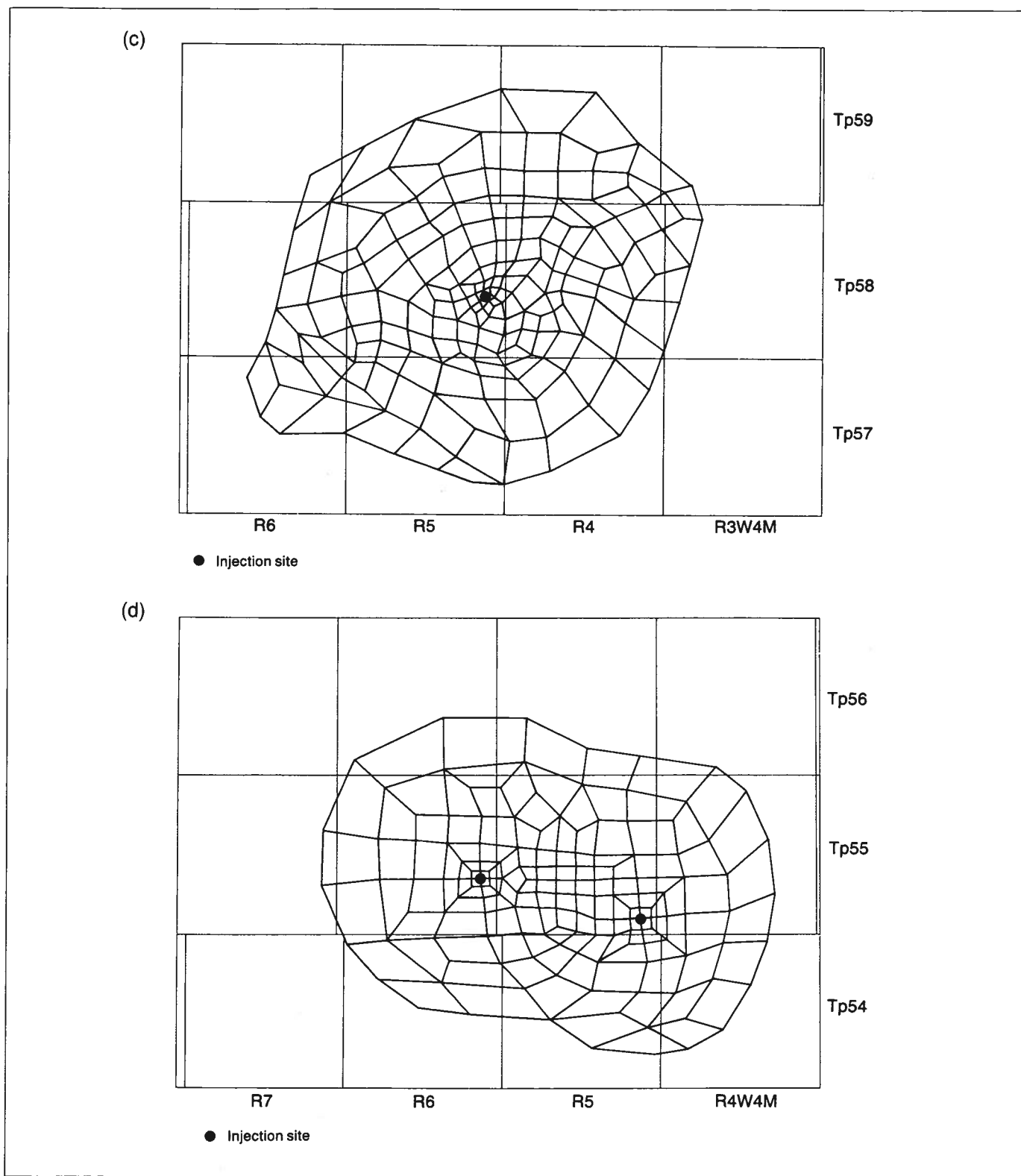


**Figure 25.** (continued)

area (figure 25c) is centred around a site at 5-13-58-5-W4M where injection takes place in both the Lower Grand Rapids Formation at 510 m depth, and in the Cooking Lake Formation at 600 m depth. Finally, a southern model area (figure 25d) includes two injection

sites: at 11-1-55-5-W4M with injection in the Lloydminster sandstone, and at 3-13-55-6-W4M with injection in the Cooking Lake Formation. Table 19 presents the characteristics of the finite element grids and the computer resources (CPU time) required to

**Table 19.** Characteristics of the finite element grids and CPU time used for local simulations of deep waste disposal at selected sites in the Cold Lake area.

Model area	Surface nodes	Surface elements	Total nodes	Total elements	Boundary condition nodes	Unknowns	CPU time for 183 timesteps
Lower Paleozoic	269	250	1016	716	35	981	40 min
Northern Post-Prairie	210	194	2099	1800	330	1769	2 h 20 min
North-central Post-Prairie	103	93	1338	1122	175	1163	1 h 3 min
South-central Post-Prairie	174	160	2216	1964	252	1964	2 h 50 min
Southern Post-Prairie	148	136	1652	1458	192	1460	1 h 53 min

simulate the deep injection of liquid wastes over a period of 30 a with a time step of 60 d.

The finite element grids covering these model areas have a higher resolution than the grids used for the regional simulations of the effects of injection. As a result, each injection node represents an equivalent distance (radius) of 80-160 m from the actual well; this is 5-10 times smaller than the equivalent radius for the injection sites in the regional simulations. The numerical solution depends on the grid resolution in such a way that the value of the hydraulic head buildup at the injection site is larger for smaller finite elements around it (smaller equivalent radius). Therefore, if all other parameters and conditions are the same, the hydraulic head buildups at the injection sites will be larger in local simulations than in regional simulations. However, the values of the hydraulic parameters used in the local simulations are different from those used in the regional simulations (table 18). The final result therefore depends on the interplay between greater hydraulic conductivity values, smaller or larger specific storage values, and greater resolution of the areal finite element grids. The magnitude of the vertical dimension of the three-dimensional finite elements is unchanged in the local simulations versus the regional simulations. This is a result of the vertical dimension being defined by the actual thicknesses of the hydrostratigraphic units in the succession. It must be stressed that the aquifer geometry used in these simulations was determined on a regional scale and may not correspond to the actual thickness of the strata at a particular site. The results and conclusions of sensitivity analysis and calibration of modelling on the regional scale were also considered to be valid for the simulations on the local scale.

Simulation of injection in the Basal Cambrian aquifer at the BP and Dome sites confirmed the previous results indicating that there is no interference in terms of pressure buildup between the two sites (figure 26). The variations in hydraulic head at the nodes representing the injection sites are presented in figure 26. The hydraulic head increase is greater in local simulations than in regional simulations, as would be expected for a smaller equivalent radius. However, the

difference is not proportionally larger because of the attenuating effect of the larger hydraulic conductivity and specific storage values used in local simulations (table 18). The changes (breaks) in the patterns of hydraulic head increase are the result of significant and sudden changes in injection rates (table 1). Although the injection rates are higher at the BP site than at the Dome site by a factor of 3 to 4, the hydraulic head increase is greater at the Dome site because the host aquifer is thinner.

With respect to fracturing, comparison of the hydraulic head increases at these two sites with the respective values of breakdown pressures (table 14) shows that the fracturing threshold will be reached after a few years of operation. After initiation of vertical fractures, the flow regime will change as a result of corresponding changes in hydraulic parameters, such that the results of the present modelling would no longer be valid. The study of the effects of injection in terms of fracturing must be undertaken at the scale of the well site using different mathematical and numerical models which take into account the stress regime and the fracturing process (initiation, propagation, etc.). It is suggested that the fractures would not propagate all the way up to the post-Prairie succession because of the thicknesses of the intervening strata, particularly the salt beds (Lotsberg, Cold Lake, Prairie), which exhibit elastoplastic properties.

Local simulations of injection at the Dome and BP sites in the post-Prairie succession (northern model area) again show a greater increase in hydraulic heads (figure 27) than is seen in regional simulations, with no interference between the sites (figure 27). This is mainly due to a higher resolution finite element grid. The local values for hydraulic conductivity and specific storage are of the same magnitude as the regional ones at the BP site, so the numerical increase is clearly a result of a smaller equivalent radius. Comparison with the fracturing threshold (table 14) at the BP site in the Grand Rapids (Mannville) aquifer shows that the fracturing threshold will be reached after 15 to 20 a of injection. The fractures will be vertical, but will probably be deflected at the top of the Mannville Group and change from being vertical to being horizontal before

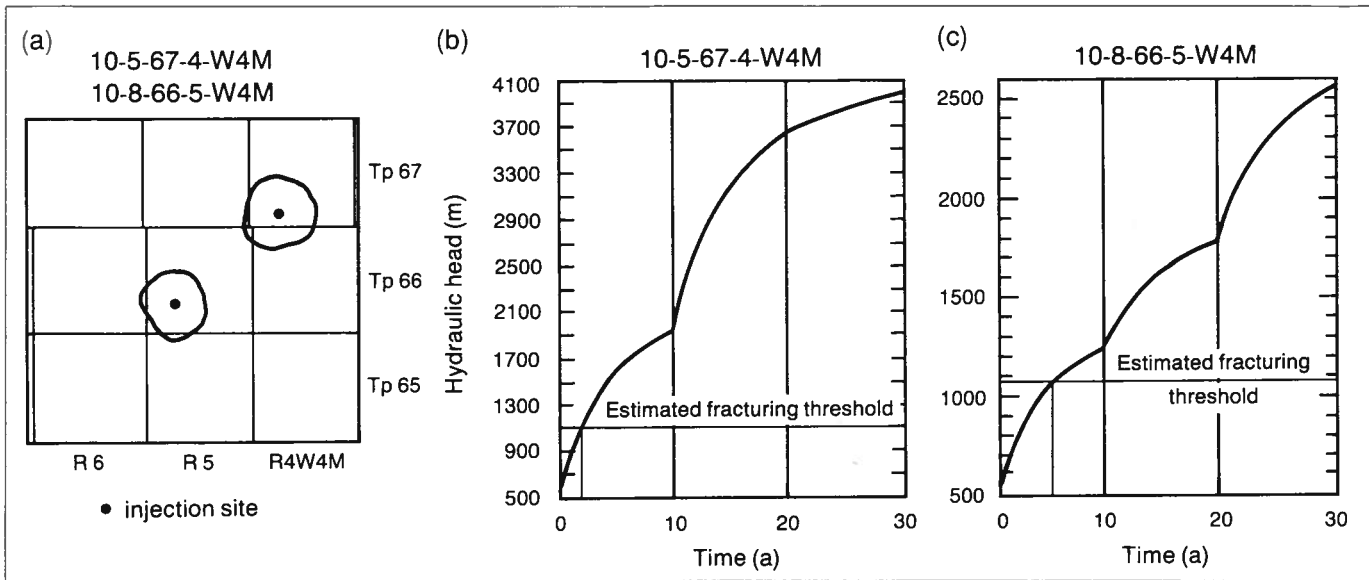


**Figure 26.** Predicted effects of injection in Lower Paleozoic (Cambrian) aquifers at Dome (10-5-67-4-W4M) and BP (10-8-66-5-W4M) sites. (a) spread of hydraulic head buildup (the contour represents the 10 m isoline of hydraulic head increase after 30 a); (b) hydraulic head increase at Dome site; and (c) hydraulic head increase at BP site.

reaching the top of the bedrock (Dusseault and Simmons 1982). At the Dome site, the increase in hydraulic head is still below the fracturing threshold for the McMurray Formation (the effect of higher resolution of the finite element grid is attenuated by a four-fold increase in the value of hydraulic conductivity).

The injections at the Suncor sites in the north-central model area were simulated previously on a regional scale at a single injection node because of the limits imposed by the finite element grid. The higher resolution of the grid used for local simulations allowed them to be modelled individually. The varia-

tions in hydraulic head at the respective sites are shown in figure 28, while the radii of influence are shown in figure 29. The decrease in hydraulic head after 20 a is a result of corresponding decreases in injection rates. The combined effect of greater hydraulic conductivity values (table 18) and higher grid resolution is such that, while greater than in regional simulations, the hydraulic head increase at these two sites is still significantly lower than the fracturing threshold. This fact allows for extrapolation from the radius of equivalence to the well and the assumption that fracturing will not occur. This assumption should still be

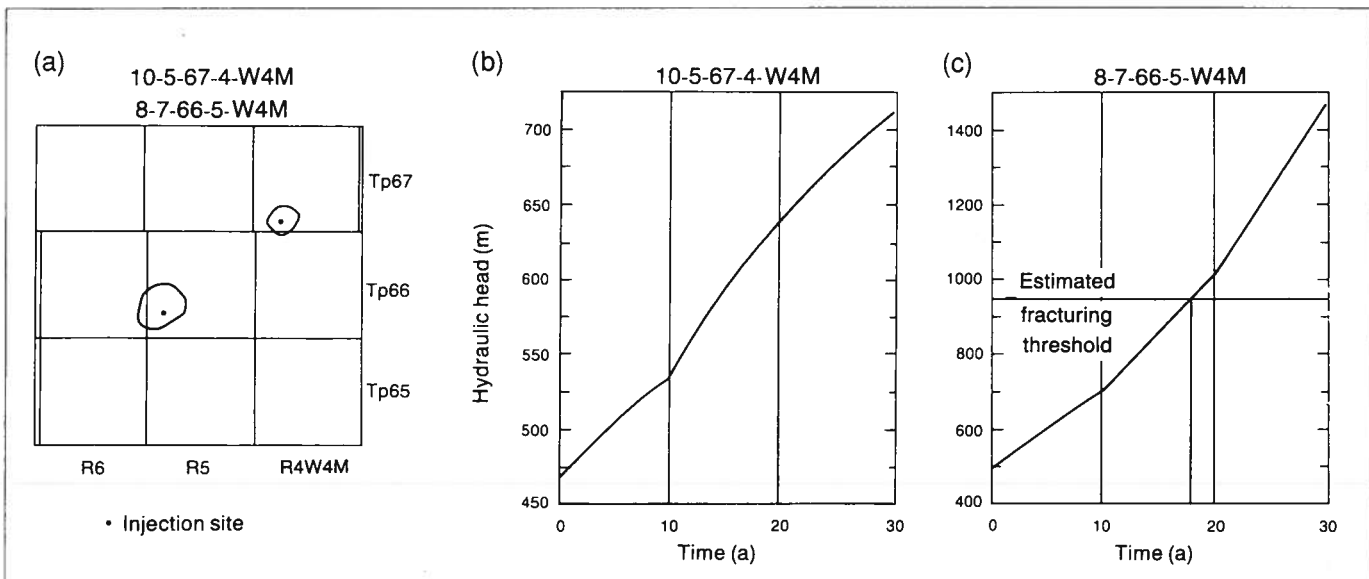


**Figure 27.** Predicted effects of injection in post-Prairie aquifers at Dome (10-5-67-4-W4M) and BP (10-8-66-5-W4M) sites. (a) spread of hydraulic head buildup (the contour represents the 10 m isoline of hydraulic head increase after 30 a); (b) hydraulic head increase at Dome site; and (c) hydraulic head increase at BP site.

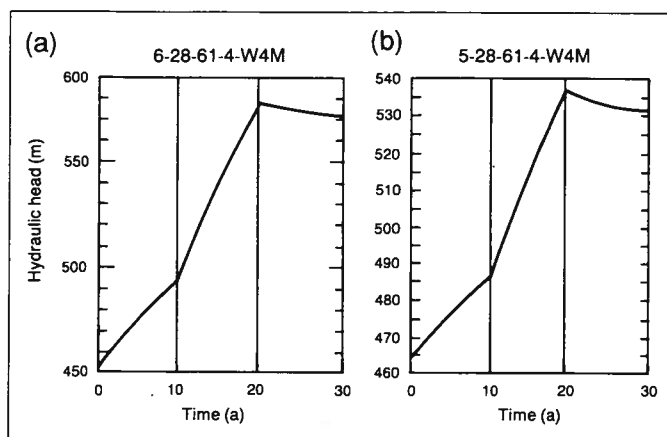


**Figure 28.** Predicted increase in hydraulic head at Suncor sites as a result of injection in (a) Cummings Member at 6-28-61-4-W4M; and (b) Clearwater Formation at 5-28-61-4-W4M.

verified by modelling fracture initiation at the injection wells themselves.

In the south-central model area, injection was simulated at the same location in the Lower Grand Rapids and Cooking Lake Formations. At the Cooking Lake site (Beaverhill Lake aquifer system), the hydraulic conductivity has a local value seven times greater than the regional one and a slightly larger specific storage value (table 18). This explains why the hydraulic head increase (figure 30a), although higher than is seen in regional simulations, is still significantly lower than the fracturing threshold. Again, it can be assumed that at this site fracturing will not occur. At the Lower Grand Rapids site (figure 30b), the hydraulic head increase is below the fracturing threshold, but not by a significant amount. In this case, the effects of a threefold increase in the hydraulic conductivity values used in local simulations are cancelled by the effects of a tenfold decrease in the value of specific storage (table 18). It can be assumed that at the injection well itself fracturing may occur near the

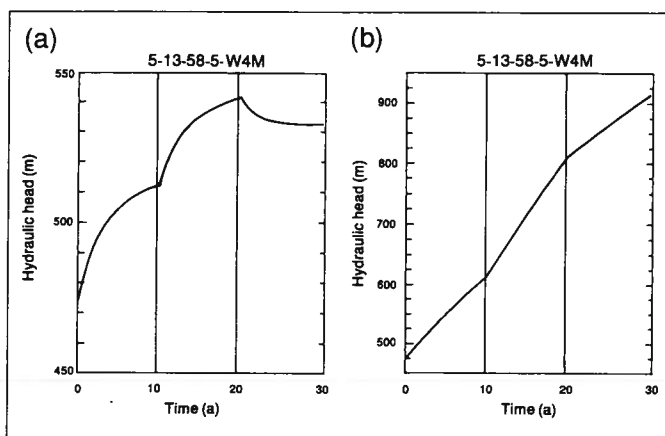


**Figure 30.** Predicted increase in hydraulic head at Murphy site (5-13-58-5-W4M) as a result of injection in (a) Cooking Lake Formation; and (b) Lower Grand Rapids Formation.

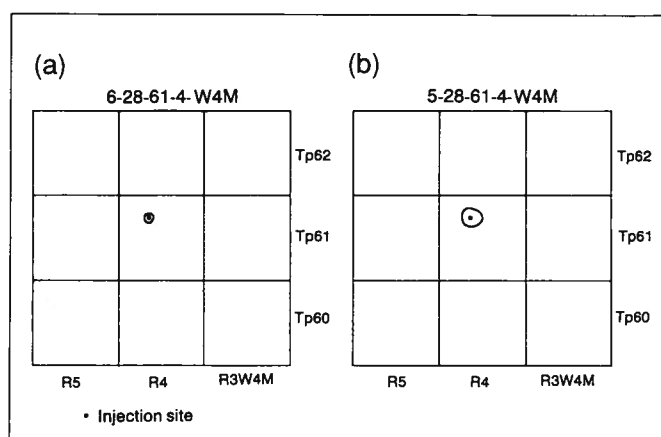


**Figure 29.** Predicted spread of hydraulic head buildup at Suncor sites as a result of injection in (a) Cummings Member at 6-28-61-4-W4M; and (b) Clearwater Formation at 5-28-61-4-W4M (the contour represents the 10 m isoline of hydraulic head increase after 30 a).

end of the injection period depending on the real values of hydraulic and stress characteristics at the site. However, as before, a vertical fracture will probably be deflected at the top of the Mannville Group and change to a horizontal fracture (Dusseault and Simmons 1982). The shapes of the curves of hydraulic head increase are a result of variations in injection rates (table 1) and the different geometry of the two injection aquifers. The radius of influence around these injection sites is shown in figure 31.

In the southern model area, local simulations were carried out for both Westmin sites, one in the Lloydminster sandstone and one in the Cooking Lake Formation. The hydraulic head increase as a result of injection in the Cooking Lake Formation is very small, and the effect of using a higher resolution grid is cancelled by significant increases in the values of hydraulic parameters used in modelling (table 18). For injection into the Lloydminster sandstone, the hydraulic head increase (figure 32) is larger than is

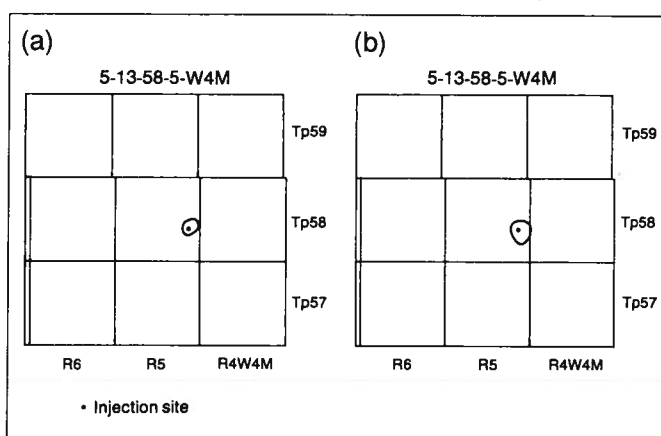


**Figure 31.** Predicted spread of hydraulic head buildup at Murphy site (5-13-58-5-W4M) as a result of injection in (a) Cooking Lake Formation; and (b) Lower Grand Rapids Formation (the contour represents the 10 m isoline of hydraulic head increase after 30 a).

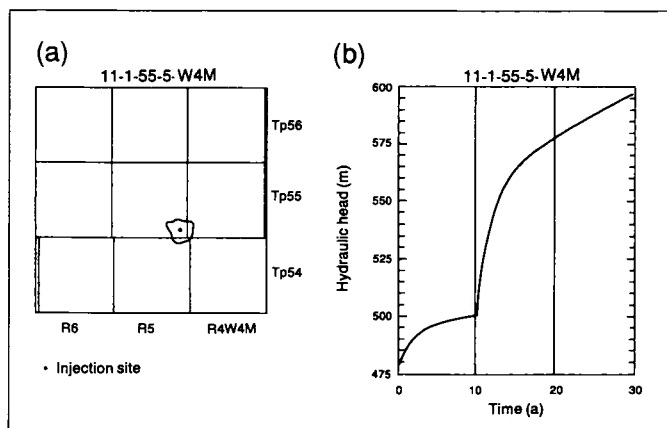


**Figure 32.** Predicted effects of injection at Westmin site (11-1-55-5-W4M) in the Lloydminster sandstone. (a) spread of hydraulic head buildup (the contour represents the 10 m isoline of hydraulic head increase after 30 a); and (b) hydraulic head increase.

seen in regional simulations. This is a result of a fivefold increase in the grid resolution versus only a threefold increase in the hydraulic conductivity value used in local simulations. However, the increase in hydraulic head is still significantly lower than the fracturing threshold; therefore, by extrapolation, it is assumed that fracturing will not occur at either site during the projected period of injection. The radius of influence of injection around the Lloydminster site is shown in figure 32.

The local simulations performed for selected sites confirmed the conclusion that there is no interference between injection sites. According to the results of these simulations, the fracturing threshold will be reached at sites injecting into the Basal Cambrian aquifer and at some sites injecting into the post-Prairie succession. Vertical fractures initiated in Cambrian rocks will probably be interrupted by the overlying thick salt formations, while the vertical fractures initiated at some sites of injection into the Mannville Group will probably be deflected and transformed into horizontal fractures before reaching the top of the bedrock. The above conclusions should be confirmed by studies of hydrofracturing at the scale of the injection sites using values for the parameters involved that are measured at the sites.

## Evaluation of the results

The evaluation of effects of deep waste disposal in the Cold Lake area was based so far on data generally available from regulatory agencies, mainly the ERCB. Virtually no information used in the simulation of injection and in the evaluation of breakdown pressures is site specific. Even the rates of injection, as supplied by Alberta Environment, are predicted averages over ten-year intervals. The immediate question arising from these facts is the issue of the applicability of the results. In order to validate the results obtained so far,

an attempt was made to compare computed with actual pressure buildups.

The ERCB requires submission of monthly disposal water well injection data, which comprise maximum monthly pressure at the wellhead, total monthly injection volume, and hours of injection. The operating license issued by the ERCB sets a maximum operating pressure. When this maximum pressure is reached, the injection well is shut down for a period of time.

The National Hydrology Research Institute awarded a contract to Stanley Associates Engineering Ltd. (SAEL) of Edmonton to search the ERCB files and compile the data necessary for validation of the predicted pressure buildups as a result of deep waste injection in the Cold Lake area. The results of the data search and processing were presented in an interim report (SAEL 1988). The main conclusions of the study performed by SAEL are that ERCB information is of no use in defining a pressure-volume relation, and that these data are not useful in the validation of the numerical model used to predict pressure buildups. Taking the data search a step further, SAEL contacted the operators of waste injection wells and gained access to confidential daily injection data. These data, again, show no correlation between the injected volume and the recorded wellhead pressure, which is relatively constant. As a result of the SAEL study, it became apparent that validation of the numerical simulations through history matching is not possible because of the absence of reliable injection data. For proper comparison of computed and actual pressure buildups there is need for rigorous recording of injected volumes and downhole pressures.

Another aspect which has to be taken into account when considering the results in this bulletin is the absence of any evidence and information about the existence and characteristics of natural and induced fractures close to the injection wells. The estimation of characteristic values for hydraulic conductivity and specific storage is based on information within a certain distance from the injection wells, usually of the order of  $10^0$ - $10^1$  km. No well-specific information was available for these estimations. If microfractures are present, their effect would be to increase the hydraulic conductivity of the host aquifer, with the consequence of decreased pressure buildups. If large fractures are present, the characteristics of the flow would change from single porous medium to dual porosity. However, it has to be emphasized here that in most cases injection takes place in the unconsolidated sands of the Mannville Group. In this case, the existence of large fracture systems is highly improbable. The complexity of the problem is increased if there are natural or induced fractures in the overlying aquitards, or improperly abandoned wells in the close vicinity of the injection wells. These fractures and wells could constitute vertical conduits for the upward migration of

contaminants to the shallow aquifers used as sources of water.

Chia and Chiu (1989) used both a single and a dual porosity model (three-dimensional, finite-difference) for mass transport in fractured porous media to assess the upward migration of underground injected wastes. The results of their analysis show that in a typical injection aquifer, over a period of 20 a, the contaminants can move laterally up to a few hundred metres and regional upward migration through an extensive, con-

fining formation is a very slow process. Nevertheless, injected wastes can move rapidly upward through microannuli and channels in the cement sheath of the injection well, through improperly abandoned wells in the immediate vicinity, and through fractures in the disturbed zone. The work of Chia and Chiu (1989) confirms the results of the present evaluation and strengthens the conclusion that a site-specific assessment should be undertaken.

## Conclusions

The baseline natural hydrogeological regime was determined for the entire Phanerozoic succession in a region defined as Tp 50-70, R 15 W3M to R 17 W4M (60 000 km<sup>2</sup>) in the Cold Lake area (Hitchon et al. 1989). The local effects of present and future deep waste injection in the area were studied at ten individual sites in terms of geochemical processes, fracturing thresholds, and hydraulic head buildups. The sites were chosen based on data availability and their representativeness, such that all injection aquifers (Basal Cambrian, Cooking Lake, McMurray, Clearwater, and Grand Rapids) were examined. The regional effects were studied at 27 sites in terms of hydraulic head buildups using projected rates of injection to the year 2015.

Water-rock interaction effects were evaluated for the Basal Cambrian, Beaverhill Lake, McMurray, Clearwater, and Mannville aquifers using the computer code SOLMINEQ.88. Reservoir mineralogy was determined from selected cores and representative formation water analyses were reevaluated because of incomplete determinations and saturation with minerals in the aquifers. Twenty wastewaters from the Cold Lake area were used in the modelling. The most important minerals which may precipitate from or dissolve into the fluid are quartz and calcite. Calculations indicate that 20% of the available silica will precipitate from solution in 30 a if the solution is supersaturated with quartz. For a solution supersaturated with calcite, 50% of the amount of calcite that can form will do so in 3-4 d. This suggests that the most important change that can be made to wastewater is softening or the removal of CO<sub>2</sub>.

Fracturing thresholds were evaluated using accurate calculations of overburden stresses and Poisson's ratios derived from digitized density and acoustic geophysical logs. The hydraulic head buildups were simulated using regional and local values for hydraulic conductivity and specific storage. The results are representative for distances of approximately 100-500 m from the injection wells,

depending on the resolution of the finite element grid used in numerical simulations. The results show that there is no interference between the different injection sites, and depending on the rates of injection and aquifer characteristics, vertical fracturing may occur close to the injection wells at some sites. Vertical fractures initiated in Cambrian rocks will probably be stopped by the overlying thick salt formations, while vertical fractures initiated at some sites in the Mannville Group will probably be deflected and transformed into horizontal fractures before reaching the top of the bedrock. At the beginning of the study it was thought that there was enough information in the Cold Lake area for a complete evaluation of the effects of deep waste disposal. For a regional-scale evaluation this is indeed the case. As the study progressed, however, it became clear that an accurate local-scale evaluation cannot be performed because of lack of data. For this reason, some of the results are speculative, inasmuch as they have a degree of associated uncertainty. It can be stated with a high degree of confidence, however, that the injection of residual wastewaters in the Cold Lake area has only local effects which are limited to the area surrounding the injection wells. The lack of site-specific data makes this study of local effects of injection indicative only of the probable response of the system, without being able to provide definite answers to be used by operators and regulatory agencies. This lack of data at the injection well includes the aquifer mineralogy, the composition of formation and injected waters, the mechanical and hydraulic properties of the rocks, and the injected volumes with corresponding downhole pressures. Despite these deficiencies due to lack of site-specific data, the present study is important because it helps to clarify and eliminate some concerns, such as the possibility of liquid waste migration over large distances to the shallow aquifers in Saskatchewan. Also, the study is indicative of at least the order of magnitude of the effects of injection, and provides a basis for the development and implementation of a successful



monitoring program. An indirect result of the present study is the conclusion that more emphasis should be placed by the pilot operators and by regulatory agencies on the capture and collection of all the pertinent data needed for an accurate evaluation of the effects of deep liquid waste disposal at the local scale.

The effects of injection in the area surrounding the well should be studied and predicted on a case by case basis using locally (site) measured values of the parameters involved, any natural or artificial vertical conduits for fluid migration, and actual field injection

data for model calibration and history matching. If site-specific modelling can predict pressure buildups over the respective fracturing thresholds, the initiation, orientation, propagation, and extent of fractures should be studied further. This may be accompanied by using geomechanical modelling in conjunction with fluid flow models (hydrofracturing models) in order to assess the possibility of inducing hydraulic connectivity with the shallow groundwater aquifers used for water supply.

## References

- Anderson, R.A., D.S. Ingram and A.M. Zanier (1973): Determining fracture pressure gradients from well logs; *Journal of Petroleum Technology*, v. 25, pp. 1259-1268.
- Bachu, S., C.M. Sauveplane, A.T. Lytviak and B. Hitchon (1987): Analysis of fluid and heat regimes in sedimentary basins: techniques for use with large data bases; *American Association of Petroleum Geologists Bulletin*, v. 71, pp. 822-843.
- Balmer, G.G. (1953): Physical properties of some typical foundation rocks, Denver, Colorado; Design and Construction Division, U.S. Bureau of Reclamation, Engineering Laboratories Branch, Concrete Laboratory Report No. SP-39.
- Basin Analysis Group (1985): Hydrogeology of the Cold Lake study area, Alberta, Canada; Consultant report prepared for Alberta Environment.
- (1987): Evaluation of deep waste disposal, Cold Lake area, Alberta and Saskatchewan: regional effects; Consultant report prepared for Alberta Environment.
- (1988): Evaluation of deep waste disposal, Cold Lake area, Alberta and Saskatchewan: local effects; Consultant report prepared for Alberta Environment.
- Bear, J. (1972): Dynamics of fluids in porous media; Elsevier, 764 pp.
- Beljin, M.S. (1987): Representation of individual wells in two-dimensional ground water modelling; *in* Proceedings of the NWWA/IGWMC Conference – Solving ground water problems with models, February 10-12, 1987, Denver, Colorado, National Water Well Association, Dublin, Ohio, pp. 340-351.
- Bell, J.S. and E.A. Babcock (1986): The stress regime of the Western Canadian Sedimentary Basin and implications for hydrocarbon production; *Bulletin of Canadian Petroleum Geology*, v. 34, pp. 364-378.
- Biot, M.A. (1941): General theory of three-dimensional consolidation; *Journal of Applied Physics*, v. 12, pp. 155-164.
- Biot, M.A., W.L. Medlin and L. Masse (1983): Fracture penetration through an interface; *Society of Petroleum Engineers Journal*, v. 23, pp. 857-869.
- Bredehoeft, J.D., R.G. Wolff, W.S. Keys and E. Shuler (1976): Hydraulic fracturing to determine the regional in situ stress field, Piceance Basin, Colorado; *Geological Society of America Bulletin*, v. 87, pp. 250-258.
- Charbeneau, R.J. and R.L. Street (1979): Modeling groundwater flow fields containing point singularities: a technique for singularity removal; *Water Resources Research*, v. 15, pp. 583-594.
- Chia, Y. and J. Chiu (1989): Upward migration of underground injected wastes through hydrologic conduits around the wellbore; *in* Proceedings, Fourth Canadian/American Conference on Hydrogeology – Fluid flow, heat transfer and mass transport in fractured rocks (S. Bachu and B. Hitchon, editors). National Water Well Association, Dublin, Ohio, (in press).
- Chouet, B. (1986): Dynamics of a fluid-driven crack in three dimensions by the finite difference method; *Journal of Geophysical Research*, v. 91, no. B 14, pp. 13967-13992.
- Davies, P.B. (1987): Modeling areal, variable density, groundwater flow using equivalent head-analysis of potentially significant errors; *in* Proceedings of the NWWA/IGWMC Conference – Solving ground water problems with models, February 10-12, 1987, Denver, Colorado, National Water Well Association, Dublin, Ohio, pp. 888-903.
- Dusseault, M.B. and J.V. Simmons (1982): Injection-induced stress and fracture orientation changes; *Canadian Geotechnical Journal*, v. 9, pp. 483-493.

- Eaton, A.B. (1969): Fracture gradient prediction and its application in oil field operations; *Journal of Petroleum Technology*, v. 21, pp. 1353-1360.
- Gunter, W.D., B.J. Fuhr and B. Young (1986): Composition of water in waste well disposal from oil sands and heavy oil field pilots of Alberta; *in* Proceedings, Third Canadian/American Conference on Hydrogeology – Hydrogeology of sedimentary basins: application to exploration and exploitation (B. Hitchon, S. Bachu and C.M. Sauveplane, editors), National Water Well Association, Dublin, Ohio, pp. 233-249.
- Gupta, S.K., C.R. Cole, F.W. Bond and A.M. Monti (1984a): Finite-element three-dimensional groundwater (FE3DGW) flow model formulation, program listings and users' manual; Pacific Northwest Laboratory, Richland, Washington.
- Gupta, S.K., C.R. Cole and G.F. Pinder (1984b): A finite-element three-dimensional groundwater (FE3DGW) model for a multiaquifer system; *Water Resources Research*, v. 20, pp. 553-563.
- Haimson, B. (1968): Hydraulic fracturing in porous and non-porous rock and its potential for determining in situ stresses at great depth; Ph.D thesis, University of Minnesota, Minneapolis.
- Haimson, B. and C. Fairhurst (1969): Hydraulic fracturing in porous permeable materials; *Journal of Petroleum Technology*, v. 21, pp. 811-817.
- Harrison, D.B., R.P. Glaister and H.W. Nelson (1981): Reservoir description of the Clearwater oil sands, Cold Lake, Alberta; *in* The future of heavy crude and tar sands, McGraw-Hill, Inc., New York, pp. 264-280.
- Hitchon, B., G.K. Billings and J.E. Klován (1971): Geochemistry and origin of formation waters in the western Canada sedimentary basin – III. Factors controlling chemical composition; *Geochimica et Cosmochimica Acta*, v. 35, pp. 567-598.
- Hitchon, B., S. Bachu, C.M. Sauveplane and A.T. Lytviak (1987): Dynamic basin analysis: an integrated approach with large data bases; *in* Fluid flow in sedimentary basins and aquifers (J.C. Goff and B.P.J. Williams, editors), Geological Society Special Publication No. 34, pp. 31-44.
- Hitchon, B., S. Bachu, C.M. Sauveplane, A. Ing, A.T. Lytviak and J.R. Underschultz (1989): Hydrogeological and geothermal regimes in the Phanerozoic succession, Cold Lake area, Alberta and Saskatchewan; *Alberta Research Council Bulletin* 59, 84 pp.
- Hubbert, M.K. (1945): Strength of the earth; *American Association of Petroleum Geologists Bulletin*, v. 29, pp. 1630-1653.
- Hubbert, M.K. and D.G. Willis (1957): Mechanics of hydraulic fracturing; *American Institute of Mining Engineers Transactions*, v. 210, pp. 153-168.
- Jaeger, J.C. and N.G.W. Cook (1976): *Fundamentals of rock mechanics*; Chapman and Hall, 2nd edition, London.
- James, D.P. and T.A. Oliver (1977): The sedimentology of the McMurray Formation, East Athabasca; *in* The oil sands of Canada-Venezuela 1977; (D.A. Redford and A.G. Winestock, editors) The Canadian Institute of Mining and Metallurgy, pp. 17-26.
- Kharaka, Y.K., W.D. Gunter, P.K. Aggarwal, E.H. Perkins and J.D. DeBraal (1988): SOLMINEQ.88: A computer program code for geochemical modelling of water-rock interaction; U.S. Geological Survey, Water Resources Investigation Report 88-4227, 420 pp.
- Labudovic, D. (1984): The effect of Poisson's ratio on fracture height; *Journal of Petroleum Technology*, v. 36, pp. 287-290.
- Lama, R.D. and V.S. Vutukuri (1978): *Handbook on mechanical properties of rocks*; Vol. II-IV, Trans. Tech. Publications.
- MacDonald, J. (1987): The Basal Cambrian sandstone, mineralogy and diagenesis; Unpublished MSc. thesis, The University of Alberta.
- McLennan, J.D., J. Elbel, E. Mattheis and L. Lindstrom (1982): A critical evaluation of the Mechanical Properties Log (MPL) on a Basal Quartz well in the Caroline area, Alberta; 33rd Annual Technical Meeting of the Petroleum Society of the Canadian Institute of Mining and Metallurgy, 6-9 June 1982, Calgary, Alberta, Paper 82-33-45, 11 pp.
- Mossop, G.D., J.W. Kramers, P.D. Flach and B.A. Rottenfusser (1981): Geology of Alberta's oil sands and heavy oil deposits; *in* The future of heavy crude and tar sands, McGraw-Hill, Inc., New York, pp. 197-207.
- Nordgren, R.P. (1972): Propagation of a vertical hydraulic fracture; *Transactions of the Society of Petroleum Engineers of AIME*, v. 253, pp. 306-314.
- Peaceman, D.W. (1983): Interpretation of well-block pressures in numerical reservoir simulation with nonsquare grid blocks and anisotropic permeability; *Society of Petroleum Engineers Journal*, v. 23, no. 3, pp. 541-543.
- Pickett, G.R. (1963): Acoustic character logs and their application in formation evaluation; *Journal of Petroleum Technology*, v. 15, pp. 659-667.
- Porter, J.W., R.A. Price and R.G. McCrossan (1982): The Western Canada Sedimentary Basin; *Philosophical Transactions of the Royal Society of London, Series A*, v. 305, pp. 169-192.
- Pugh, D.C. (1973): Subsurface Lower Paleozoic stratigraphy in northern and central Alberta; Geological Survey of Canada, Paper 72-12, 29 pp.

SAEL (1988): Subsurface well practices. Interim report prepared for the National Hydrology Research Institute.

Settari, A. and M.P. Cleary (1984): Three-dimensional simulation of hydraulic fracturing; *Journal of Petroleum Technology*, v. 36, pp. 1177-1190.

Vissen, K., P.H.M. Dankers, D. Lechie and A.G.P. Van der Marel (1985): Mineralogy and geology of the Clearwater reservoir sands in the Wolf Lake area,

Cold Lake, Alberta; *in* Proceedings of the Third International Conference on Heavy Crude and Tar Sands, United Nations Development Program, v. 1, p. 380.

Warpinski, N.R., P. Branagan and R. Wilmer (1985): In-situ stress measurements at US's DOE's Multiwell Experiment site, Mesaverde Group, Rifle, Colorado; *Journal of Petroleum Technology*, v. 37, pp. 517-536.